



---

# PhD THESIS

---

**Ramavath Naresh Naik**



**JANUARY 29<sup>th</sup>, 2021**  
**UNIVERSITÀ DEL PIEMONTE ORIENTALE**  
**Via Solaroli 17, Novara-28100, ITALY**



UNIVERSITÀ DEL PIEMONTE ORIENTALE

Dipartimento di Scienze della Salute

Corso di Dottorato di Ricerca in  
SCIENZE E BIOTECNOLOGIE MEDICHE

XXXIII Ciclo

# **Role of immune cell interactions in the evolution of nonalcoholic steatohepatitis (NASH)**

SSD: MED/04 – Patologia Generale

Coordinatore

Prof. Marisa GARIGLIO

Tutor

Prof. Emanuele ALBANO

Dottorando

Ramavath Naresh Naik

ANNO ACCADEMICO 2017/2018

# Table of Contents

<i>General Abstract</i> .....	4
<i>Introduction</i> .....	6
Epidemiology and Clinical Features of NAFLD.....	6
Pathogenesis of NAFLD/NASH.....	9
The role of innate immunity cells in NAFLD.....	14
The role of adaptive immune system in NAFLD.....	17
<i>Aims of Project</i> .....	24
<i>Materials and Methods</i> .....	25
<i>Results-Section 1</i> .....	30
Characterization of the role of B-lymphocytes in NASH progression.....	30
<i>Results- Section 2</i> .....	53
Role of the fractalkine receptor CX <sub>3</sub> CR1 in the development of monocytes derived dendritic cells during hepatic inflammation.....	53
<i>Results- Section 3</i> .....	73
Role of ICOS/ICOSL dyad in the interaction between T-cell and macrophages during NASH evolution.....	73
<i>General Discussion</i> .....	88
<i>References</i> .....	92
<i>Acknowledgements</i> .....	107

## General Abstract

Recent evidence implicates adaptive immunity as a key player in the mechanisms supporting hepatic inflammation during the progression of nonalcoholic steatohepatitis (NASH). In these settings, oxidative stress-derived epitopes (OSE) have been documented as the antigens triggering NASH-associated immune responses. My doctoral project has investigated different aspects of the involvement of immune mechanisms in NASH. From the observation that B-lymphocytes were evident in liver biopsies from NASH patients and localized in cell aggregates resembling lymphoid structures we investigated the role of B cell in NASH showing that in mice the onset of steatohepatitis was characterized by hepatic B2-lymphocytes maturation to plasma cells. B-cell responses preceded T-cell activation and were accompanied by the up-regulation in the hepatic expression of B-cell Activating Factor (BAFF). Selective B2-cell depletion in mice over-expressing a soluble form of the BAFF/APRIL receptor Transmembrane Activator and Cyclophilin Ligand Interactor (TACI-Ig) or BAFF neutralization with anti-BAFF monoclonal antibodies prevented Th-1 activation of liver CD4<sup>+</sup> T-lymphocytes and ameliorate liver damage and NASH progression to fibrosis. These data indicate that B2-lymphocyte activation is an early event in NAFLD evolution and contributes to the disease progression through the interaction with T-cells.

A still poorly explored aspect in the development of adaptive immune response in NASH concerns the mechanism by which lymphocyte interacts with other myeloid cell within the liver. By investigating the co-stimulatory molecules Inducible T-cell Co-Stimulator (ICOS; CD278) and its ligand ICOSL (CD275) we observed that the serum content of the soluble forms of both ICOS and ICOSL were significantly higher in NAFLD/NASH patients than in healthy individuals. In mice NASH was characterized by an enhanced expression of ICOS by liver CD8<sup>+</sup> T-cells and a concomitant up-regulation of ICOSL in monocyte/macrophages (MoMFs). Steatohepatitis as well as hepatic fibrosis were significantly lower in ICOSL deficient (ICOSL<sup>-/-</sup>) than in wild type mice. Flow cytometry analysis of liver MoMFs revealed that the lack of ICOSL selectively reduced the fraction of pro-inflammatory Ly6C<sup>high</sup> MoMFs and this paralleled with a lowering in the expression of the Triggering Receptor Expressed on Myeloid cells 1 (TREM-1), a surface receptor involved in maintaining MOMF M1 activation. Similar effects were also observed in ICOS

deficient mice, suggesting that CD8<sup>+</sup> T cells can sustain TREM-1 mediated macrophage M1 through signals involving ICOS/ICOSL dyad.

The activation of immune responses in NASH requires antigen presentation to lymphocytes by specialized cells among which the most important are dendritic cells (DCs). Although previous studies have documented an early expansion of hepatic myeloid DCs in NASH and their involvement in sustaining lobular inflammation, the feature of these cells were not investigated. Here we show that hepatic inflammation in experimental NASH associates with a massive expansion of myeloid DCs expressing monocyte markers along with CX<sub>3</sub>CR1, allowing their tentative identification as monocyte-derived DCs (moDCs). The lack of CX<sub>3</sub>CR1 affected the maturation of monocytes into moDCs both *in vitro* and in a model of acute liver injury induced by CCl<sub>4</sub> poisoning. Moreover, the treatment with the CX<sub>3</sub>CR1 antagonist, CX3-AT before CCl<sub>4</sub> administration reduced liver moDCS and significantly ameliorated hepatic injury and inflammation, highlighting a novel role of CX<sub>3</sub>CR1-mediated signals in driving the differentiation of hepatic moDCs in response to tissue injury.

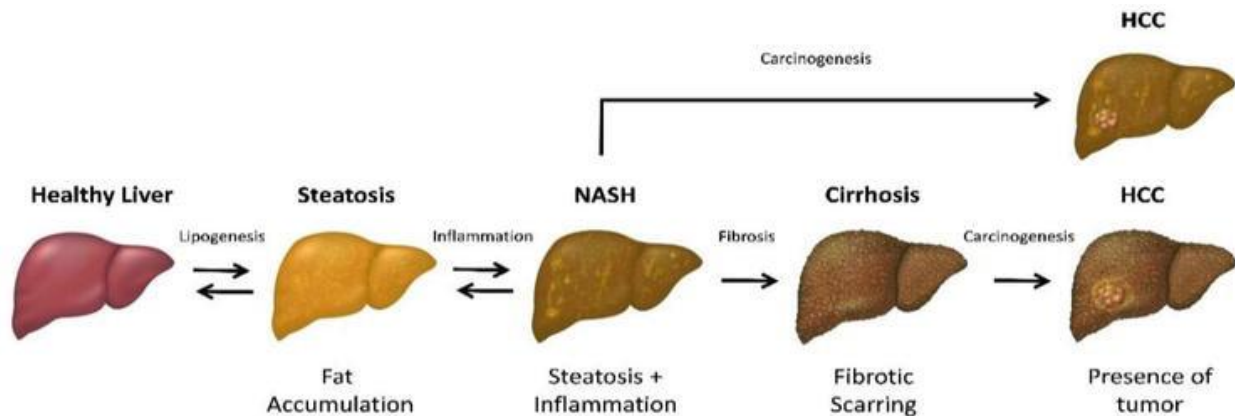
In conclusion the data obtained during my doctoral training further highlight the complexity of the mechanisms involved in the progression of NASH pointing to the importance of specific interactions between adaptive and innate immunity cells. Targeting these interactions might offer the possibility for developing novel therapeutic approaches to NASH.

## Introduction

### Epidemiology and Clinical Features of NAFLD.

Nonalcoholic fatty liver disease (NAFLD) is presently considered as the most common liver diseases worldwide with an overall prevalence of about 25% and is emerging as one of the leading causes of end-stage liver disease in western world involving both the adolescent and the adult populations (Younossi, et al. 2018). NAFLD is characterized by excessive fat, mainly triglycerides, accumulation within the liver, a process known as “steatosis”, in the absence of considerable alcohol ingestion (Chalasani, et al. 2012). NAFLD/NASH is considered the hepatic manifestation of the so called Metabolic Syndrome (MS) (Yki-Jarvinen, et al. 2014), a complex of clinical condition associated to obesity and over-weight that includes diabetes, hypertension, hypertriglyceridemia, and low high-density lipoprotein (HDL) cholesterol. It is estimated that about 47 million U.S. individuals suffer of metabolic syndrome and more than 80% of such subjects develop NAFLD (Younossi, et al. 2012). On the other hand, more than 90% of NAFLD patients have obesity associated with some features of metabolic syndrome. As mentioned above, the prevalence of NAFLD in the general population is estimated to about 25% worldwide. The highest rate of NAFLD is evident in the middle east (32%), south America (31%), with lowest rate found in Africa (13%). It is estimated that by 2030 NAFLD population will be increase by 18% in USA and 15% in Germany (Younossi, et al. 2016; Estes, et al. 2018). NAFLD occurs in all age groups, including children and is equally frequent in both genders (Sheth and others 1997). The prevalence of NAFLD is directly related to Body Mass Index (BMI) and waist circumference, in fact subjects having BMI more than >30 as well as waist circumference more than >94 cm of men or >80 cm for women have greater chance to develop NAFLD (Chaney, et al. 2015). In addition, multiple factors influence the prevalence of NAFLD/NASH, among the different ethnic groups, as African-American have lower (24%) prevalence whereas the highest (45%) is observed among Hispanics, indicating that NAFLD also reflect complex interactions between environmental, lifestyle related factors and genetic predisposition (Younossi, et al. 2016).

The histopathologic features of adult NAFLD are characterized by macrovesicular steatosis, mainly involving centrilobular areas, (Brunt, et al. 2011; Brunt, et al.2003). Nonalcoholic steatohepatitis (NASH) is an inflammatory subtype of NAFLD characterized by presence of steatosis along with evidence of hepatocyte injury, lobular inflammation and eventually fibrosis. The inflammation associated with steatohepatitis is generally modest and has mainly lobular distribution. However, portal inflammation can be detected in specific individuals, particularly in pediatric subjects and in those who are morbidly obese (Gramlich, et al. 2004). In the majority of NAFLD patients, steatosis is the main feature and these subjects generally do not face a significant risk of liver-related adverse outcomes (Rinella, et al. 2015). Conversely in about 20–30% of NAFLD subjects, the development of NASH represents the key feature in the evolution of the disease as it is frequently associated with the progression to liver cirrhosis and eventually to hepatocellular carcinoma (HCC) (Caligiuri, et al. 2016; Brunt, et al. 2011).



#### Natural progression of NASH/NAFLD

Hepatic fibrosis is by now the strongest predictor for disease-specific mortality in NAFLD/NASH and the death rate ascribed to NASH-related cirrhosis accounts for 12-25% and end-stage NASH is becoming an increasingly common indication for liver transplantation (Lindenmeyer, et al. 2018). A further aspect related to NAFLD evolution concerns its association with hepatocellular carcinoma (HCC) (Baffy, et al. 2012; Younes, et al. 2018]. NAFLD-related cirrhosis is a rising cause of HCC in Western countries accounting for 10-34% of the known aetiologies. Nonetheless, growing evidence points out that roughly 13-49% of all HCCs develop in non-cirrhotic NASH patients (Younes, et al. 2018). All together, these data indicate that

NAFLD/NASH substantially contributes to the prevalence of cirrhosis and HCC worldwide. Such a scenario is forecasted to worsen in the near future as a result of the expected rise in NAFLD prevalence (Estes, et al. 2018) and the diffusion of effective treatments for viral hepatitis.

The majority of the patients with diagnosis of NAFLD are asymptomatic (Johannes, et al. 2014; Bhriony, et al. 2011) and clinical symptoms of NAFLD are nonspecific. NAFLD subjects often have hepatomegaly variably associated with general malaise, abdominal discomfort, vague right upper quadrant abdominal pain, nausea. Jaundice and features of portal hypertension, such as ascites and variceal hemorrhage, are the initial findings in a small minority of subjects with advanced liver disease. (Ahmed, et al. 2015). From the laboratory point of view there is no single biochemical marker that can confirm the diagnosis of NAFLD or distinguish between steatosis, steatohepatitis and cirrhosis. It has been reported that mildly elevated level of liver enzymes serum aminotransferases is the primary abnormality seen in NAFLD patients. An elevation of alanine aminotransferase (ALT) and aspartate aminotransferase (AST) greater than four times the upper limit of AST/ALT ratio (Pratt, et al. 2000; Torres, et al. 2008) indicates abnormalities in liver function, however most of NAFLD subjects shows normal levels of liver enzymes. (Johannes, et al. 2014; Mofrad, et al. 2003). Therefore, liver enzyme levels are not sensitive for the diagnosis of NAFLD. Serum gamma-glutamyl transferase (GGT) is frequently elevated in patients with NAFLD and elevated levels of GGT has shown been to be associated with fibrosis (Tahan, et al. 2008). Furthermore, an elevated ferritin level has been reported in up to 50% of NASH patients, (Angulo, et al. 1999). However, these findings do not appear to correlate with an elevated iron concentration in the liver, and the role of hepatic iron in the pathogenesis of NASH is unclear. Several clinical investigators have proposed other different biomarkers, but their use has been limited due to the reproducibility or inability to accurately distinguish advanced form of steatosis (Sumida, et al. 2009). Therefore, liver biopsy remains the gold standard for diagnosing steatohepatitis and for staging the liver disease, unless clinically evident cirrhosis is present.



## **Pathogenesis of NAFLD/NASH**

The molecular mechanism underlying the development and progression of NAFLD is complex and multifactorial. Different theories have been formulated, leading initially to the 'two hits hypothesis'. According to this theory, the first hit is caused by the hepatic accumulation of lipids as consequence of obesity and insulin resistance. Steatosis sensitizes the liver to further insults acting as a 'second hit' activating inflammatory cascades and fibrogenesis (Day and James, 1998). However, soon it became evident that this view is too simplistic to recapitulate the complexity of the human NAFLD where multiple environmental and genetic factors can contribute to the disease evolution. Consequently, a multiple-hit hypothesis has now substituted the outdated two-hit hypothesis for the progression of NAFLD.

### **i) Mechanism of steatosis:**

As mentioned above, steatosis is a key feature of NAFLD and the mechanisms responsible for the impairment of lipid metabolism within the liver play a key role in the disease pathogenesis. Liver plays a major role in lipid metabolism, as hepatocytes utilize Free Fatty Acids (FFAs) as energy source, but a large amount of FFA is re-esterified to triglycerides and exported as very low-density lipoproteins (VLDL). Nonetheless, FFAs are also produced by liver cells from glucose and fructose through de novo lipogenesis (DNL). Thus, any derangement in this process can lead to development of NAFLD (Musso, et al. 2009). Under physiological conditions non-esterified FFAs can derive from dietary short chain fatty acids or are released from the adipose tissue and within the liver may follow three different pathways such as beta-oxidation in mitochondria or the synthesis of triglycerides that are then exported as VLDL into the blood with help of apolipoprotein B (APOB) (Lonardo, et al. 2002). The liver responds to elevated circulating FFAs as well as to increased lipogenesis by promoting triglyceride synthesis and by favoring intrahepatic triglyceride accumulation thus leading to steatosis. Hence hepatic fat accumulation can result from increased fat synthesis, increased fat delivery, decreased fat export, and/or decreased fat oxidation (Postic and Girard, et al. 2008). Lipid metabolism in the liver and adipose tissue is controlled by insulin-mediated signals. Insulin binding to insulin receptors leads to

phosphorylation of insulin receptor substrates IRS 1,2,3 and to the activation of intracellular phosphoinositide 3-kinase (PI3K) and AKT/PKB (protein kinase B) pathways, which are intimately involved in mediating the metabolic effects of insulin including glucose uptake, the expression of key lipogenic genes and decrease in gluconeogenic genes. Insulin has also a potent action in suppressing adipose tissue lipolysis (Bugianesi and others, et al. 2010). Obesity and metabolic syndrome are characterized by an impairment of the insulin signal pathway, a condition known as insulin resistance (IR). NAFLD contribute both hepatic and systemic IR. As a result, insulin-mediated suppression of lipolysis is impaired resulting in an increased efflux of FFA from the adipose tissue. Hyper-insulineamia associated with IR leads also to an up-regulation of the transcription factor sterol regulatory element binding protein-1c (SREBP-1c), which is a key transcriptional regulator of genes involved in DNL as well as to the inhibition of  $\beta$ -oxidation of FFA thus further promoting hepatic lipid accumulation (Hooper et al., 2011). The expression FAT/CD 36 (Fatty acid translocase) is also upregulated via transcription factor forkhead box protein (FoxO1) thus enhancing the FFAs uptake by the hepatocytes (Mastrodonato, et al. 2011). A further aspect in the mechanisms leading to hepatic steatosis directly involves the changes in adipokine production by the adipose tissue. In obesity adipocytes that accumulate triglycerides modify their pattern of adipokine secretion leading to higher secretion mediators promoting IR such as pro inflammatory cytokines, visfavin and resistin and lowering the synthesis of adiponectin, a adipokine that favour liver insulin response (Marra, et al. 2005). In fact, the circulating levels of adiponectin are inversely proportional to body fat content and are reduced in patients with NAFLD. The importance of adiponectin in NAFLD is supported by studies showing that serum adiponectin levels can help to distinguish NASH from simple steatosis.

## **ii) Mechanism of Hepatocyte Injury**

NASH is characterized by parenchymal injury involving hepatocyte ballooning, the presence of Mallory-Denk bodies and extensive liver cell apoptosis (Duwaerts and Maher, et al. 2014). In line with these findings, recent studies have proposed the measure of serum levels of caspase-cleaved cytokeratins (CK) 8 and 18 as specific marker of NASH (Eguchi, et al. 2014). Several mechanisms have been invoked to explain the proapoptotic state in NASH. Triglyceride

accumulation itself can increase hepatocyte apoptosis by facilitating the synthesis of ceramide that triggers cell death via an inducible nitric oxide synthetase (iNOS)-mediated pathway (Harbrecht and others, et al. 2012). It has also been shown that hepatocyte incapability to esterify the excess of FFAs consequent to increased peripheral lipolysis promotes apoptosis through a process known as lipotoxicity. In this setting endoplasmic reticulum (ER) stress and the activation of signal pathways associated to the unfolded protein response (UPR), stress kinases, which eventually results in the activation of homologous protein (CHOP), a potent apoptosis-inducing factor, and in the up-regulation of the proapoptotic proteins Bim and PUMA (Cazanave, et al. 2009; Masukoa, et al. 2009; Akazawa, et al. 2013). Recent studies have reported that patients with NAFLD have a variable degree of UPR and c-jun N-terminal kinase (JNK) activation (Malhi and others, et al. 2008). Accordingly, JNK activation and pharmacological or genetic JNK inhibition prevents lipotoxicity “in vitro” and ameliorates steatohepatitis in rodent models of NASH (Cazanave and Gores, et al. 2010; Czaja, et al. 2010). Thus, it has been proposed that the development of progressive NAFLD in some patients but not in others may be the result of increased susceptibility of steatotic hepatocytes to apoptosis arising from JNK activation (Li, et al. 2014; Malhi, et al. 2008). Additional mechanisms of hepatocyte injury in NAFLD/NASH involve the cytotoxic effects of pro-inflammatory cytokine TNF- $\alpha$  and oxidative stress (Marra, et al. 2008).

Oxidative stress is defined as the imbalance between the production of reactive oxygen species (ROS) and the scavenging capacity of the antioxidant (Takaki, et al. 2013). ROS, including superoxide anion radicals ( $O_2^{\bullet-}$ ) and hydrogen peroxide ( $H_2O_2$ ), are continuously produced intracellularly as byproducts of energetic metabolism in mitochondria, peroxisomes, endoplasmic reticulum (Masarone, et al. 2018). In liver cells mitochondria are considered the most relevant ROS generators and they are especially important when considering ROS derived from energetic metabolism (Mansouri, et al. 2018; Figueira, et al. 2013). In NAFLD/NASH the disturbances in mitochondrial electron transport chain represent an important source for ROS production within hepatocytes, nonetheless the upregulation of microsomal cytochromes CYP2E1 and CYP4A by excess of FFA could also contribute to ROS generation (Vernon et al. 2011; Williams, et al. 2010). By interacting with lipids, DNA and proteins ROS causes cellular and tissue injury. In particular, ROS reaction with lipids produces hydroperoxides and endoperoxides,

which undergoes fragmentation to generate reactive intermediates, such as malondialdehyde (MDA) and 4-hydroxynonenal (4-HNE), resulting in cell death and activation of inflammatory mechanisms (Ray, et al. 2012). The contribution of oxidative stress to the pathogenesis of NASH is supported by studies showing that ROS contribute to the death of fat-laden hepatocytes (Marr, et al. 2008; Gambino, et al. 2011), while the supplementation with antioxidant reduces liver injury in experimental rodent models of NASH (Laurent, et al. 2004). In the same vein, an increase in oxidative stress markers, is evident in the liver and in the serum of both adult and paediatric NAFLD/NASH patients (Seki, et al. 2002; Chalasani, et al. 2004; Ikura, et al. 2006; Nobili, et al. 2010).

### **iii) Mechanisms of fibrosis.**

Hepatic cirrhosis represents the final outcome of NAFLD/NASH and end-stage NASH is becoming an increasingly important cause of liver cirrhosis world wide. NASH-related fibrosis develops primarily in the pericentral areas, where thin bundles of fibrotic tissue surround groups of hepatocytes and thicken the space of Disse, with a pattern called “chicken wire” (Brunt, et al. 2010). As in other type of chronic liver diseases hepatic stellate cells (HSCs) are the main responsible for extracellular matrix deposition. These cells respond to tissue damage and to the macrophage production of transforming growth factor  $\beta$ 1 (TGF- $\beta$ 1), platelet-derived growth factor (PDGF) and fibroblast-derived growth factors by trans-differentiating into myofibroblast-like cells (HSC/MSs) that secrete large amount of collagen and extracellular matrix components (Friedman, et al. 2008). Collagen accumulation is further favored by a decrease in hepatic matrix degradation due to a reduced production of matrix metalloproteases (MMPs) and/or an increased synthesis of matrix metalloprotease inhibitors (Friedman, et al. 2008). Several factors such as oxidative stress and lymphocyte-derived cytokines influence HSC proliferation and transformation to collagen-producing myofibroblasts (Novo, et al. 2008). In this latter respect the production of OPN by NKT cells might be particularly relevant in NASH evolution as OPN has been shown to directly stimulate collagen synthesis by hepatic stellate cells (HSCs) through a TGF- $\beta$ 1-independent pathway (Urtasum, et al. 2012). Although the development of fibrosis in NASH does not appears to be appreciably different from those in other liver diseases, alterations in adipokine

secretion consequent to obesity might have a specific role for the induction of fibrogenesis in this condition. Activated HSCs selectively express leptin receptors and leptin stimulates HSC survival, the expression of pro-inflammatory and angiogenic cytokines (Wang, et al. 2008). The pro-fibrogenic action of leptin might be enhanced by the combined lowering of adiponectin as adiponectin reduces proliferation and increases apoptosis of cultured HSC (Wang, et al. 2008).

#### **iv) Mechanisms of Inflammation**

Inflammation, along with hepatocyte damage and fibrosis is the main feature of the progression from simple steatosis to NASH. Both the innate and adaptive immunity have a role in the initiation and maintenance of lobular inflammation and understanding the interplay between these two systems represents the challenge in unravelling the disease pathogenesis. In fact, current view sees inflammation as the driving force in NASH progression and a key therapeutic target since the factors promoting inflammation crosstalk with those responsible for hepatocellular damage and fibrosis.

Several mechanisms contribute to the recruitment and activation of inflammatory cells in the liver during the evolution of NAFLD. As mentioned above, hepatocyte FFA overload causes cellular stress and cell death causes the release of damaged associated molecular patterns (DAMPs) in the hepatic circulation (Feldstein, et al. 2003). Several molecules have been recognized as DAMPs including nuclear factors such as the high-mobility group box 1 (HMGB1), nuclear and mitochondrial DNA, purine nucleotides (i.e., ATP, UTP), lipid peroxidation products and uric acid. In addition to DAMPs, gut dysbiosis associated with obesity promotes an increased enteral adsorption of bacterial products such as lipopolysaccharide (LPS) and peptidoglycans and their increase in the portal circulation also contributes to inflammatory response in NAFLD/NASH (Ganz, et al. 2013; Brandl and Schnabl, et al. 2017; Huebener, et al. 2015). DAMPs and pathogen associated molecular patterns (PAMPs) bind to a variety of cell receptors known as pattern recognition receptors (PRRs), that are responsible for triggering a local inflammatory including the production of inflammatory cytokines such as tumor necrosis factor-alpha (TNF-a) and interleukin-6 (IL-6). (Feldstein, et al. 2010; Seki, et al. 2008]. Among PRRs, Toll-like receptors (TLRs) are highly conserved receptors expressed on hepatocytes, Kupffer cells, hepatic stellate

cells, biliary epithelial cells (Kesar, et al. 2014; Petrasek, et al. 2013; Strowig, et al. 2012). The most studied TLRs in the liver, and particularly in NASH, are TLR2, TLR4 and TLR9 (Kesar, et al. 2014; Strowing, et al.2012). These receptors recognize specific variant motifs present in pathogen molecules. While TLR2 recognizes peptidoglycans, TLR4 and TLR9 recognize bacterial LPS and DNA, respectively (Bieghs, et al. 2014]. The nucleotide oligomerization domain (NOD)-like receptors (NLRs) also belong to the PRR family and can recognize DAMPs and PAMPs. NLR activation in response to DAMPs or PAMPs leads to the assembly of inflammasome, a multiprotein complex required for caspase-1 activity and initiation of inflammatory signals. Full activation of inflammasome, results in secretion of mature IL-1 and IL-18 (Martinon, et al. 2002; Szabo, et al. 2012). Both these cytokines elicit inflammatory signals in liver as well as in the adipose tissue and intestine, triggering steatosis, insulin resistance, inflammation and cell death (Dixon, et al. 2013).

## **The role of innate immunity cells in NAFLD**

In recent years, the role of the innate immune response in NAFLD has been the focus of intense research. Lobular inflammation in NASH involves hepatic infiltration of innate immune cells such as macrophages, granulocytes and natural killer (NK) and natural killer T cells (NKT) which have a key role in sustaining the disease progression.

*Neutrophils:* Neutrophil accumulation is frequently seen in NASH as a results of CXCL1 production in hepatocytes (Tacke, et al. 2017). Neutrophils critically contribute to hepatocellular damage by releasing ROS, myeloperoxidase (MPO), and proteases, such as neutrophil elastase (NE), proteinase 3, cathepsins, and matrix metalloprotease (MMP)-9 into the extracellular environment. MPO also enhances inflammation by recruiting macrophages and promotes the pro-fibrogenic activation of hepatic stellate cells (HSCs) (Xu, et al. 2014). Accordingly, neutrophil depletion with the antibody, 1A8 or impairment of MPO, NE, or proteinase-3 expression improve liver damage in experimental model of NASH (Cai, et al. 2019)

*Macrophages:* Liver macrophages are a heterogeneous population consisting of yolk sac-derived tissue-resident macrophages or Kupffer cells (KCs) and bone marrow monocyte-derived macrophages. In healthy liver, KCs reside in the hepatic sinusoids (Duarte, et al. 2015), their major functions include phagocytosis of pathogen or bacterial-derived products coming from the portal vein circulation, and present antigens to cytotoxic and regulatory T cells (Lanthier, et al. 2015). The phenotype of macrophages depends upon the stimuli of local environment (Duarte, et al. 2015), and they have been classified as M1 classical activated macrophages and alternative M2 macrophages. While M1 phenotype is regarded as “proinflammatory”, M2 is considered as “anti-inflammatory”. Nonetheless, such a distinction is now considered over simplified and the phenotype of hepatic macrophages is still a matter of research (Tacke, et al. 2014). During the evolution of NAFLD quiescent KCs are activated during by the release of damage associated molecular patterns (DAMPs), including mitochondrial DNA (mtDNA) from steatotic hepatocytes or cells dying because of lipotoxicity and oxidative stress. The release of DAMPs triggers Toll-like receptor (TLR) activation (TLR9, TLR 4) in KCs stimulating the secretion of proinflammatory cytokines (IL-6, tumor necrosis factor (TNF)  $\alpha$ , IL-1 $\beta$ , and chemokine such as CCL2, CCL5, ROS and NO generated by inducible NO synthase-iNOS (Tacke et al. 2017; Garcia, et al. 2016; Mridha, et al. 2017). On their turn, CCL2 and CCL5 recruit the circulating monocytes promoting the expansion of hepatic macrophages. Other chemokine receptors, namely C-X-C motif receptor (CXCR) such as CXCR2 and CXCR3 leads instead to reduced recruitment of infiltration of macrophages, improved hepatic inflammation and fibrosis (Ye, et al. 2016; Zhang, et al. 2016). Monocyte-derived macrophages (MoMFs) represent the majority of mononucleated cells infiltrating the liver and are key players in modulating lobular inflammation as well as NASH evolution to fibrosis (Tacke, et al. 2017). Liver macrophages are very plastic and adapt their phenotype according to signals derived from the hepatic microenvironment, thus explaining their apparent opposing functions during the disease evolution. In fact, beside promoting inflammation, the expansion of liver macrophage pool has also a key role in stimulating HSC activation to myofibroblast and fibrogenetic responses (Tacke, et al. 2017). Accordingly, the infiltration of Ly-6C<sup>+</sup> monocytes has been identified as a crucial factor in the progression toward NASH and fibrosis in mice (Baek, et al. 2012; Lefebvre, et al. 2016). In line with these findings

blocking CCL2 and CCL5 receptors ameliorates experimental NASH (Tacke, et al. 2017) and reduces fibrosis evolution in a phase 2 clinical trial (Friedman, et al. 2018). Conversely the interference with anti-inflammatory mediators that control macrophage responses such annexin A1 or adenosine worsen NASH evolution (Locatelli, et al. 2014; Cai, et al. 2018).

*Natural Killer Cells:* NK cells are enriched in the liver, they account 10 to 20% of total liver lymphocytes in mouse and almost 40 to 50% in humans (Peng, et al. 2016; Tiang, et al. 2013). NK cells are an important component of the innate immune response since they can kill virus-infected cells and by secreting some a variety of cytokines such TNF- $\alpha$ , INF- $\gamma$  and IL-4 that inhibit viral replication and recruit/activate cells involved in adaptive immune response, thus playing a critical role in bridging the innate and adaptive arms of the immune response (Yoon, et al. 2009). In experimental models of NAFLD NK cells have been shown to contribute in maintaining M1 polarization of hepatic macrophages by releasing INF- $\gamma$  (Tosellom and Trampont, et al. 2016). Nonetheless, a recent study in mice suggests that NK cells have also an anti-fibrotic effect by favoring the killing of activated hepatic stellates cells (HSC) through the secretion of tumor necrosis factor – related apoptosis inducing ligand (TRAIL) and NKG2D (Radaeva, et al. 2006; Oh et al. 2016).

Natural Killer T cells (NKT): NKT cells comprise a unique immune cell subtype that expresses specific NK cell surface receptors (NK1.1 in mice or CD161/CD56 humans) as well as conventional T cells antigen receptor (TCR) (Marrero, et al. 2018). NKT cells mainly reside in the sinusoids and can be differentiated in two sub-sets. The large majority (95%) of liver NKT cells is represented by type I or invariant NKT (iNKT), that use an invariant TCR encoded by V $\alpha$  gene. The remaining 5% consists of type II NKT cells, which relay instead an oligoclonal TCR repertoire (Marrero, et al. 2018). NKT cells recognize as antigens glycolipids presented by antigen presenting cells (APCs) expressing CD1d cell surface molecules. Upon activation NKT cells secrete a variety of cytokines (IL-4, IL-10, INF- $\gamma$ , and TNF- $\alpha$ ) that can promote Th-1, Th-2 and T-regulatory (Treg) activities (Marrero, et al. 2018). Thus, NKT cells can both stimulate or suppress immune/inflammatory responses. During NAFLD evolution the prevalence of liver NKT cells varies a lot since in steatosis and during the early phases of steatohepatitis (Kremer, et al. 2010), while NKT cell expansion is evident in advanced NASH (Tajiri, et al. 2009; Wolf, et al. 2014). The involvement of NKT cells in



the pathogenesis of NASH is demonstrated by several paper showing that interfering with NKT cells effectively improves hepatic parenchymal injury, inflammation and prevent NASH progression to fibrosis and hepatocellular carcinoma in different experimental models (Wolf, et al. 2014; Bhattacharjee, et al. 2017; Syn, et al. 2012; Maricic, et al. 2018). On this respect it has been proposed that NKT cells production of the lymphotoxin Lymphotoxin-like Inducible protein that competes with Glycoprotein D for Herpesvirus entry on T cells (LIGHT or TNFSF14) contributes to cause liver steatosis by increasing hepatocyte lipid uptake (Wolf, et al. 2014), while their production of production of osteopontin (OPN) and Heedhogh ligand (Syn, et al. 2012) are implicated in the promotion of NASH-associated liver fibrosis. Furthermore, the lack of iNKT cells in  $J\alpha 18^{-/-}$  mice or NKT cells inhibition by mice treatment with retinoic acid receptor- $\gamma$  agonist tazarotene reduces  $CD8^{+}$  T-cell infiltration in NASH livers (Maricic, et al. 2018), suggesting a strict interplay between cytotoxic T-cells and iNKT cells in the mechanisms supporting steatohepatitis.

### **The role of adaptive immune system in NAFLD**

Adaptive immune response involves the activation and the functional activities of B- and T-lymphocytes that are involved in the production of lymphocyte-derived cytokines regulating inflammatory responses, antibody production and cytotoxicity in response to specific antigens as well as the regulatory functions mediated by regulatory T cells (Treg). These adaptive immune responses require lymphocytic cell trafficking between the bone marrow, lymphoid organs and peripheral tissues using blood and lymphatic vessels as a vehicle (Cyster, et al. 2003).

Histology in human liver biopsies has first suggested the involvement of adaptive immunity in NAFLD/NASH by showing the presence of lymphocytes NASH lobular infiltrates (Yeh, et al. 2014) as well as in periportal infiltrates associated with NASH ductular reactions (Gadd, et al. 2014). The hepatic infiltration by B- and  $CD4^{+}$  and  $CD8^{+}$  T-lymphocytes is also evident in different experimental models of NASH where it parallels the worsening of parenchymal injury and lobular inflammation (Sutti, et al. 2014; Wolf MJ, et al. 2014; Weston, et al.2015; Grohmann, et al.2018). These T-lymphocytes express the memory/effector markers CD25, CD44 and CD69, along with an enhanced production the cytokine LIGHT, indicating their functional activation (Sutti, et al. 2014; Wolf, et al. 2014; Grohmann, et al.2018). In line with these findings Wolf and co-workers (2017)

have observed that Rag1<sup>-/-</sup> mice which lack mature B, T and NKT cells and are unable to mount adaptive immune responses develop less steatosis, parenchymal injury and lobular inflammation when feed with a choline deficient high fat diet (CD-HFD). Liver lymphocyte infiltration is also evident in association with severe steatohepatitis and fibrosis following the administration of a high fat diet to mice carrying the hepatocyte specific deficiency for T Cell Protein Tyrosine Phosphatase (TCPTP) (AlbCre;Ptpn2<sup>fl/fl</sup>), which is responsible for the de-phosphorylation of the transcription factors STAT-1, STAT-3 and STAT-5 in the nucleus (Grohmann, et al.2018). In these mice, hepatocyte STAT-1 activity favors the liver lymphocyte recruitment through an increased production chemokine CXCL9 (Grohmann, et al.2018). In this setting, reducing STAT-1 activation lowers CXCL9 expression and reduces the hepatic recruitment of activated CD4<sup>+</sup> and CD8<sup>+</sup> T-cells ameliorating fibrosis (Grohmann et al.2018).

#### **i) T-lymphocytes**

As mentioned above, the liver infiltration by helper CD4<sup>+</sup> T-lymphocytes is commonly seen in several experimental models of steatohepatitis as well as in NASH patients (Sutti, et al. 2014; Wolf, et al.2014; Weston, et al. 2015; Grohmann, et al.2018; Li, et al. 2005; Luo, et al. 2013; Inzaugarat, et al. 2011; Ferreyra, et al.2012). From the functional point of view, CD4<sup>+</sup> T lymphocytes show features of interferon- $\gamma$  (IFN- $\gamma$ )-producing T-helper 1 (Th-1) cells (Sutti, et al. 2014; Li, et al. 2005) and IFN- $\gamma$  deficient mice develop less steatohepatitis and fibrosis than wild-type littermates when fed with a methionine/choline deficient (MCD) diet (Luo, et al. 2013). The importance of CD4<sup>+</sup> Th-1 cells in NASH is supported by the clinical observations showing that both pediatric and adult NASH are characterized by an increase in liver and circulating IFN- $\gamma$ -producing CD4<sup>+</sup> T-lymphocytes (Inzaugarat, et al. 2011; Ferreyra, et al. 2012). In response to inflammatory stimuli CD4<sup>+</sup> T-lymphocytes can also differentiate to T-helper 17 (Th-17) cells which are characterized by the expression of the nuclear receptor retinoid-related orphan receptor  $\gamma$ t (ROR $\gamma$ t) and by the production of interleukin-17 (IL-17) and, to a lesser extent, IL-21, IL-22, IFN- $\gamma$  and TNF- $\alpha$  [Tang, et al.2011]. The IL-17-family (IL-17A-F) is a group of structurally related cytokines that have been implicated in the pathogenesis of both acute and chronic liver injury (Molina, et al.2018). The possible involvement of Th-17 responses in NASH has been suggested

by the observation that liver and circulating Th-17 CD4<sup>+</sup> T-cells increase in NAFLD/NASH patients in parallel with Th-1 lymphocytes (Rau, et al. 2016). Interestingly, the progression from NAFLD to NASH associates with a more pronounced liver accumulation of Th-17 cells, while all these changes normalize in the patients undergoing bariatric surgery (Rau, et al. 2016). In a similar manner, Th-17 cells and IL-17A are required for the development of fat inflammation, insulin resistance and steatohepatitis in mice over-expressing the hepatic unconventional prefoldin RPB5 interactor (URI), which is postulated to couple nutrient surplus to inflammation (Gomes, et al.2016). In these animals, the genetic ablation of the myeloid cell IL-17A receptor prevents NASH development (Gomes, et al.2016). Time-course experiments using mice fed with the MCD diet have also revealed that the number of liver Th-17 cells fluctuates during the disease evolution, peaking at the onset of steatohepatitis and then in the late phase of the disease [Rolla, et al. 2016]. Opposite variations are instead evident in intrahepatic IL-22 producing CD4<sup>+</sup> T-lymphocytes (Th-22) that are prevalent between the first and the second expansion of Th-17 cells [Rolla, et al. 2016]. An extensive hepatic infiltration of Th-22 cells is also evident in MCD-fed IL-17-deficient (IL-17<sup>-/-</sup>) mice, which display milder steatohepatitis [Rolla, et al. 2016], suggesting a possible antagonist action between the Th-17 and Th-22 lymphocyte in modulating NASH. Altogether, these data indicate a complex role of Th-17 cells in NASH that is also likely influenced by the concomitant differentiation of Th-22<sup>+</sup> CD4<sup>+</sup> T-lymphocytes as well as the possible contribution of type 3 innate lymphoid cells (ILC3) producing both IL-17A and IL-22 (Li, et al. 2017).

In addition to the changes in CD4<sup>+</sup> T-cells NAFLD/NASH evolution in either humans or rodents is accompanied by an increase in the liver prevalence of activated cytotoxic CD8<sup>+</sup> T-lymphocytes (Sutti, et al.2014; Wolf, et al. 2014; Grohmann, et al. 2018; Ghazarian, et al.2017). These cells appear to be mainly recruited in response to signals mediated by IFN- $\alpha$  (Ghazarian, et al. 2017), but their role in the disease evolution is less well characterized as compared to that of CD4<sup>+</sup> T-cells. On this respect, Ghazarian and co-workers have observed that lowering CD8<sup>+</sup> T-cells ameliorates insulin resistance and liver glucose metabolism in mice receiving a high-fat diet (Ghazarian, et al. 2017), while  $\beta 2m^{-/-}$  mice lacking CD8<sup>+</sup> T- and NKT cells are protected from both

steatosis and NASH when fed with CD-HFD diet in relation to the capacity of CD8<sup>+</sup> T- and NKT cells to produce LIGHT (wolf, et al.2014). The selective ablation of CD8<sup>+</sup> T-cells is also effective in ameliorating steatohepatitis in wild-type mice receiving a high fat/high carbohydrate (HF/HC) diet (Bhattacharjee, et al. 2017), suggesting an effective role in the pathogenesis of NASH. Nonetheless, additional studies are required to better characterize CD8<sup>+</sup> T-cell functions in relation to the disease progression.

## ii) B-lymphocytes

Beside T-cells, B-lymphocytes are detectable within inflammatory infiltrates in liver biopsies from NASH patients (Bruzzi, et al.2018; Grohmann, et al.2018). In mice models of NASH, we have observed that B-cells activate in parallel with the onset of steatohepatitis and mature to plasma blasts and plasma cells. Mice liver B-lymphocytes mainly consist of bone marrow-derived mature B220<sup>+</sup>/IgM<sup>+</sup>/CD23<sup>+</sup>/CD43<sup>-</sup> B2-cells resembling spleen follicular B-cells. However, a small fraction of B220<sup>+</sup>/IgM<sup>+</sup>/CD23<sup>-</sup>/CD43<sup>+</sup> B1-cells is also detectable (Novobrantseva, et al.2005). The functions of the two B-cell sub-sets are not overlapping, as upon antigen stimulation B1-cells mature in a T-cell independent manner to plasma cells producing IgM natural antibodies (Tsiantoulas, et al.2015). Natural antibodies are pre-existing germline-encoded antibodies with a broad specificity to pathogens, but also able to cross-react with endogenous antigens, such as oxidized phospholipids and protein adducted by end-products of lipid peroxidation (Tsiantoulas, et al.2015). Conversely, the B-2 sub-set requires helper-T cells to proliferate and to undergo antibody isotype class switching which leads to plasma cells producing highly specific IgA, IgG or IgE (Tsiantoulas, et al.2015). Previous studies have shown that B-cell can contribute to autoimmune hepatitis (Béland, et al.2015) and liver fibrogenesis (Novobrantseva, et al.2005; Thapa, et al.2015). According to Thapa and co-workers the pro-fibrogenic role of B-cells involves the production of pro-inflammatory mediators which stimulate hepatic stellate cell (HSC) and liver macrophage, while, in turn, activated HSCs support liver B-cell survival and maturation to plasma cells by secreting retinoic acid (Thapa, et al.2015). However, so far, the relevance of the above findings to the pathogenesis of NASH has not been investigated in detail.

It is noteworthy that the involvement of adaptive immunity in NASH outlined above has many analogies with the data concerning the role of lymphocytes in supporting insulin resistance and

visceral adipose tissue (VAT) inflammation in obesity (McLaughlin, et al.2017). In fact, obesity in either rodent and humans associates with an expansion and activation of VAT CD4<sup>+</sup> and CD8<sup>+</sup> T-cells, while T-cell blockage or IFN- $\gamma$  neutralization improve fat inflammation and insulin resistance (McLaughlin, et al.2017). These data can explain why in several experimental model of NASH the interference with adaptive immunity ameliorate liver lipid metabolism and steatosis by improving insulin resistance. Furthermore, they suggest the possibility that in patients with metabolic syndrome lymphocytes may support VAT and liver inflammation through similar mechanisms.

### **iii) Mechanisms possibly involved in promoting adaptive immune response in NASH.**

It is known that under physiological conditions the liver has important immunosuppressive functions inducing tolerance to autoantigens and antigens from ingested food or commensal bacteria (Rahman, et al.2013; Eckert, et al.2016). These actions are mediated by a complex network of signals involving professional antigen presenting cells (APC) such as Kupffer cells and dendritic cells as well as non-professional APC including hepatocytes, hepatic sinusoidal endothelial cells, hepatic stellate cells (HSCs) (Eckert, et al.2016). These cells present antigens to T-cells in combination with signals that lead to T-cell apoptosis, anergy or differentiation into CD4<sup>+</sup>/CD25<sup>+</sup>/Foxp3<sup>+</sup> regulatory T-cells (Tregs) (Eckert, et al.2016). Additional immuno-suppressive signals can also derive from NKT and NK cells and myeloid suppressor cells (MSCs) (Eckert, et al.2016). At present, the mechanisms responsible for triggering adaptive immunity in NASH are still poorly characterized. The issue still open regard the antigens responsible for triggering lymphocyte responses as well as how the liver immunosuppressive environment is modified to allow such responses. Regarding the first issue it is known that oxidative stress derived epitopes (OSEs) are presently implicated in the stimulation of immune reactions responsible for plaque evolution in atherosclerosis (Papac-Milicevic, et al.2016) as well as in the breaking of self-tolerance in several autoimmune diseases (Smallwood, et al.2018). OSEs include oxidized lipids and protein adduct with reactive aldehydes generated during lipid peroxidation, such as malondialdehyde (MDA) or 4-hydroxynonenal (4-HNE) and condensation products generated by the interaction between malonyl dialdehyde and acetaldehyde, known as

malonyl dialdehyde-acetaldehyde adducts (MAA) (Papac-Milicevic, et al.2016; Rolla, et al. 2000). The involvement of OSEs in driving NAFLD/NASH associated immune responses has emerged from the observations that elevated titers of anti-OSE IgG are detectable in about either adult and paediatric NAFLD/NASH patients (Nobili et al.2008; Albano, et al.2005) and that anti-OSE IgG in adult NAFLD/NASH patients target the cyclic MAA adduct methyl-1,4-dihydropyridine-3,5-dicarbaldehyde (Albano, et al.2005). Experiment in rodents have confirmed the association of humoral and cellular responses against OSEs with hepatic inflammation and parenchymal injury (Sutti, et al. 2014; Baumgardner, et al. 2008), while reducing lipid peroxidation by supplementation with N-acetylcysteine prevent antibody responses (Baumgardner, et al. 2008). Conversely, mice pre-immunized with MDA-protein adducts before receiving the MCD diet show enhanced liver lymphocyte infiltration and more severe parenchymal injury, lobular inflammation and fibrosis (Sutti, et al.2014). Such an effect involves Th-1 activation of liver CD4<sup>+</sup> T-lymphocytes which, in turn promote the M1 activation of hepatic macrophage by releasing CD40 ligand (CD154) and IFN- $\gamma$  (Sutti, et al.2014). These observations are consistent with data obtained by feeding a high-fat/cholesterol diet to Ldlr<sup>-/-</sup> mice, an established rodent model of atherosclerosis, in which OSE formation leads to NASH in combination with the development of atherosclerotic plaques. (Hendrikx, et al. 2016; Ketelhuth, et al.2016).

For an effective development of immune reactions antigens need to be presented to lymphocytes together with suitable co-stimulatory signals by the, so called, antigen presenting cells (APCs). Within the livers major APCs are represented by activated macrophages and hepatic dendritic cells (HDCs). HDCs account for less than 1% of total liver myeloid cells (Heier, et al. 2017) and are distributed within the portal areas and under liver capsule (Segura, et al.2013). Based on specific membrane markers and functional features HDCs can be distinguished into plasmacytoid and myeloid or classical subsets. Myeloid HDCs are further sub-grouped in type 1 (CD103<sup>+</sup>/CD11b<sup>-</sup> in mice; CD141<sup>+</sup>/CD14<sup>-</sup> in humans) and type 2 (CD103<sup>-</sup>/CD11b<sup>+</sup> in mice; CD1c<sup>+</sup>/CD14<sup>-</sup> in humans) cells (Heier, et al.2017; Sutti, et al. 2019). In healthy livers, HDCs have a predominant immature phenotype with low capacity to endocytose antigens and to stimulate T-lymphocytes. In these conditions HDCs produce interleukin-10 (IL-10), interleukin-27 (IL-27) and kinurenin which contribute to the tolerogenic environment of healthy livers (Tsong , et al.2007;

Tosello-Trampont, et al.2016). In response to hepatic injury HDCs expand and activate becoming efficient APCs and a source of pro-inflammatory cytokines (Ley, et al.2013). The pro-inflammatory and immune-stimulating functions of HDCs involve sub-set of cells with high lipid content, while low-lipid HDC have immuno-suppressive functions (Seijkens, et al.2014). At present, the contribution of HDCs to immune responses in NASH is still controversial. Henning and co-workers have reported that myeloid HDCs expand and activate already in the early phases of MCD-induced NASH acquiring the capacity to specifically stimulate CD4+ T-cells (Henning, et al. 2013). However, mice lacking type 1 myeloid HDC have an increased susceptibility to steatohepatitis (Liu, et al.2017), suggesting that different HDC sub-sets might have opposite roles in the disease evolution. Recently, Sutti and coworkers have proposed that monocyte derived dendritic cells (moDCs) expressing the fractalkine receptor CX3CR1 infiltrated the liver of mice with advanced NASH and contribute to hepatocyte injury (Sutti et al. 2017). Nonetheless, unspecific HDC depletion induced by the administration of diphtheria toxin in transgenic mice expressing the toxin receptor under the control of the dendritic cell marker CD11c (CD11c-DTR) does not prevent NASH-associated hepatic inflammation and liver injury (Henning, et al. 2013).

Altogether, available evidence indicates the possibility that NAFLD livers might lose their tolerogenic environment in relation to a variety of intra- and extra-hepatic stimuli. In these circumstances antigen presentation by activated HDCs, liver macrophages and other non-professional APCs within an inflammatory milieu can trigger lymphocyte stimulation. However, a better characterization of these mechanisms is needed to define the factors that influence the inter-individual variability in adaptive immune reactions among NAFLD/NASH patients.

## Aim of Project

So far, several studies have investigated the involvement of adaptive immune mechanisms in the pathogenesis of NASH/NAFLD in the attempt of characterizing their contribution in mechanism supporting the hepatic inflammation and in driving the disease evolution to fibrosis/cirrhosis and/or HCC. Nonetheless, several issues remain poorly understood as regard to the specific role of different lymphocyte subsets and the characterization of the network of cellular interactions that allow the stimulation of specific immune responses.

In my doctoral project, I have investigated some of these aspects focalizing my work on:

- a) the role of B-lymphocytes in the pathogenesis of NASH;
- b) the characterization of dendritic cells associating to NASH evolution;
- c) the role of the lymphocyte co-stimulatory signals involving ICOS/ICOSL dyad in sustaining hepatic inflammation in NASH.

These issues were addressed using experimental models of NASH based on mice feeding with methionine/choline deficient (MCD) and choline-deficient and amino acid defined (CDAA) diets which allows to reproduce liver lymphocyte responses associated to human NAFLD/NASH and as well as NASH-associated fibrosis (Pitzalis, et al.2014) and in using liver section from biopsies obtained from NAFLD/NASH patients at various stage of the disease evolution.



## Materials & Methods

*Human specimen analysis.* Liver biopsies and sera from 41 consecutive patients with NAFLD/NASH, referring to the Liver Unit of the University Hospital of Novara from 2011 to 2016, were analyzed. All samples were collected at the time of first diagnosis. Patients were characterized by anthropometric, clinical and biochemical data and liver biopsies were evaluated for the severity of steatohepatitis and fibrosis according to Kleiner et al. [24]. All subjects gave informed consent to the analysis and the study was planned according to the guidelines of the local ethical committee. The clinical and biochemical features of patients are reported in Table 1.

Table 1.

Clinical and biochemical characterization of NAFLD patients investigated.

	Patients
Patients (Male/Female)	41 (17/24)
Age (Years)	51 (47-55)
BMI	30 (28-32)
HOMA-IR (n.v. <2.5)	5.8 (1.04-14.6)
AST (U/L n.v. 5–40)	43 (36-51)
ALT (U/L n.v. 5–40)	64 (51-77)
$\gamma$ -GT (U/L n.v. 5–45)	117 (58-177)
Albumin (g/L n.v. 36-49)	39.9 (28.2-44-5)
Total $\gamma$ -globulins (g/L n.v. 9-14)	10.4 (6.7-14.1)
Fasting Glucose (mg/dL n.v. <100)	123 (112-134)
Cholesterol (mg/dL n.v. <200)	175 (160-189)
Triglycerides (mg/dL n.v. <160)	131 (113-148)
Steatosis score	2 (1-3)
Inflammation score	1 (0-2)
Balloning score	1 (0-3)
Fibrosis score	2 (0-4)
NAS score	4 (1-7)

The values are expressed as median and inter-quartile range (IQR). For histological scores the range of variability is included.

BMI, body mass index; AST, alanine aminotransferase; ALT, aspartate aminotransferase;  $\gamma$ -GT, gamma-glutamyl transpeptidase; HOMA-IR, homeostatic model assessment-insulin resistance; ISI, insulin sensitivity index; n.v., normal values; NAS, NAFLD activity score.

Serum samples from NAFLD/NASH patients together with those of 32 age/gender matched healthy subjects recruited among blood donors were investigated for the presence of IgG reactivity toward OSE by an in house enzyme-linked immunosorbent assay (ELISA) using as antigen malonyl-dialdehyde adducts with human serum albumin (MDA-HSA). Circulating interferon- $\gamma$  (IFN- $\gamma$ ) was also measured in 34 sera of these patients by commercial kits supplied by Peprotech (Milano, Italy).

*Rodent model of NASH.* Transgenic *TACI-Ig* mice on C57BL/6 background were a kind gift of Dr. A. Villunger (Division of Developmental Immunology, Biocenter, Medical University Innsbruck, Innsbruck, Austria). These mice overexpress a soluble form of the BAFF/APRIL receptor Transmembrane Activator and Cyclophilin Ligand Interactor (TACI; TNFRSF13B) fused with the Fc portion of human IgG1 and are characterized by an impaired B-cell maturation in the periphery, leading to a severe depletion of marginal zone and follicular B2-lymphocytes, but not of peritoneal B1-cells (Kleiner et al. 2005). ICOSL deficient mice (ICOSL<sup>-/-</sup>) on C57BL/6 background (B6.129P2-Icosl<sup>tm1Mak</sup>/J, stock number 004657) were obtained from Jackson Laboratories. Eight-week-old male wild type and *TACI-Ig* mice were fed *ad libitum* with either methionine/choline deficient (MCD) diet for 1 or 4 weeks or with a choline deficient and amino acid defined (CDAA) diet for 12 or 24 weeks (Laboratorio Dottori Piccioni, Gessate, Italy). Control animals received the same diets supplemented by either choline/methionine or choline alone. In the experiments using ICOSL<sup>-/-</sup> mice eight-week-old male wild type and ICOSL<sup>-/-</sup> mice were fed *ad libitum* with either the MCD for 6 weeks or a high fat/high carbohydrate diet enriched with 1,25% of cholesterol (Western Diet) for 24 weeks (Laboratorio Dottori Piccioni, Gessate, Italy). Control animals received the same diets supplemented by either choline/methionine or normal chow pellets.

In some experiments, mice receiving the MCD diet were injected intra-peritoneally with the BAFF neutralizing monoclonal mouse IgG1 Sandy-2 (Kowalczyk-Quintas et. 2016) (2  $\mu$ g/g body weight; Adipogen, Liestal, Switzerland) at the start and after two weeks of MCD diet. Control animals received isotype-matched IgG. The animals were housed at 22°C with alternating 12 hours light/dark cycles. The mice were not fasted before sample collections. In all the experiments euthanasia was performed under isoflurane anesthesia between 9 a.m. and 12 a.m. The

experimental procedures complied with the EU guidelines for animal experimentation and were approved by the Italian Ministry of Health.

*Mice model of acute liver injury.* C57BL/6 wild type and CX<sub>3</sub>CR1-deficient homozygous mice having the green fluorescent protein (gfp) inserted in the CX<sub>3</sub>CR1 gene (CX<sub>3</sub>CR1<sup>gfp/gfp</sup>) were housed in pathogen-free conditions and fed ad libitum with standard chow diet and water. Liver injury was induced by injecting intra-peritoneally eight-week-old male mice with CCl<sub>4</sub> (0.6 ml/kg in olive oil). Control animals received an injection with olive oil alone. The CX<sub>3</sub>CR1 antagonist CX3-AT (European Patent EP2913060A1) (Mionnet et al. 2010; Staumont-Sallé et al 2014) was kindly supplied by Dr V. Julia (University of Nice, France). In some experiments wild type mice received an intraperitoneal injection of CX3-AT solution in sterile saline (150 µg/mice) 24 hours after the administration of CCl<sub>4</sub>. Control animals received a similar amount of saline alone. All animals were euthanized 36 hours after CCl<sub>4</sub> administration.

*Biochemical analysis.* Plasma alanine aminotransferase (ALT) and liver triglycerides were determined by spectrometric kits supplied by Gesan Production S.r.l. (Campobello di Mazara, Italy) and Sigma Diagnostics (Milan, Italy), respectively. Circulating TNF-α was evaluated by commercial ELISA kits supplied by Peprotech (Milano, Italy). Anti-OSE IgG reactivity in mice sera was evaluated as previously reported (Sutti et al. 2014).

*Histology and immunohistochemistry.* Serial sections from paraffin-embedded human liver biopsies were immune-stained with anti-CD20 and anti-CD3 antibodies (Roche/Ventana, Tucson, AZ, USA) using Bond Polymer Refined Detection kit on the Bond Max auto-stainer (Leika Biosystems, Wetzlar, Germany). The presence of B-/T-cell aggregates was evaluated semi-quantitatively according to the size and number. Hematoxylin/eosin stained mouse liver sections were scored blindly for steatosis, lobular inflammation and fibrosis (Sutti et al. 2014). Collagen deposition was detected by Picro-Sirius Red staining. Liver activated hepatic stellate cells were evidenced in formalin-fixed sections using an α-smooth muscle actin (α-SMA) polyclonal antibody (Labvision, Bio-Optica, Milan, Italy) in combination with a horseradish peroxidase polymer kit (Biocare Medical, Concord, CA, USA). The extension of Sirius Red and α-SMA-positive areas was quantified by histo-morphometric analysis using the ImageJ software (<https://imagej.nih.gov/ij/>).

*Intrahepatic mononucleated cell isolation and flow cytometry analysis.* Liver mononucleated cells were isolated from the livers of naive and MCD-fed mice and purified on a density gradient (Lympholyte<sup>®</sup>-M, Cedarlane Laboratoires Ltd. Burlington, Canada) as described by Crispe (1996). Cells were washed with Hank's medium and incubated 30 min with de-complemented mouse serum to block nonspecific immunoglobulin binding. The cells were then stained with fluorochrome-conjugated antibodies for CD45, CD3, CD4, CD8, B220, IgM, CD69, CD23, CD43, MHCII CD11c, CD80 (eBiosciences, San Diego CA, USA), CD138 (BD Biosciences, Franklin Lakes, NJ, USA) and analyzed with a FACScalibur (Becton Dickinson, Franklin Lakes, NJ, USA) or Attune™ NxT (Thermo Fischer Scientific, Waltham, MS, USA) flow cytometers. Intracellular staining for TNF- $\alpha$ , IFN- $\gamma$  and IL-10 was performed using specific fluorochrome-conjugated antibodies (eBiosciences, San Diego CA, USA) after cell permeabilization with saponin (Permeabilization Kit, eBiosciences, San Diego CA, USA). Single cells were pre-gated on CD45<sup>+</sup>.

*Cell sorting of liver leukocytes.* Livers were digested by type IV collagenase (Worthington, USA) and intrahepatic leukocytes were isolated by multiple differential centrifugation steps according to Heymann et al. (2012). The cell preparations were then subjected to red cell lysis by Pharmlyse (BD Bioscience) and stained using combinations of the following monoclonal antibodies: CD25, I-Ab, Ly6G (BD Bioscience), CD3, CD4, CD19, CD11b, CD11c, CD45, CD80, CD40, CD88, CD26, CD35, CD105, F4-80, NK1.1, MHCII (eBioscience), CD8, CX<sub>3</sub>CR1, Ly6C, Ly6G (Biolegend). After surface staining, cells were fixed using 2% formalin and permeabilized using 0.5% saponin (Sigma). Total cell numbers were determined by adding fixed numbers of Calibrite APC beads (BD Bioscience) before measurement as internal reference (Heymann et al. 2012). Sample cell sorting FACS Aria-II cytometer (BD Bioscience). Sorted cells (20,000) were analysed using the Nanostring Immunology gene array kit covering 561 genes (NanoString Technologies, Inc), according to the manufacturer instructions. Differential gene expression was calculated using the R package DESeq2. A log<sub>2</sub> fold change threshold greater than 2 and an adjusted P value of <0.01 was used for comparison.

*mRNA extraction and Real time PCR.* Liver RNA was retro-transcribed with the High Capacity cDNA Reverse Transcription Kit (Applied Biosystems Italia, Monza, Italy) in a Tecne TC-312 thermocycler (TecneInc, Burlington NJ, USA). Real Time PCR was performed in a CFX96™ Real-time PCR System (Bio-Rad, Hercules, California, USA) using TaqMan Gene Expression Master Mix and TaqMan Gene Expression probes for mouse TNF- $\alpha$ , IL-12p40, CCL2, CXCL10, IFN- $\gamma$ , CD154, T-bet, BAFF, TREM1,  $\alpha$ 1-procollagen, TGF- $\beta$ 1,  $\alpha$ -SMA and beta-actin (Applied Biosystems Italia, Monza, Italy). All samples were run in duplicate and the relative gene expression was calculated as  $2^{-\Delta Ct}$  over that of  $\beta$ -actin gene. The values were expressed as fold increase over control samples.

*In vitro moDC differentiation from bone marrow myeloid cells.* Myeloid cells were isolated from the tibia and femur bone marrow of CX<sub>3</sub>CR1<sup>gfp/+</sup> and CX<sub>3</sub>CR1<sup>gfp/gfp</sup> mice according to [27]. Red blood cells were removed with BD FACST™ lysing solution (BD Bioscience) and the myeloid cells were cultured for seven days in RPMI-1640 medium supplemented with 10% fetal bovine serum (FBS) with or without the addition of granulocyte-macrophage colony stimulating factor (GM-CSF; 20 ng/mL) and IL-4 (10 ng/mL). In some experiments, myeloid cells isolated from wild-type mice were cultured for seven days in 10% FBS RPMI-1640 medium in the presence of fractalkine (40 ng/mL).

*Data analysis and statistical calculations.* Statistical analyses were performed by SPSS statistical software (SPSS Inc. Chicago IL, USA) using one-way ANOVA test with Tukey's correction for multiple comparisons or Kruskal-Wallis test for non-parametric values. Significance was taken at the 5% level. Normality distribution was preliminarily assessed by the Kolmogorov-Smirnov algorithm.

## Results

### Section 1

#### Characterization of the role of B-lymphocytes in NASH progression.

Data published on Free Radic Biol Med. 2018;124:249-259. doi:

10.1016/j.freeradbiomed.2018.06.015.

#### Foreword

An emerging body of evidence indicates that, besides the role of innate immune responses, NASH is also characterized by the involvement of adaptive immunity. Indeed, lobular and portal lymphocyte infiltration is a histological feature of human NASH (Wolf, et al.2014), while experimental NASH models show that CD4<sup>+</sup> and CD8<sup>+</sup> T-lymphocytes, B-lymphocytes and natural killer T-cells (NKT) are recruited within the liver in parallel with the worsening of steatohepatitis (Sutti, et al.2014; Giles, et al. 2016). T-cell subsets in NASH livers express activation markers (CD44, CD69) and show an enhanced production of interferon- $\gamma$  (IFN- $\gamma$ ), interleukin (IL)-17A, IL-17F and LIGHT, indicating that lymphocytes infiltrating the liver are functionally activated (Wolf et al.2014; Sutti, et al.2014; Giles, et al. 2016). These findings are supported by clinical observations showing that human NASH is characterized by an increase in circulating IFN- $\gamma$ -producing CD4<sup>+</sup> T-cells as well as enhanced IFN- $\gamma$  production within the liver (Inzaugarat, et al. 2011; Ferreyra Solari, et al. 2012) in relation to CD8<sup>+</sup> T- and NKT-cell infiltration (Wolf, et al.2014; Tajiri, et al. 2009). Conversely, the severity of experimental NASH is greatly lowered in Rag1<sup>-/-</sup> mice, which are unable to mount adaptive immune responses (Wolf, et al.2014). Nonetheless, in either human or experimental animals NASH is also characterized by humoral immune responses involving the production of IgG against epitopes derived from oxidative stress (OSE) (Sutti, et al. 2014; Baumgardner, et al.2008). Elevated titers of the same antibodies are detectable NAFLD/NASH patients in whom are associated with increased hepatic inflammation

(Albano, et al. 2005; Nobili, et al. 2010) and are an independent predictor of advanced fibrosis (Albano, et al. 2005). These data suggest the possibility that beside a role of T-cell in supporting steatohepatitis, B cells and humoral immunity might also play a role in the pathogenesis of NASH associated immune responses. Such a hypothesis is supported by the observation that B-lymphocytes infiltrating the adipose tissue as important players in causing insulin resistance and systemic inflammation in obesity (Sell, et al. 2012; McLaughlin, et al.2017). In more detail, B-cells isolated from visceral fat of obese mice show an increased production of pro-inflammatory cytokines, while their accumulation in the adipose tissue associates with T-cell and macrophage activation (DeFuria, et al. 2013; Winner, et al.2011, Zhang, et al. 2016). Moreover, fat inflammation and insulin resistance are lowered in mice lacking B-cells or following B-cell depletion using anti-CD20 antibodies (Zhang, et al. 2016).

From this background this work aims to investigate the role of B-lymphocytes in the pathogenesis of NASH.

## Results

### *Changes in liver B-lymphocytes during the evolution of experimental NASH*

Based on the notion that obesity promotes B-cell activation that, on its turn, influences insulin resistance and systemic inflammation (Sell, et al. 2012; McLaughlin, et al.2017), for studying the role of B cells in NASH tackled the problem by using an obesity-independent models of steatohepatitis based on the administration of a methionine/choline deficient (MCD) (Mackay, et al. 2009). Such a model was also chosen because, according to previous studies, it reproduces liver lymphocyte responses associated to human NAFLD/NASH (Wolf et al.2014; Sutti, et al. 2014) and is characterized by an early development of liver inflammation which is already appreciable after one week of treatment and further progresses in the following weeks (Fig. 1).

Flow cytometry analysis of liver myeloid cells revealed that the onset of steatohepatitis in mice receiving the MCD diet for one week was associated with a significant decline in the number of IgM<sup>+</sup>/B220<sup>+</sup> hepatic B-lymphocytes (Fig. 2A). Such an effect specifically involved the fraction of B220<sup>+</sup>/CD43<sup>-</sup>/CD23<sup>+</sup> B2-lymphocytes, while the pool of B220<sup>+</sup>/CD43<sup>+</sup>/CD23<sup>-</sup> B1-cells was unmodified (Fig. 2B). Liver B-cell lowering was accompanied by a concomitant up-regulation in the expression of the early lymphocyte activation marker CD69 among B220<sup>+</sup> cells (Fig. 2C).

In the same animals, we also detected the expansion of B220<sup>+</sup>/CD138<sup>+</sup> plasma blasts and B220<sup>-</sup>/CD138<sup>+</sup> plasma cells (Fig. 3A) and an increase in the titers of circulating anti-OSE IgG (Fig. 3C), without changes in IgM reactivity against the same antigens (Fig. 3D), indicating B2-cell maturation toward IgG-producing plasma cells. B-cell responses in NASH were associated to the up-regulation in the liver expression of B-cell Activating Factor (BAFF; TNFSF13b), one of the cytokines regulating B-cell survival and maturation (Mackay, et al. 2009) (Fig. 3D). No changes were instead observed for the other B-cell regulating cytokine A Proliferation Inducing Ligand (APRIL; TNFSF13) (Fig. 3E).



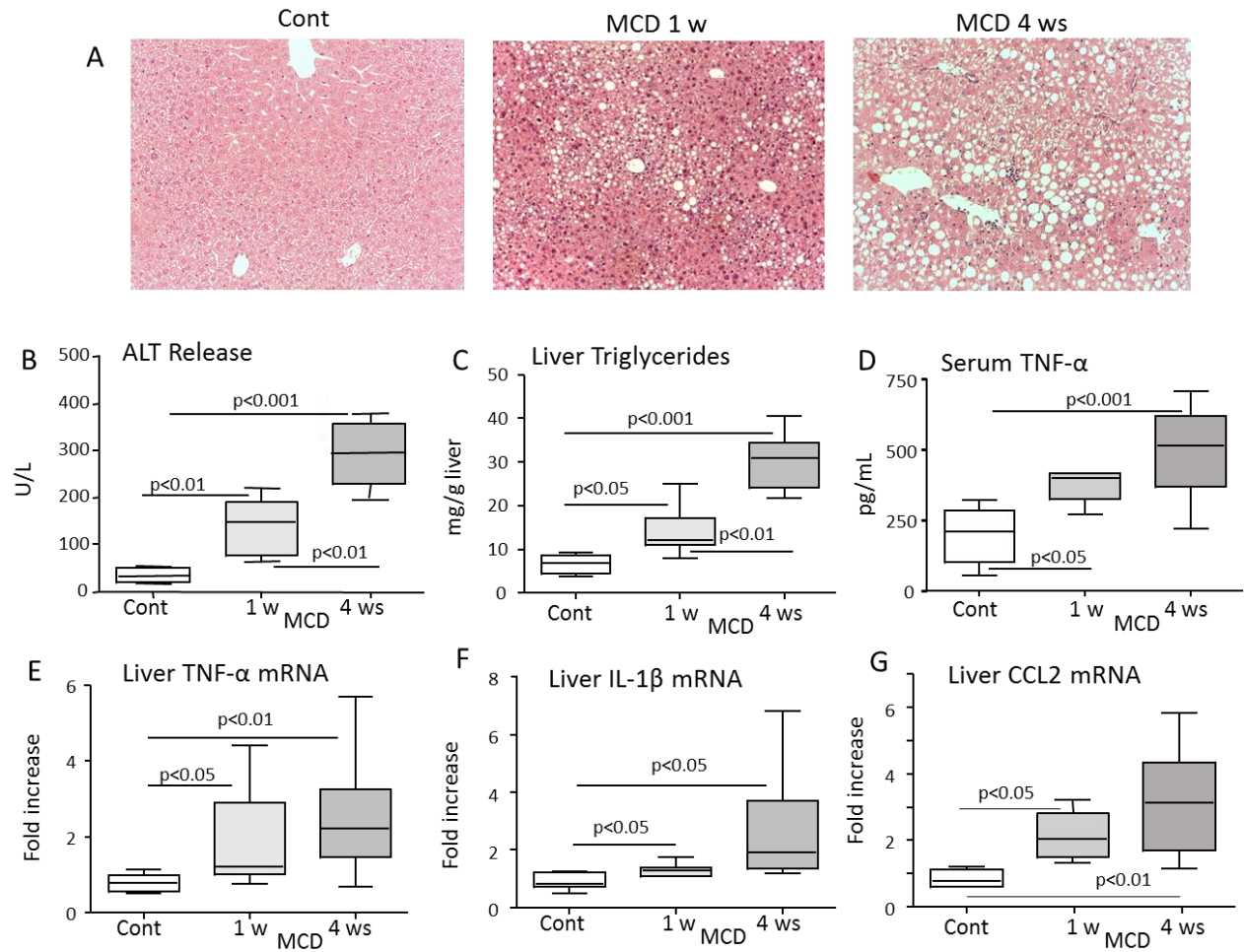


**Figure 1:** Time dependent variations of hepatic injury and inflammation during the evolution of NASH induced by mice feeding with a methionine/choline deficient (MCD) diet.

Wild type C57BL/6 mice received MCD or control diets for up to 4 weeks. (A) Hematoxylin/eosin staining of liver sections (magnification 200x). (B-C) Alanine aminotransferase (ALT) release and hepatic triglyceride content. (Panel D) Immuno-enzymatic determination of circulating TNF- $\alpha$ . (E-G) The hepatic mRNA levels of pro-inflammatory mediators TNF- $\alpha$ , IL-1 $\beta$  and CCL2. RT-PCR values are expressed 2 as fold increase over control values after normalization to the  $\beta$ -actin gene. The values refer to 8-9 animals per group and the boxes include the values within 25<sup>th</sup> and 75<sup>th</sup> percentile, while the horizontal bars represent the medians. The extremities of the vertical bars (10<sup>th</sup>-90<sup>th</sup> percentile) comprise 80 percent of the values.

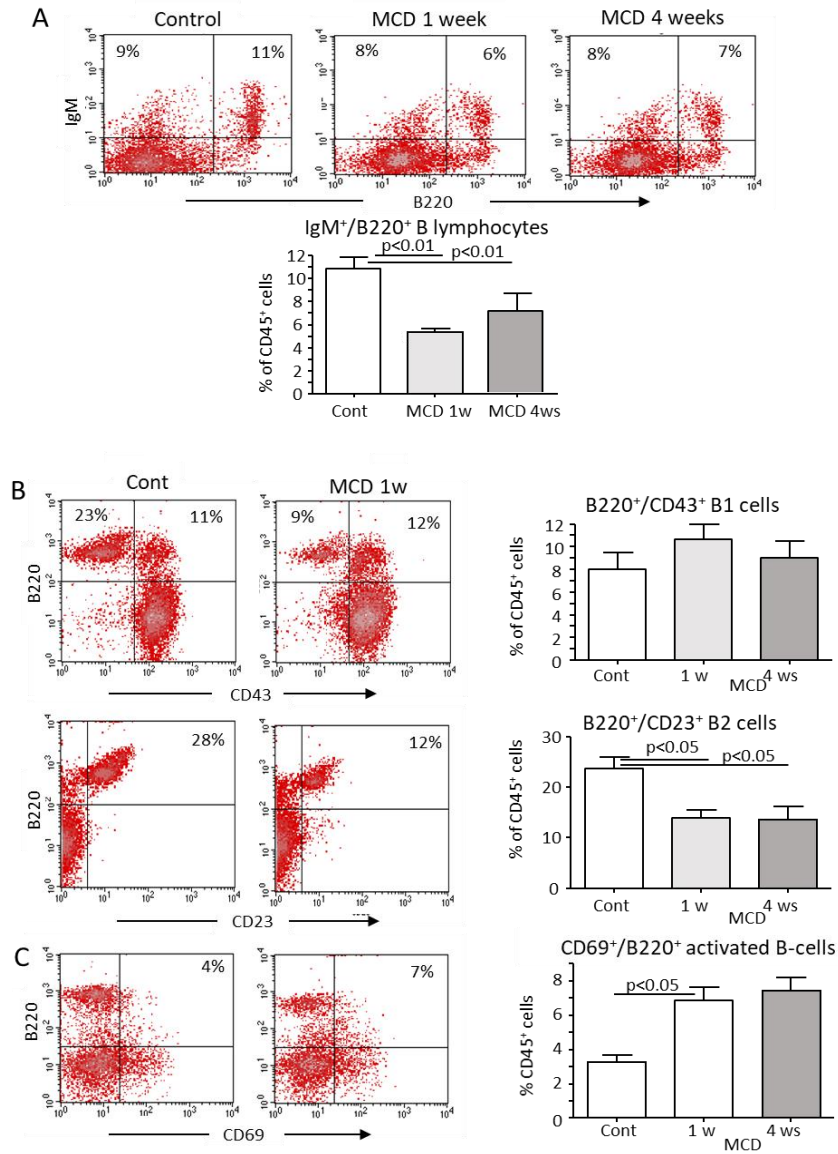


**Figure 2:** Changes in liver B-cells during the evolution of experimental NASH.

Wild type mice were fed with the MCD diet for either 1 or 4 weeks. The intrahepatic distribution of B-lymphocytes was evaluated by flow cytometry. (A) Changes in the liver distribution of total IgM<sup>+</sup>/B220<sup>+</sup> B-lymphocytes at different stages of NASH evolution. (B) Changes in the liver distribution of B220<sup>+</sup>/CD43<sup>+</sup>/CD23<sup>-</sup> B1- and B220<sup>+</sup>/CD43<sup>-</sup>/CD23<sup>+</sup> B2-lymphocytes at different stages of NASH evolution. (C) Increase of activated intrahepatic B-cells expressing CD69 at the onset of steatohepatitis. The values are means ± SD of cell preparation from 3 animals per group.

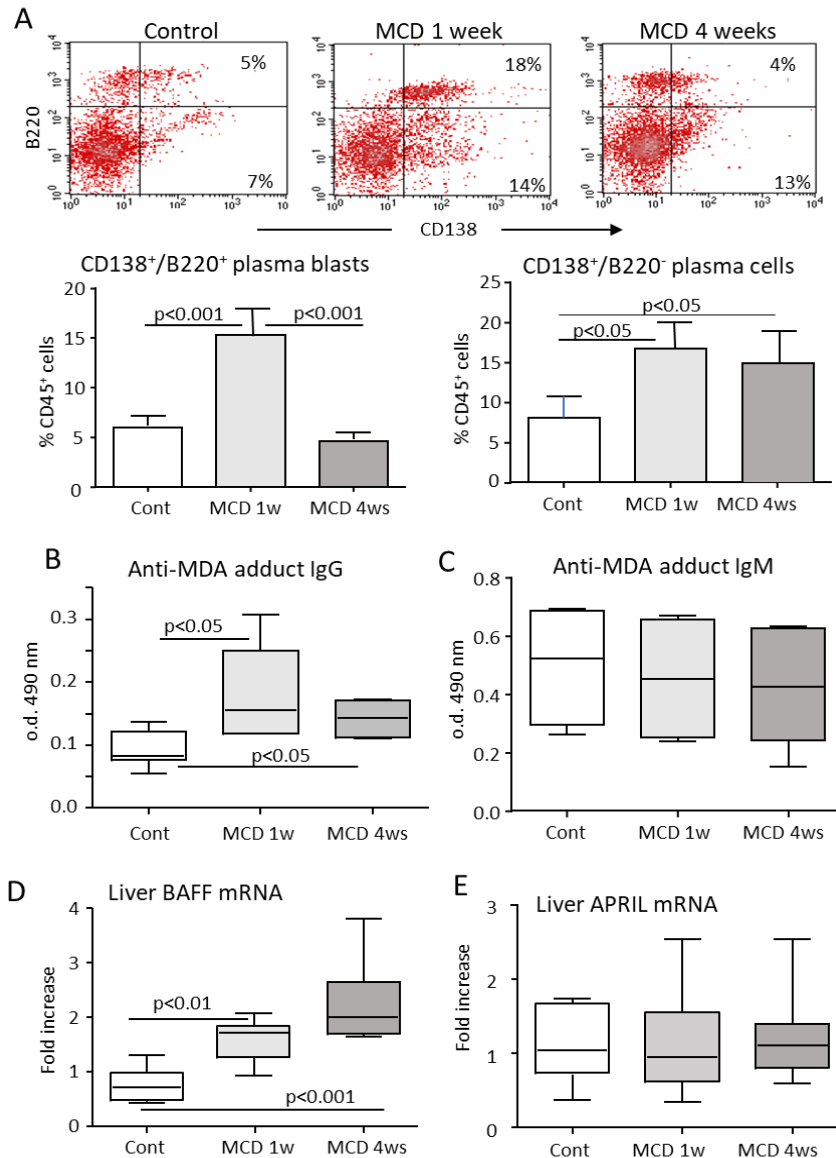


**Figure 3:** B cell responses associated with the evolution of NASH.

Wild type mice were fed with the MCD diet for either 1 or 4 weeks. The intrahepatic distribution of plasma blasts and plasma cells were evaluated by flow cytometry in parallel with the production of IgG targeting OSE and the liver expression of BAFF. (A) Changes in the liver distribution of total IgM<sup>+</sup>/B220<sup>+</sup> B-lymphocytes at different stages of NASH evolution. (B) The changes in anti-OSE antibody titres, were measured by IgG and IgM targeting malonyl-dialdehyde (MDA) adducts in the sera of mice with NASH. (D-E) Real Time PCR analysis of hepatic BAFF and APRIL expression, as measured by RT-PCR analysis, during the evolution of steatohepatitis. The values in are means  $\pm$  SD of 8-10 animals per group and the boxes include the values within 25<sup>th</sup> and 75<sup>th</sup> percentile, while the horizontal bars represent the median. The extremities of the vertical bars (10<sup>th</sup>-90<sup>th</sup> percentile) include 80% of the values.

It is well known that B-lymphocytes can act as antigen presenting cells for CD4<sup>+</sup> T-cells through the expression of class II Major Histocompatibility Complex (MHCII) and costimulatory molecules (Zhang, et al. 2016). Time-course experiments revealed that an early up-regulation of MHCII among CD138<sup>+</sup> plasma blasts and plasma cells (Supplementary Fig. 4 A). Furthermore, B-cell activation preceded the liver recruitment/activation of both CD4<sup>+</sup> and CD8<sup>+</sup> T-lymphocytes as well as the up-regulation of liver mRNAs for the Th-1 activation markers IFN- $\gamma$ , T-bet and CD40 ligand (CD154) (Fig. 4B & C).

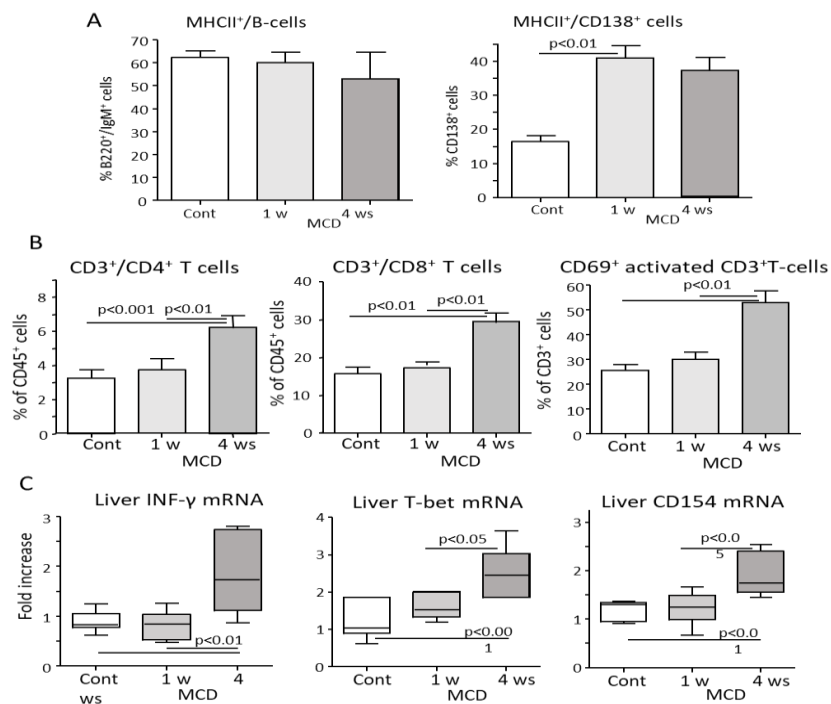


**Figure 4:** The development of the antigen presentation capability of B cells precedes T cell responses in NASH.

Wild type mice were fed MCD or control diets for either 1 or 4 weeks. B cell expression of class II Major Histocompatibility Complex (MHCII) by liver B-cells was evaluated by flow cytometry in parallel with the prevalence of CD3<sup>+</sup> T-lymphocytes, the lymphocyte activation marker CD69 and the hepatic expression of Th-1 activation markers. (A) Changes in the expression of MHCII by liver IgM<sup>+</sup>/B220<sup>+</sup> B-cells and CD138<sup>+</sup> plasma blasts and plasma cells during NASH evolution. The values are means  $\pm$  SD of cell preparation from 3 animals per group. (B) Changes in the liver distribution of CD4<sup>+</sup> and CD8<sup>+</sup> T-lymphocytes and their expression of CD69 during NASH evolution. The values are means  $\pm$  SD of cells preparation from 3-4 animals per group. (C) Hepatic mRNA levels of interferon- $\gamma$  (IFN- $\gamma$ ), T-bet, and CD40 ligand (DC154). RT-PCR values are expressed as fold increase over control values after normalization to the  $\beta$ -actin gene. The values refer to 5-6 animals per group and the boxes include the values within 25<sup>th</sup> and 75<sup>th</sup> percentile, while the horizontal bars represent the medians. The extremities of the vertical bars (10<sup>th</sup>-90<sup>th</sup> percentile) comprise 80% of the values.

*B2-lymphocyte deficiency interferes with the onset of immune response in NASH*

To investigate the possible role of B2-lymphocytes in modulating NASH-associated T-cell responses, we took advantage of transgenic *TACI-Ig* mice that overexpress a soluble form of the BAFF/APRIL receptor TACI and are characterized by the selective depletion of B2-lymphocytes (Schneider, et al. 2001). In our hands, *TACI-Ig* mice showed a marked lowering of hepatic B-cells specifically involving the B220<sup>+</sup>/CD43<sup>-</sup>/CD23<sup>+</sup> B2-subset (Fig. 5A). Conversely, no significant changes were appreciable in the fraction of B220<sup>+</sup>/CD43<sup>+</sup>/CD23<sup>-</sup> B1-cells (Fig. 5B).

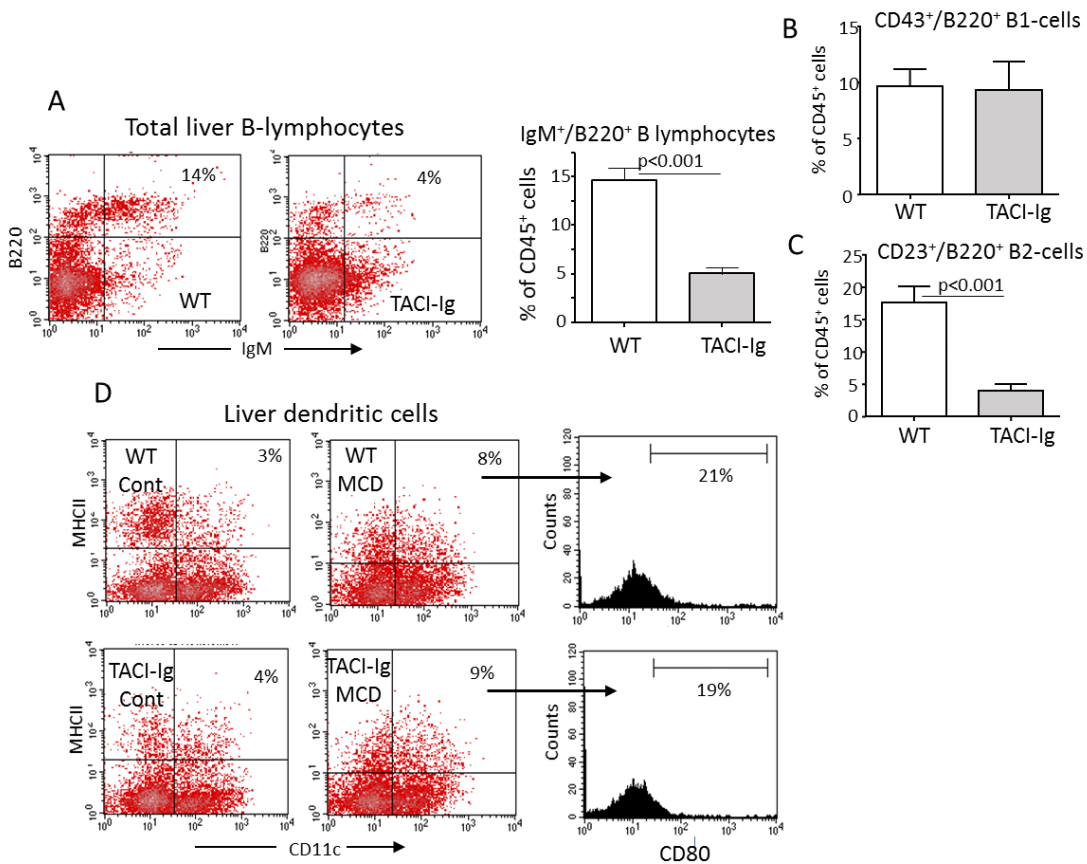


**Figure 5:** Characterization of hepatic B-cells and dendritic cells in *TACI-Ig* mice.

Untreated wild-type (WT) and *TACI-Ig* mice were investigated by flow cytometry. (A) Liver distribution of total IgM<sup>+</sup>/B220<sup>+</sup> B-lymphocytes. (B-C) and the relative prevalence of B220<sup>+</sup>/CD43<sup>+</sup> B1- and B220<sup>+</sup>/CD23<sup>+</sup> B2-subsets. (D) Evaluation of the fraction of CD11c<sup>+</sup>/MHCII<sup>+</sup> hepatic dendritic cells and their expression of the activation marker CD80 in WT and *TACI-Ig* mice receiving the MCD diet for 4 weeks mice.

In subsequent experiments NASH was induced in *TACI-Ig* mice by feeding the MCD diet for 4 weeks. We observed that liver plasma cell maturation, as well as the production of anti-OSE IgG, were impaired in *TACI-Ig* mice as compared to wild-type littermates (Fig. 6A-B). In line with a role of B2-cells in promoting T-cell responses, the liver recruitment of CD4<sup>+</sup> and CD8<sup>+</sup> T-lymphocytes, as well as their CD69 expression, were significantly reduced in *TACI-Ig* mice receiving the MCD diet (Fig. 6C-D), in spite the expansion and activation of hepatic dendritic cells were not affected (Fig. 5C). Moreover, the hepatic expression of Th-1 activation markers IFN- $\gamma$ , CD154 and T-bet was also decreased in *TACI-Ig* mice (Fig. 6E). These effects were specific for liver immune responses associated with NASH, as no difference in the development of anti-OSE immunity were evident between wild-type and *TACI-Ig* mice following immunization with bovine serum albumin complexed with malonyl-dialdehyde (Fig. 7).

#### *Effects of BAFF neutralization ameliorates the evolution of NASH*

The evaluation of the severity of NASH in *TACI-Ig* mice showed that the lack of B2-cells appreciably ameliorated lobular inflammation score ( $2.3 \pm 0.5$  vs  $1.6 \pm 0.5$ ;  $p < 0.05$ ) and the prevalence of necrotic foci ( $7.3 \pm 3.31$  vs  $4.0 \pm 1.3$ ;  $p < 0.05$ ) without affecting the extension of steatosis ( $2.8 \pm 0.4$  vs  $2.5 \pm 0.5$ ;  $p = 0.39$ ). These observations suggested the possibility that B-cell activation in the early phase of NASH might be critical for the further evolution of the disease. In line with that previous studies have shown that circulating levels of BAFF are higher in patients with NASH than in those with simple steatosis, and correlate with the severity of steatohepatitis and fibrosis (Mackay, et al. 2009). Thus, in further experiments we investigated the effects of interfering with BAFF on the evolution of steatohepatitis taking advantage of a BAFF neutralizing monoclonal antibody Sandy-2 (Kowalczyk-Quintas, et al. 2016). Preliminary tests demonstrated that the treatment for one week with Sandy-2 ( $2 \mu\text{g/g}$  body weight) reduced by about 40% circulating and liver B-cells, specifically affecting the B2-subset (Fig. 8A-B). Accordingly, the administration of Sandy-2 prevented liver plasma cell maturation in mice fed with the MCD diet for 1 week (Fig. 8C). From these data we went on testing the effect of Sandy-2 on the severity to NASH by injecting Sandy-2 mAb ( $2 \mu\text{g/g}$  body weight) or isotype-matched IgG at the start of MCD diet administration and then after 2 weeks. In the animals receiving the MCD diet for 4

weeks, BAFF neutralization ameliorated histological scores for steatosis ( $2.8 \pm 0.4$  vs  $1.7 \pm 0.8$ ;  $p < 0.05$ ) and lobular inflammation ( $2.7 \pm 0.5$  vs  $1.8 \pm 0.4$ ;  $p < 0.05$ ) as well as ALT release and liver triglycerides (Fig. 9 A-C). Differently from what observed in TACI-Ig mice, Sandy-2 treatment did not appreciably affect the prevalence of liver infiltrating CD4<sup>+</sup> and CD8<sup>+</sup> T-cells (not shown). Nonetheless, Th-1 activation of liver CD4<sup>+</sup> T-lymphocytes, as evaluated by IFN- $\gamma$  production, was significantly lowered by Sandy-2 treatment (Fig. 9D). BAFF blockage also decreased the hepatic expression of pro-inflammatory mediators such as TNF- $\alpha$ , IL-12 and CXCL10 (Fig. 9E).

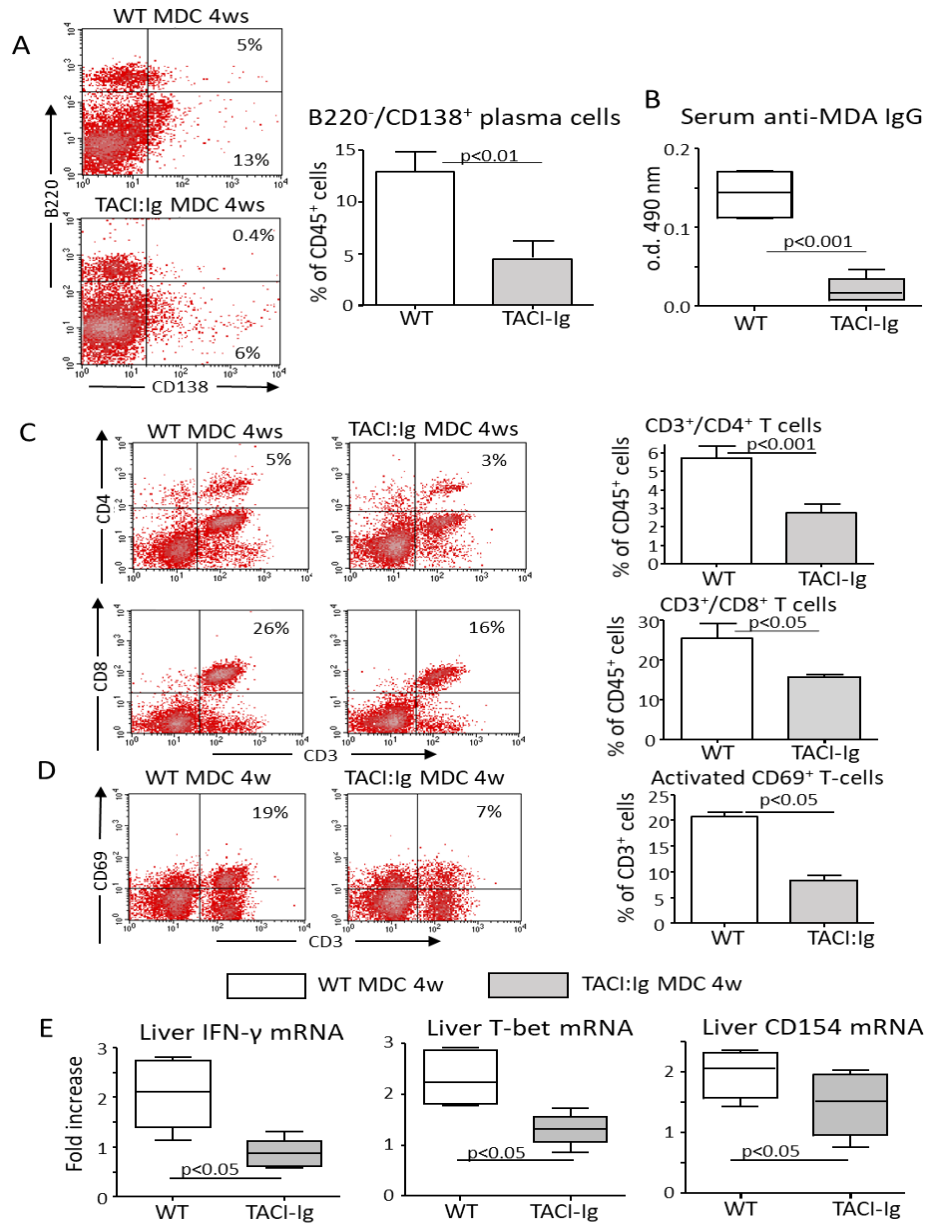


**Figure 6:** B2-lymphocyte deficiency interferes with the onset of immune responses in NASH.

B2-cell deficient *TACI-Ig* and wild type mice were fed with control or MCD diet for 4 weeks. The intrahepatic distribution of T-lymphocytes and plasma cells was evaluated by flow cytometry in parallel with the production of IgG targeting OSE and the liver expression of Th-1 activation markers. (A) Effect of B2-cell depletion on the liver expansion of B220<sup>+</sup>/CD138<sup>+</sup> plasma cells and (B) the increase of circulating anti-OSE antibody titres, as measured by IgG targeting malonyl-dialdehyde (MDA) adducts. (C) The liver distribution of CD4<sup>+</sup> and CD8<sup>+</sup> T-lymphocytes and (D) their expression of the activation marker CD69 in *TACI-Ig* and wild-type mice with NASH. The values in panels A-C are means  $\pm$  SD of three different experiments with 3-4 animals for each group. (E) Down-modulation in the expression of Th-1 activation markers interferon- $\gamma$  (IFN- $\gamma$ ), T-bet and CD40 ligand (CD154) in the liver of *TACI-Ig* mice. The values of RT-PCR analysis are expressed as fold increase over their relative controls and are means  $\pm$  SD of 8-10 animals per group. The boxes in panels B and E include the values within 25<sup>th</sup> and 75<sup>th</sup> percentile, while the horizontal bars represent the median. The extremities of the vertical bars (10<sup>th</sup>-90<sup>th</sup> percentile) include 80% of the values.



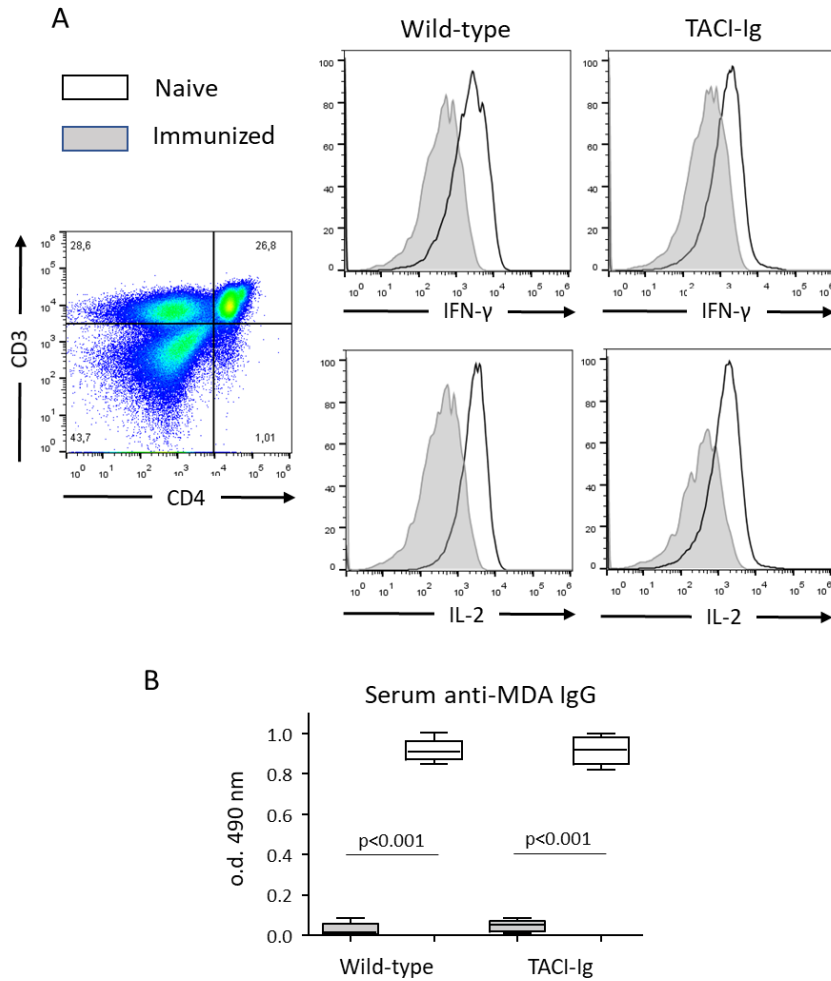


**Figure 7:** B2-cell deficiency in *TACI-Ig* mice does not affect the development of anti-OSE immunity.

Wild-type and *TACI-Ig* mice were immunized with bovine serum albumin adducted with malonyldialdehyde (MDA) and incomplete Freund's adjuvant as previously reported [10]. (A) Lymphocytes were isolated from spleens of naïve and immunized animals and the production of IFN- $\gamma$  and IL-2 by CD4<sup>+</sup> T-lymphocytes was evaluated by flow cytometry. One experiment representative of two. (B) Circulating IgG targeting MDA adducts were measured by ELISA assay in the sera of the same animals. The bars represent medians  $\pm$  S.D.

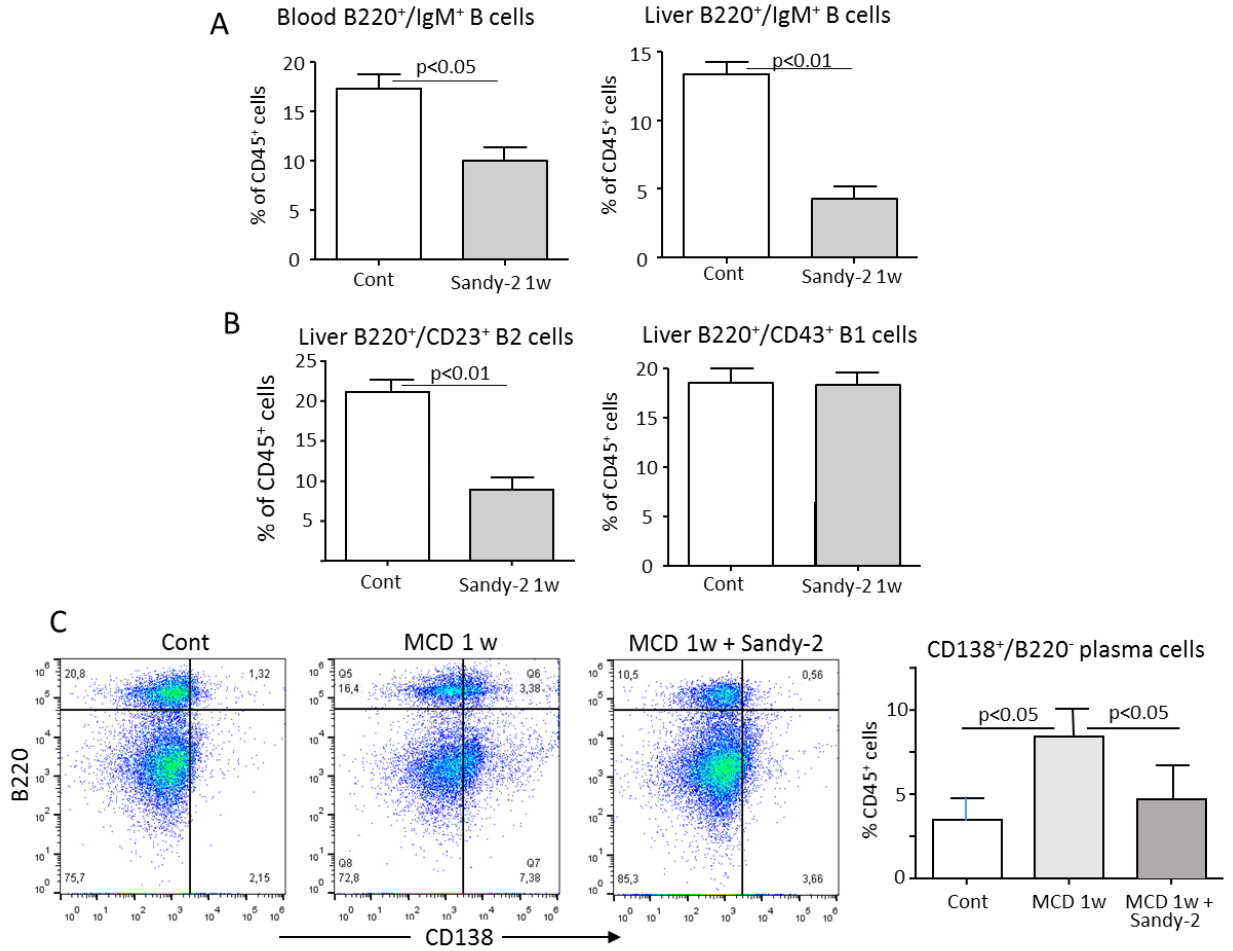


**Figure 8:** Effects of BAFF-neutralizing monoclonal antibody Sandy-2 on circulating and hepatic B cells.

Wild type mice received one injection of Sandy-2 mAb or isotype-matched IgG and B-cell distribution was evaluated by flow cytometry one week after the treatment. (A) Total circulating and liver IgM<sup>+</sup>/B220<sup>+</sup> B-lymphocytes. (B) The relative prevalence of liver B220<sup>+</sup>/CD43<sup>+</sup> B1- and B220<sup>+</sup>/CD23<sup>+</sup> B2-subsets. (C) Effect of Sandy-2 administration on plasma cell expansions in mice fed with either control or MCD diets for one week. The values refer to 4-5 animals per group.

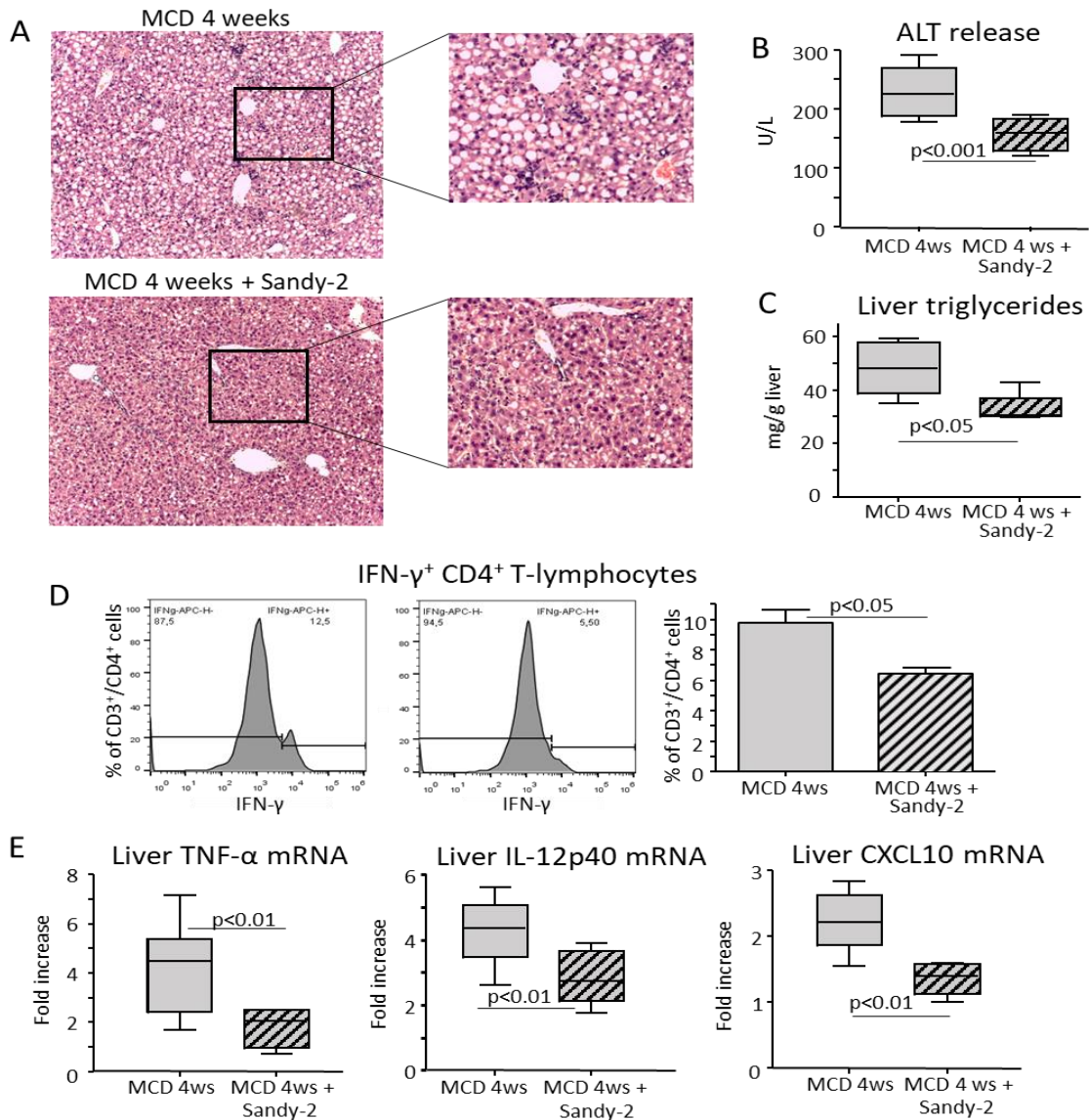


**Figure 9:** Mice treatment with the BAFF-neutralizing antibody Sandy-2 ameliorates steatohepatitis.

Wild type mice were injected with Sandy-2 mAb (2  $\mu$ g/g body weight) or isotype-matched IgG at the start and after 2 weeks of MCD diet. (A) Haematoxylin/eosin staining of liver sections (Magnification 200x). (B) Alanine aminotransferase (ALT) release and (C) liver triglyceride content. (D) Flow cytometry evaluation of interferon- $\gamma$  (IFN- $\gamma$ ) production by CD3<sup>+</sup>/CD4<sup>+</sup> helper T-lymphocytes. The values are means  $\pm$ SD of three different experiments with 4 animals per group. The hepatic mRNA levels of (E) pro-inflammatory mediators TNF- $\alpha$ , IL-12p40 and CXCL10. RT-PCR values are expressed as fold increase over control values after normalization to the  $\beta$ -actin gene. The values in the panels B, C and E refer to 6-7 animals per group and the boxes include the values within 25<sup>th</sup> and 75<sup>th</sup> percentile, while the horizontal bars represent the median. The extremities of the vertical bars (10<sup>th</sup>-90<sup>th</sup> percentile) include 80% of the values.

### *Role of B-lymphocyte in NASH progression to fibrosis*

Besides the improvement of hepatic inflammation, MCD-fed mice receiving Sandy-2 showed a descending trend in the expression of pro-fibrotic markers  $\alpha$ 1-procollagen and  $\alpha$ -smooth muscle actin ( $\alpha$ -SMA), although the differences did not reach statistical significance (not shown). Thus, in additional experiments we investigated whether lack of B2 cell might also improve NASH evolution to fibrosis. Since keeping mice under the MCD diet to the time required for the development of hepatic fibrosis leads to severe weight loss, we switched to a different experimental model of NASH based on mice feeding with a choline-deficient and amino acid defined (CDAA) diet that allows development of NASH associated fibrosis without causing severe malnutrition (Winer, et al. 2011). For the experiments wild-type and *TACI-Ig* mice were fed with CDAA diet. Preliminary experiments using WT mice receiving the CDAA diet for 12 weeks showed that the development of steatohepatitis was associated with the lowering of liver B-cell and an expansion of the plasma cell as observe with MCD-induced NASH (Fig. 10). For evaluating whether the lack of B2-lymphocytes would affect the fibrogenic evolution of NASH in subsequent experiments WT and *TACI-Ig* mice were fed the CDAA for 24 weeks. We observed that CDAA-fed *TACI-Ig* mice had hepatic expression of  $\alpha$ 1-procollagen,  $\alpha$ -SMA and Transforming Growth Factor- $\beta$ 1 (TGF- $\beta$ 1) significantly lower than wild-type littermates (Fig. 11A). Consistently, Sirius Red staining for collagen and the prevalence of  $\alpha$ -SMA-positive activated hepatic stellate cells were also significantly reduced in *TACI-Ig* mice (Fig. 11 B-D). The improvement of fibrosis observed in CDAA-fed *TACI-Ig* mice was accompanied by an improvement in the severity of steatohepatitis as indicated by the lowering of transaminases release and in the markers of lobular inflammation (Fig. 12), supporting the importance of B-cells in the mechanisms leading to steatohepatitis progression.

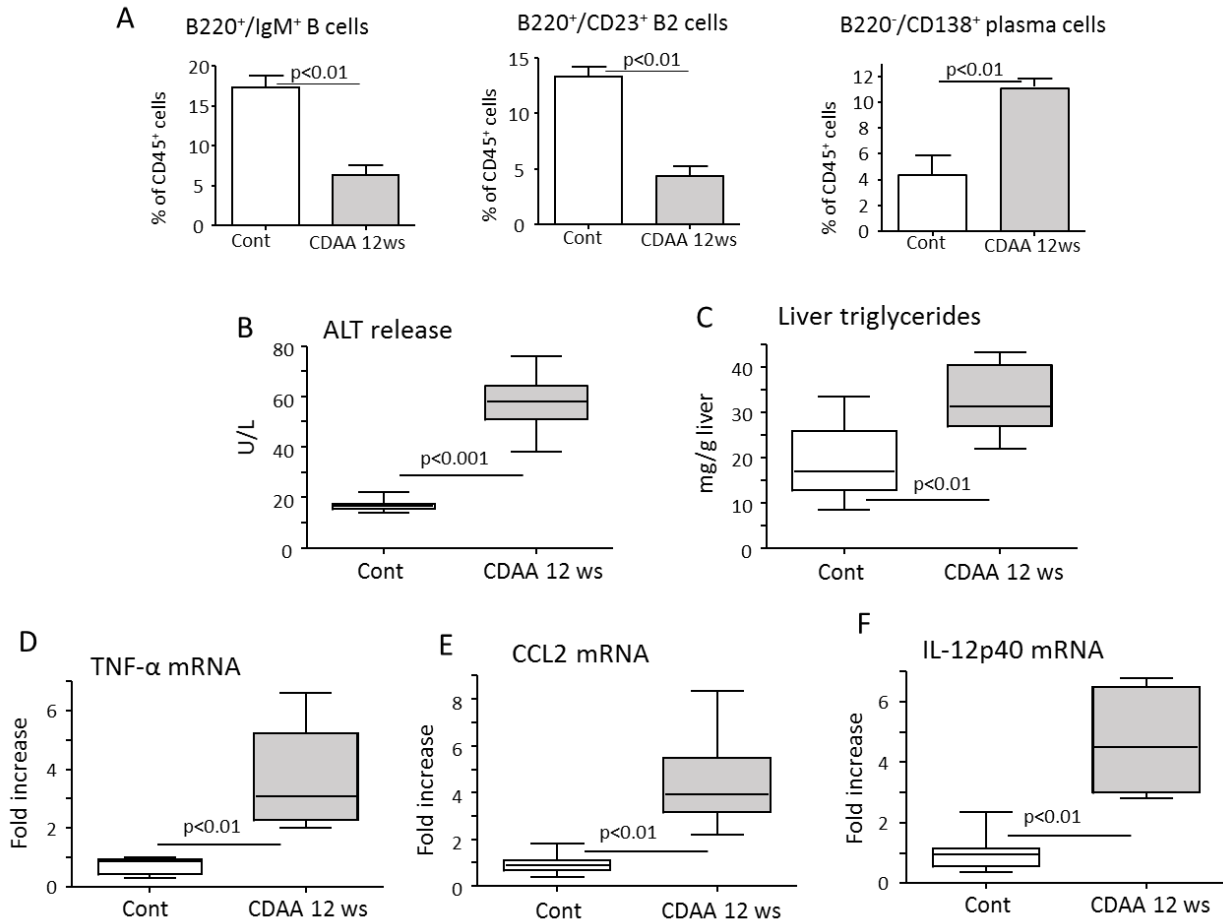


**Figure 10:** B-cell responses in experimental NASH induced by choline-deficient amino acid defined (CDAA) diet.

Wild type mice were fed with CDAA or control diets for 12 weeks. The intrahepatic distribution of B-lymphocytes, plasma blasts and plasma cells were evaluated by flow cytometry along with the development of liver injury and inflammation. (A) Liver distribution of total IgM<sup>+</sup>/B220<sup>+</sup> B-lymphocytes, B220<sup>+</sup>/CD23<sup>+</sup> B2-cells and B220<sup>-</sup>/CD138<sup>+</sup> plasma cells. (B-C) Alanine aminotransferase (ALT) release and hepatic triglyceride content as determined by enzymatic methods. (D-F) Hepatic mRNA levels of pro-inflammatory mediator TNF- $\alpha$ , IL-12p40 and CCL2. RT-PCR values are expressed as fold increase over control values after normalization to the  $\beta$ -actin gene. The values refer to 6-7 animals per group and the boxes include the values within 25<sup>th</sup> and 75<sup>th</sup> percentile, while the horizontal bars represent the medians. The extremities of the vertical bars (10<sup>th</sup>-90<sup>th</sup> percentile) comprise 80% of the values.

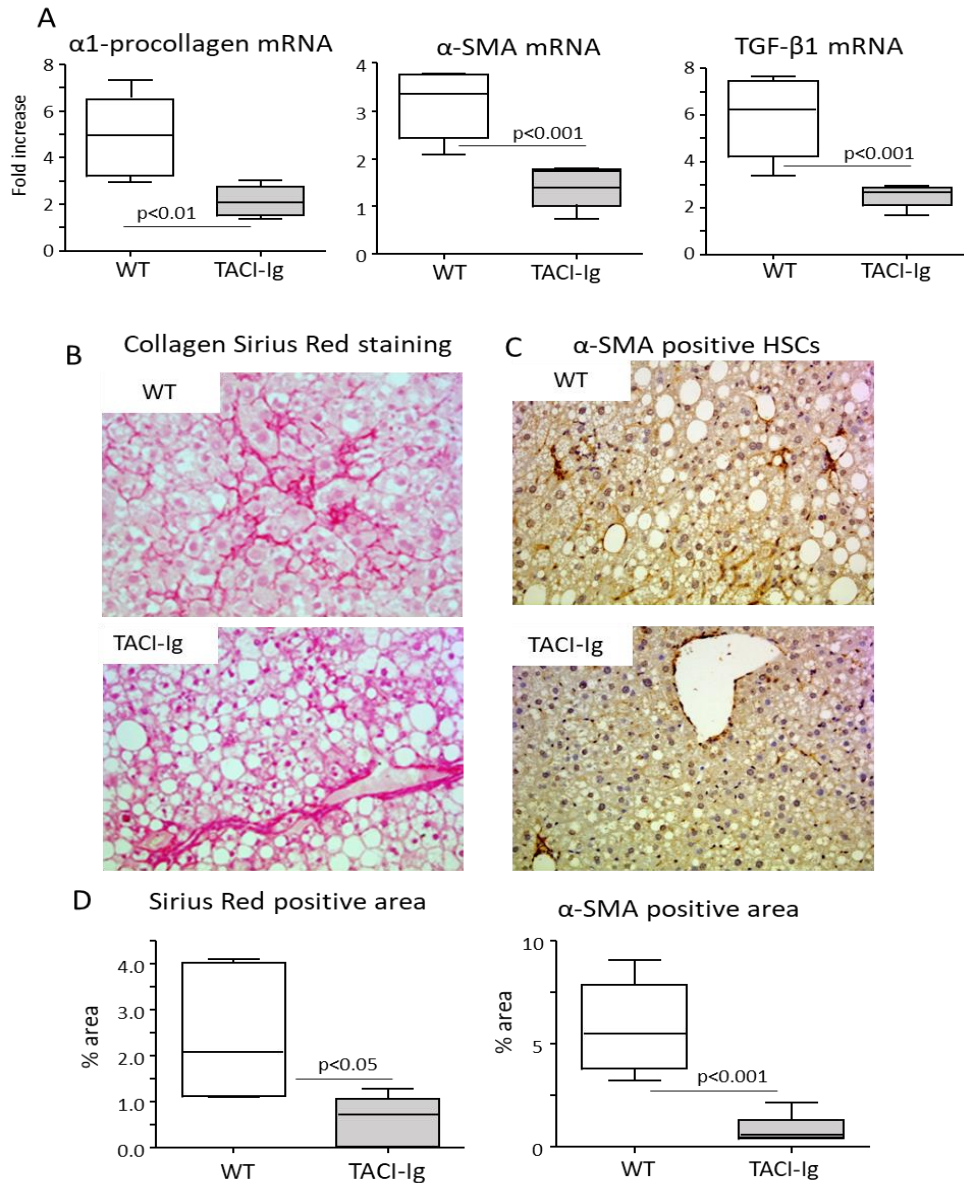


**Figure 11:** B2-lymphocyte deficiency reduces NASH evolution to fibrosis.

*TACI-Ig* and wild type (WT) mice were fed with either control or CDAA diets for 24 weeks. (A) Hepatic expression of fibrogenesis markers  $\alpha 1$ -procollagen,  $\alpha$ -smooth muscle actin ( $\alpha$ -SMA) and Transforming Growth Factor- $\beta 1$  (TGF- $\beta 1$ ). RT-PCR values are expressed as fold increase over control values after normalization to the  $\beta$ -actin gene. (B) Collagen deposition as detected by Sirius Red staining in representative liver sections from 24-week CDAA diet in WT and *TACI-Ig* mice (Magnification 200x). (C) Immuno-histochemical staining for  $\alpha$ -SMA-positive hepatic stellate cells (HSCs) liver sections from 24-week CDAA diet in WT and *TACI-Ig* mice (Magnification 200x). (D) Histo-morphometric analysis of Sirius Red and  $\alpha$ -SMA positive areas. The values refer to 5-7 animals per group and the boxes include the values within 25<sup>th</sup> and 75<sup>th</sup> percentile, while the horizontal bars represent the median. The extremities of the vertical bars (10<sup>th</sup>-90<sup>th</sup> percentile) include 80% of the values.

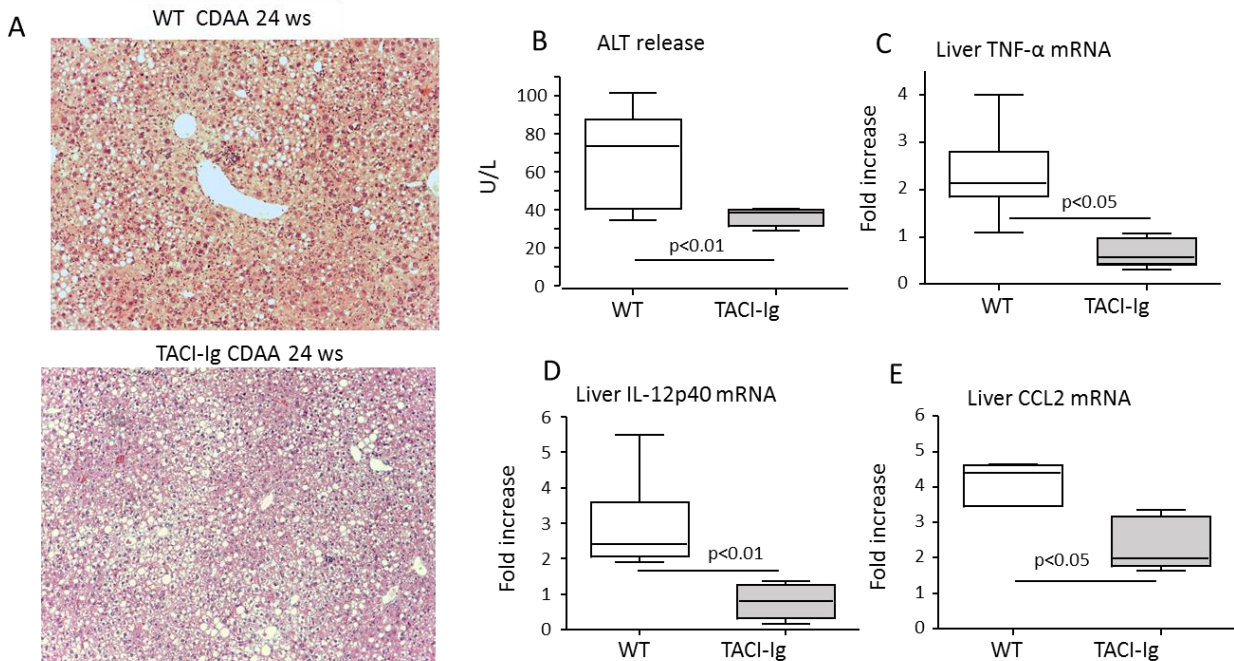


**Figure 12:** B2-cell deficiency in *TAC1-Ig* mice ameliorates experimental NASH induced by choline-deficient amino acid defined (CDAA) diet.

Wild-type (WT) and *TAC1-Ig* mice were fed with CDAA or control diets for 24 weeks. (A) Hematoxylin/eosin staining of liver sections (magnification 200x). (B) Alanine aminotransferase (ALT) release. (C-E) Hepatic mRNA levels of TNF- $\alpha$ , IL-12p40 and CCL2. RT-PCR values are expressed as fold increase over control values after normalization to the  $\beta$ -actin gene. The values refer to 6-7 animals per group and the boxes include the values within 25<sup>th</sup> and 75<sup>th</sup> percentile, while the horizontal bars represent the medians. The extremities of the vertical bars (10<sup>th</sup>-90<sup>th</sup> percentile) comprise 80% of the values.

#### *B- and T-lymphocyte responses in human NASH.*

From the data obtained with the animal models, we sought to evaluate the role of liver B-cells and humoral immunity in human NASH. We previously reported that NAFLD/NASH patients have humoral immunity against epitopes generated as a result of oxidative stress (oxidative stress derived epitopes; OSE) (Nobili, et al. 2010; Sell, et al. 2012). These findings were confirmed in the present study by measuring circulating IgG targeting MDA-derived adducts in a new cohort of 41 patients (17 male/24 female) with histological diagnosis of NAFLD/NASH. Among these patients, 10 (24%) had steatosis only, 7 (17%) steatosis with mild lobular inflammation, while the remaining 24 (59%) had NASH with variable degrees of fibrosis. As shown in Figure 13A, 18 (43%)

of NAFLD/NASH patients had titers of anti-OSE IgG above the control threshold. Furthermore, in agreement with previous observations (Albano, et al. 2005), the prevalence of advanced fibrosis or cirrhosis (staging  $\geq 2$ ) was higher among the subjects with elevated anti-OSE IgG as compared to those with anti-OSE reactivity within the control range (OR=3.25; 95% CI 1.03-15;  $p=0.05$ ). The involvement of immune response in these patients was supported by the measurement of serum interferon- $\gamma$  (IFN- $\gamma$ ) which show values significantly higher than healthy subjects (Fig. 13B). Interestingly, among NAFLD/NASH patients those showing high anti-OSE IgG reactivity also displayed higher levels of circulating IFN- $\gamma$  (Fig. 13C) and serum IFN- $\gamma$  positively correlated with the severity of fibrosis (Spearman  $r=0.59$ ; 95% CI 0.07-0.86;  $p=0.03$ ).

Immunostaining of serial sections from liver biopsies of the same patients using, respectively, the B-cell marker CD20 and the T-cell marker CD3 showed that in 26 (63%) liver specimens CD20<sup>+</sup> B-cells were evident within mononucleated cell aggregates rich of CD3<sup>+</sup> T-lymphocytes (Fig 13D). The prevalence of B/T-lymphocyte infiltration was independent from age, BMI, HOMA-IR, transaminase release and the degree of steatosis. However, NAFLD/NASH patients with marked/high B-/T-cell infiltration had elevated anti-OSE IgG titers (Fig. 13E) as well as higher scores of lobular inflammation and fibrosis than the subjects with low/mild infiltration (Fig. 13F-G). The number and size of lymphocyte aggregates also positively correlated with circulating IFN- $\gamma$  levels (Spearman  $r=0.45$ ; 95% CI 0.005-0.048;  $p=0.02$ ), lobular inflammation score (Spearman  $r=0.45$ ; 95% CI 0.17-0.67;  $p=0.003$  and  $r=0.39$ ; 95% CI 0.10-0.62;  $p=0.01$ ) and fibrosis staging (Spearman  $r=0.44$ ; 95% CI 0.15-0.66;  $p=0.004$  and  $r=0.41$ ; 95% CI 0.11-0.63;  $p=0.008$ ), further supporting a functional interplay between humoral and cellular immunity in the processes leading to human NASH progression.



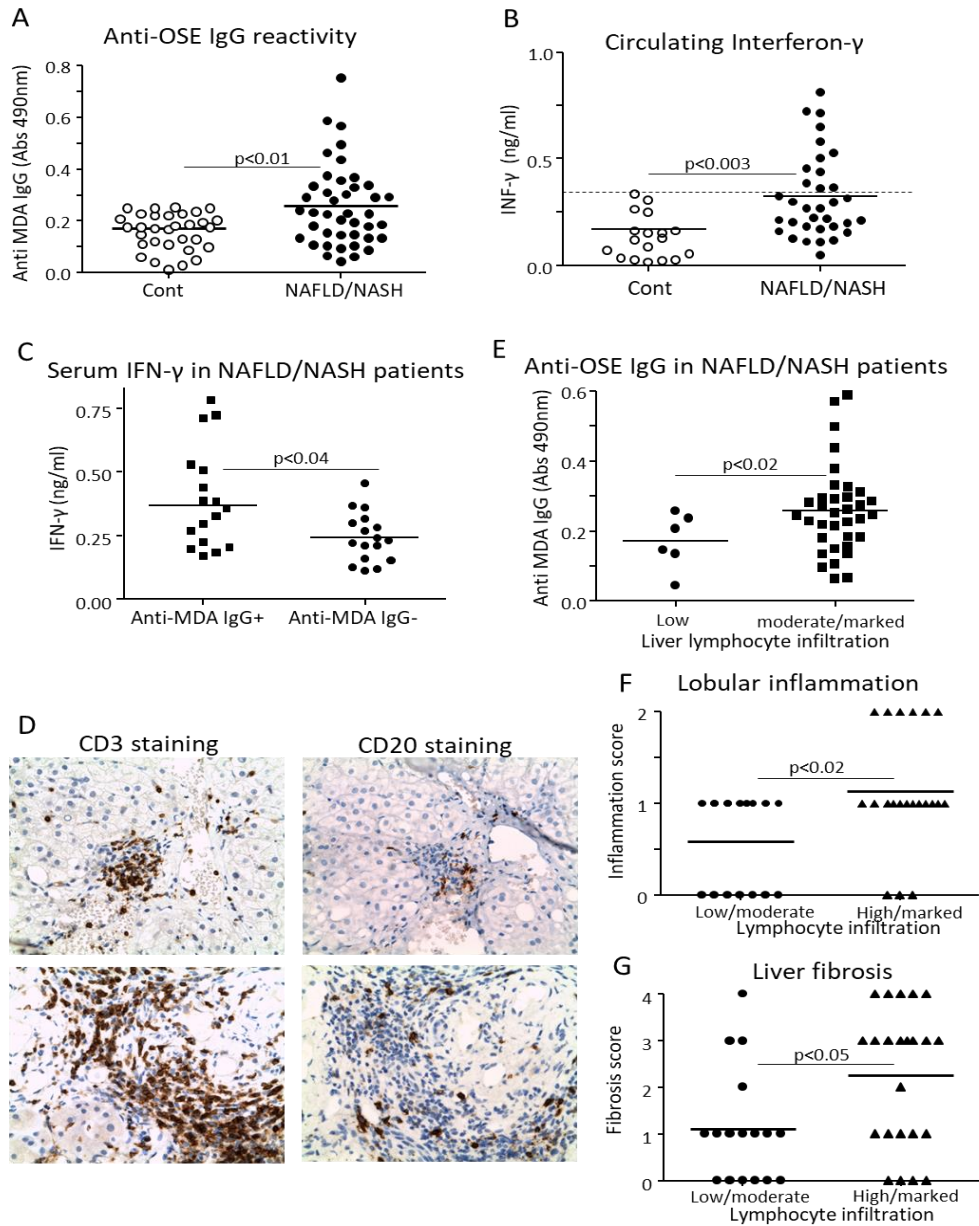


Figure 13: B- and T-lymphocyte responses associates with the evolution of human NAFLD/NASH.

(A-C) IgG reactivity toward OSE was measured in 41 NAFLD/NASH patients by in house ELISA assay using as antigen malonyl-dialdehyde (MDA) adducts with human serum albumin. For comparison 32 and 18 age/gender matched healthy subjects were used as controls. Circulating interferon- $\gamma$  (INF- $\gamma$ ) was measured in 34 of the patients and 18 age/gender matched healthy subjects. (D) Immuno-histochemical detection of cell aggregates containing CD20<sup>+</sup> B-lymphocytes and CD3<sup>+</sup> T-lymphocytes in serial sections from liver biopsies of two different representative NAFLD/NASH patients (Magnification 400x). (D-F) The prevalence of B/T-cells aggregates was associated with anti-OSE IgG titers as well as with the severity of lobular inflammation and hepatic fibrosis as estimated according to Kleiner et al. (24). Lymphocyte infiltration was evaluated semi-quantitatively taking into account the number and size of lymphocyte aggregates.

## Discussion

The possible implication of B cells in the pathogenesis of NASH has been suggested by Zhang and co-workers who have recently reported that feeding a high fat diet to mice leads to the liver recruitment of cells from B lineage (B220<sup>+</sup>) producing pro-inflammatory cytokines (Miyake, et al. 2013). However, this work did not investigate the actual role of B-cells in the pathogenesis of steatohepatitis. Our present data address this aspect by showing that B-cell activation is an early event in the evolution of experimental NASH and, even in the absence of obesity, contributes in supporting immune responses associated with the progression of steatohepatitis.

B-cells represent about 50% of intrahepatic lymphocytes. However, so far conflicting results have been obtained in studies investigating their role in liver diseases (Novobrantseva, et al. 2005; Dhirapong, et al. 2011; Beland, et al.2015). In mice, the pool of liver B-lymphocytes mainly consists of bone marrow-derived mature B220<sup>+</sup>/IgM<sup>+</sup>/CD23<sup>+</sup>/CD43<sup>-</sup> B2-cells resembling spleen follicular B-cells (Novobrantseva, et al. 2005). We have observed that B-cell changes in NASH specifically involve the B2 compartment and are characterized by their maturation to plasma cells. The circulating levels of IgG targeting OSE also increase at the onset of experimental NASH, suggesting that oxidative damage associated with the development of steatohepatitis leads to the generation of antigens recognized by B-cells that then undergo maturation to IgG-producing plasma cells. The actual relevance of B-cell responses in the pathogenesis of NASH is supported by experiments using B2-cell-deficient *TACI-Ig* mice or by using the BAFF neutralizing antibody Sandy-2. In these settings, B2-cell depletion or the interference with BAFF-mediated survival and maturation of B2- cells ameliorates both parenchymal damage and lobular inflammation and reduces the development of fibrosis. Interestingly B-cell maturation to plasma cells has been recently shown to foster HCC development in mice with steatohepatitis (Shalapour, et al. 2017). The beneficial effects connected with the interference with B-cell survival/maturation likely depend upon the reduction in the production of pro-inflammatory mediator by B-lymphocytes (Lund, et al. 2008) as well as the impairment of their antigen presenting capabilities (Di Lillo, et al.2011). On this latter respect, we have observed that B-cell activation in NASH associates with the up-regulation in MHCII molecules in plasma blasts and precedes the liver recruitment of CD4<sup>+</sup>

and CD8<sup>+</sup> T-lymphocytes, while interfering with B2-cells reduces Th-1 activation of CD4<sup>+</sup> T cells without affecting the maturation of dendritic cell. Altogether these results suggest that B2-lymphocytes can have a role in promoting OSE presentation to T-cells that, in turn, support NASH progression (Wolf, et al. 2014; Sutti, et al. 2014). Indeed, B-cells express a variety of receptors that can recognize OSE (Echeverri Tirado, et al. 2017), while Béland and co-workers have reported that B-cell depletion with anti-CD20 antibodies ameliorates experimental autoimmune hepatitis by preventing autoantigen presentation to CD4<sup>+</sup> and CD8<sup>+</sup> T-cells. It is noteworthy that the above mechanisms have several analogies with that observed in atherosclerosis, where B2-lymphocytes activation by OSE represents a key mechanism in plaque evolution. In fact, elevated circulating titers of anti-OSE IgG associate with an enhanced risk of atherosclerosis complications in humans (Tsiantoulas, et al. 2015), whereas the interference with B2-cells or BAFF-mediated signals reduces experimental atherosclerosis (Tsiantoulas, et al. 2015; Ketelhuth, et al. 2016). Although NAFLD/NASH is increasingly recognized as an independent risk factor for cardiovascular diseases [3], it is still unclear whether such association might be related to the common involvement of OSE-mediated immune responses.

Although the interference with cytotoxic and inflammatory mechanisms might account for the improvement in liver fibrosis observed in B2-cell-deficient *TACI-Ig* mice with NASH, we cannot exclude that additional mechanisms might also be involved. In fact, previous studies indicate that B-cells can directly contribute to liver fibrogenesis (Novobrantseva, et al. 2005; Thapa, et al. 2015) through the production of pro-inflammatory mediators that stimulate hepatic stellate cell (HSC) and liver macrophage activation (Thapa, et al. 2015). On the other hand, Thapa and co-workers have reported that during chronic liver injury activated HSCs can support liver B-cell survival and maturation to plasma cells by secreting retinoic acid (Thapa, et al. 2015), thus suggesting a complex interplay between B-cells and other non-parenchymal cells in the evolution of chronic liver diseases. The capacity of B-cells to stimulate inflammation and fibrogenesis through multiple interactions with T-lymphocytes and HSCs accounts for our clinical observations, showing that the prevalence of B-/T-lymphocyte aggregates in liver biopsies of NAFLD/NASH patients correlates with more severe lobular inflammation and enhanced fibrosis. In these subjects, intra-hepatic B/T-cell aggregates are also associated with elevated titers of anti-OSE IgG

and high IFN- $\gamma$  circulating levels, further supporting the clinical relevance of the interplay between B- and T-cells in the processes leading to NAFLD/NASH progression.

## **Conclusions**

Altogether these data indicate that B2-lymphocyte activation in response to OSE is an early event in NASH evolution and contributes to sustain hepatic inflammation through the interaction with T-cells. These observations, along with previous data indicating anti-OSE IgG as an independent risk factor for NASH progression to advanced fibrosis (Albano, et al. 2005), suggest that the measure of circulating anti-OSE IgG can identify a sub-set of NAFLD/NASH patients in whom adaptive immunity triggered by oxidative stress might have a relevant role in promoting steatohepatitis and the disease evolution toward fibrosis.

## Section 2

### **Role of the fractalkine receptor CX<sub>3</sub>CR1 in the development of monocyte-derived dendritic cells during hepatic inflammation.**

Data published on Cells. 2019;8:1099. doi: 10.3390/cells8091099.

#### **Foreword**

A mentioned in the introduction, the actual role of HDCs in the pathogenesis of liver diseases, including NASH, is still a matter of debate due to contradictory data obtained in experiments in which HDCs were either artificially expanded or depleted (Bamboot, et al. 2010; Connolly, et al. 2011; Zhang, et al.2013; Heier, et al.2017; Sutti, et al. 2017). These conflicting results can be explained by the low specificity of the methods used to modulate HDCs as well as by the fact that several factors including the intracellular lipid content and the interaction with other cells within the liver modify HDC functions (Ibrahim, et al. 2012; Sumpter,et al. 2012). Current view indicates that HDC expansion following liver injury mainly involves the myeloid group (Henning, et al. 2013; Connolly, et al. 2011) and that myeloid HDCs are also actively engaged in liver immune responses to infections (Krueger, et al. 2015). Nonetheless, a specific identification of the myeloid HDCs involved is uncertain, since CD141<sup>+</sup> type-1 myeloid HDCs are lowered in patients with advanced chronic liver diseases (Kelly, et al. 2014). Furthermore, in mice CD103<sup>+</sup> type-1 myeloid HDCs display a hepatoprotective action and their depletion in Batf3-deficient mice favours the onset of steatohepatitis (Heier, et al. 2017). A further element of complexity is given by the fact that in response to inflammatory stimuli monocytes can differentiate to a distinct dendritic cell subset called monocyte-derived dendritic cells (moDCs) or inflammatory dendritic cells. MoDCs have several surface markers and functional properties in common with type-2 myeloid dendritic cells, although they develop independently from the transcription factors driving myeloid dendritic cell differentiation (Segura, et al. 2013; Chow. et al, 2017; Hochheiser, et al. 2015). Furthermore, beside acting as antigen presenting cells to lymphocytes, moDCs actively produce pro-inflammatory mediators (Segura, et al. 2013; Chow. Et al, 2017; Hochheiser, et al. 2015). We have

previously reported that experimental NASH was associated with the expansion of a pool of cell co-expressing dendritic cell and macrophage markers along with the fractalkine receptor CX<sub>3</sub>CR1 and producing TNF- $\alpha$  that contribute to sustain liver injury and hepatic inflammation. These observations suggest the possibility that moDCs might be involved in the expansion of HDC pool in NASH.

In view of the importance of HDC in regulating liver immunotolerance as well as their capacity to act as APC in promoting liver immune responses, in this study we have further investigated the features of CX<sub>3</sub>CR1 expressing HDC in NASH and characterized the role of CX<sub>3</sub>CR1 in directing moDC differentiation within the liver.

## Results

### *Characterization of myeloid dendritic cells associated to NASH.*

Previous studies by Henning and co-workers (Henning et al. 2013) have shown that the expansion of myeloid HDCs is an early event in the evolution of NASH, being appreciable already after 1 week of mice feeding with the MCD diet, and precedes liver lymphocyte recruitment. Flow cytometry analysis of myeloid cells obtained from the liver of mice receiving the MCD diet for 1 week revealed an expansion of CD11c<sup>+</sup>/MHCII<sup>high</sup>/CD11b<sup>+</sup> myeloid HDCs, that occurred in parallel with the increase in the hepatic transcripts for both fractalkine (CX<sub>3</sub>CL1) and his receptor CX<sub>3</sub>CR1 (Fig. 14A). According to previous observations, CD11b<sup>+</sup> HDCs expanding in NASH were characterized by a high expression of CX<sub>3</sub>CR1 together with the monocyte/macrophage markers Ly6C (Fig. 14B), suggesting that these cells might be different from type 2 myeloid HDCs. Recently Nakano and co-workers [Nakano, et al. 2015] have reported that the presence of the complement C5a receptor (C5aR1 or CD88) is useful marker for discriminating lung infiltrating CD11b<sup>+</sup>/Ly6C<sup>+</sup> monocyte-derived dendritic cells (moDCs) that are CD88<sup>+</sup> from type-2 myeloid dendritic cells that are CD88<sup>-</sup>. In our hands, CD11b<sup>+</sup>/Ly6C<sup>+</sup>/CX<sub>3</sub>CR1<sup>+</sup> HDCs detectable in the liver of mice with NASH were largely CD88<sup>+</sup> (Fig 14B), supporting the identification of myeloid HDCs expanding at the onset of NASH as CD11b<sup>+</sup>/Ly6C<sup>+</sup>/CD88<sup>+</sup>/CX<sub>3</sub>CR1<sup>+</sup> moDCs.

### *Monocyte-derived dendritic cells in acute liver inflammation.*

From the observation that fractalkine (CX<sub>3</sub>CL1) was up-regulated during hepatic inflammation in parallel with the expansion of CX<sub>3</sub>CR1<sup>+</sup> moDCs (Figs. 14), we addressed the possible role of CX<sub>3</sub>CR1-mediated signals in modulating monocyte differentiation to moDC within the liver. Unfortunately, it is not possible to use CX<sub>3</sub>CR1 deficient mice for studying the role of this receptor in the differentiation of NASH-associated liver moDCs since Schneider and co-workers have recently reported that this strain has an increased susceptibility to steatohepatitis in relation to increased PAMP absorption in the gut secondary to altered intestinal microbiota composition and impaired intestinal barrier (Schneider, et al. 2015).

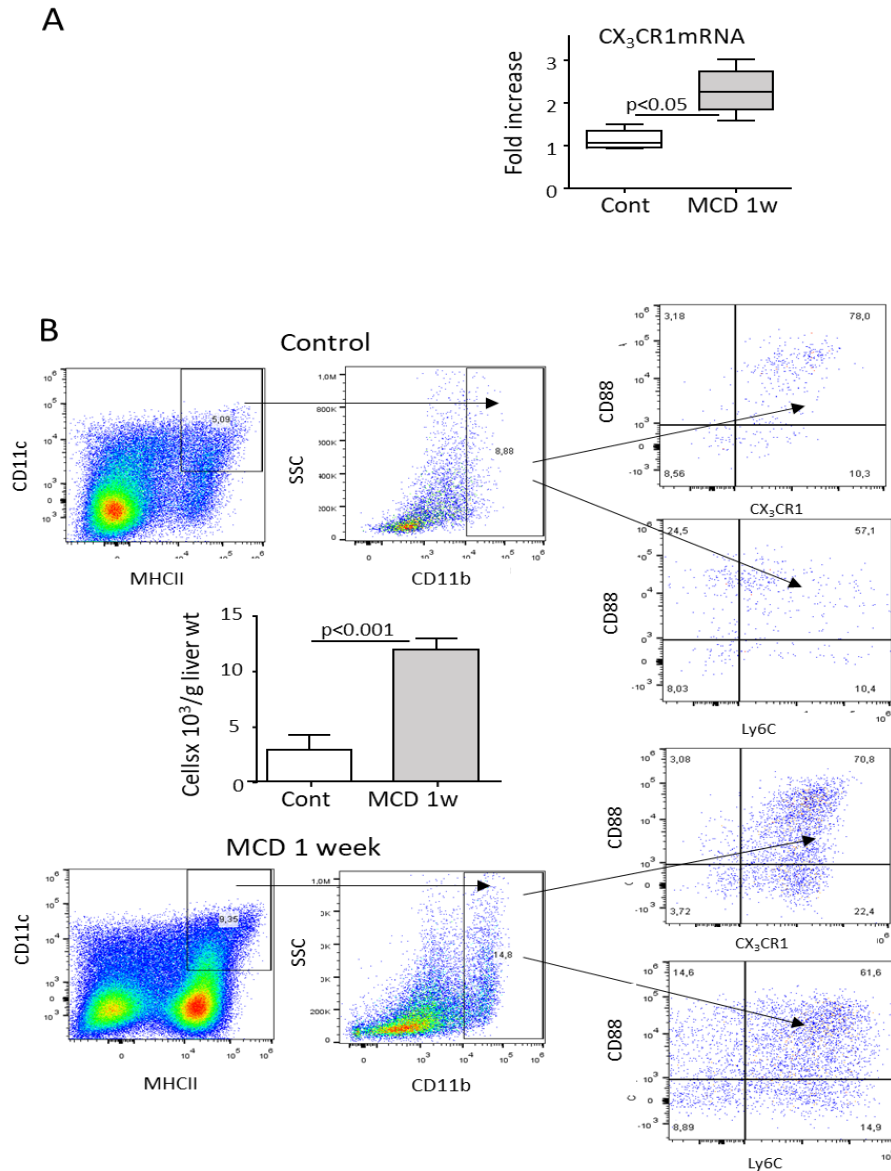


**Figure 14.** Monocyte-derived dendritic cells (moDCs) account for HDC expansion associated with the onset of nonalcoholic steatohepatitis (NASH).

Steatohepatitis was induced by feeding wild-type mice with a choline/methionine deficient (MCD) diet for one week. (Panel A) RT-PCR analysis of the hepatic expression of fractalkine (CX<sub>3</sub>CL1) and his receptor CX<sub>3</sub>CR1. The values are expressed as means ±SD of 5-6 animals in each experimental group. (Panel B) Flow cytometry analysis of the changes in the hepatic distribution CD11c<sup>+</sup>/MHCII<sup>high</sup>/CD11b<sup>high</sup>/CD88<sup>+</sup>/Ly6c<sup>+</sup> moDCs were analysed by in mice either untreated (Cont) or receiving the MCD diet. The values are expressed as means ±SD of three different cell preparations.



Thus, for further experiments we relied on a model of acute liver injury that did not involve intestinal microbiota such as the use of the hepatotoxic agent carbon tetrachloride (CCl<sub>4</sub>) poisoning. As shown in Figure 15, 36h after mice poisoning with CCl<sub>4</sub> acute liver injury was associated with massive hepatic inflammatory reactions. This injury-driven inflammation also involved an expansion of CD11c<sup>+</sup>/MHCII<sup>high</sup>/CD103<sup>-</sup>/CD11b<sup>+</sup> myeloid HDCs (Fig. 15D). Compared to healthy livers, these HDCs also underwent maturation as indicated by an increased expression of the co-stimulatory molecule CD80 (Fig. 15D). As observed in NASH, CD11b<sup>+</sup> HDCs expanding in the liver of CCl<sub>4</sub>-treated mice were characterized by a high expression of CX<sub>3</sub>CR1 (Fig. 16A) and featured the monocyte/macrophage markers Ly6C, F4-80 and CCR2, the receptor of the monocyte-recruiting chemokines CCL2/CCL7 (Fig. 16A). Furthermore, CD11b<sup>+</sup>/Ly6C<sup>+</sup>/CX<sub>3</sub>CR1<sup>+</sup> HDCs detectable in the liver of CCl<sub>4</sub>-treated mice were largely CD88<sup>+</sup> while did not express dipeptidyl peptidase-4 (CD26), a marker of Type 1 and type 2 myeloid cells (Fig 16B) and were also negative for the C3b complement receptor (CD35) (Fig. 16B), which is instead common on hepatic macrophages. In line with the pro-inflammatory features of moDCs (Segura, et al. 2013; Chow. Et al, 2017; Hochheiser, et al. 2015). Nanostring gene array comparing CX<sub>3</sub>CR1<sup>low/-</sup> and CX<sub>3</sub>CR1<sup>high</sup>/CD11b<sup>+</sup> myeloid HDCs obtained from CCl<sub>4</sub>-treated mice revealed that among the 75 genes up-regulated in the CX<sub>3</sub>CR1<sup>high</sup> sub-set there were those for interleukin-1 $\beta$  (IL-1 $\beta$ ), Toll-like receptors (Tlr-1,2,4,8), chemokines (CCL-2,3,4,6,7,9,12), immunoglobulin Fc receptors (CD16-2, CD32, CD64), CD14, macrophage scavenger receptor 1, urokinase and urokinase receptor (Supplementary Table 1). Interestingly, these cells also showed an enhanced gene expression of anti-inflammatory mediators such as interleukin-1 receptor antagonist (IL-1a) and transforming growth factor  $\beta$ -1 (TGF $\beta$ -1) (Supplementary Table 1). Altogether these data confirmed that the features of moDCs associated to acute liver injury by CCl<sub>4</sub> are similar to those identified in NASH allowing the use of this experimental model to further characterise the signals the promote their differentiation from monocytes.

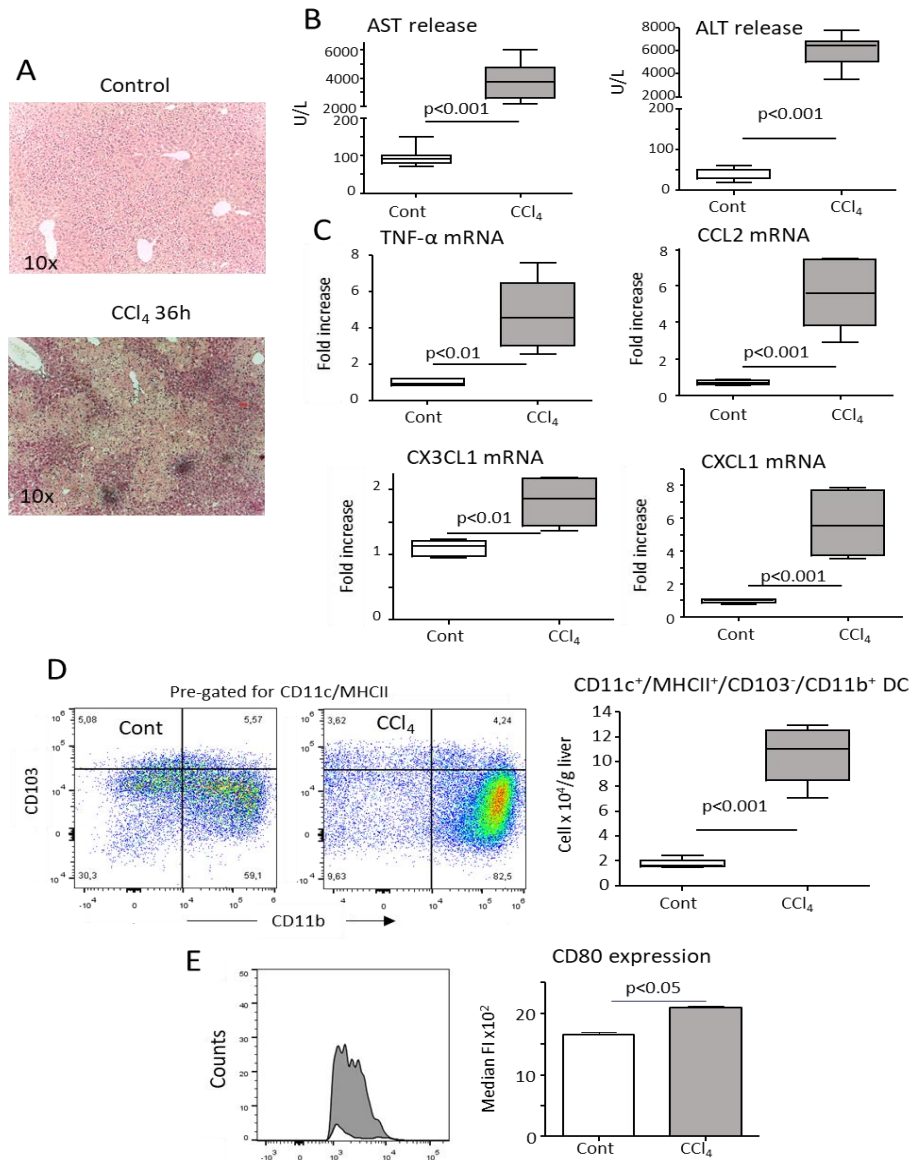


**Figure 15.** Hepatic inflammation induced by the acute administration of CCl<sub>4</sub> associates with the expansion and maturation of hepatic dendritic cells (HDCs).

Parenchymal damage and lobular inflammation were analyzed in wild-type mice either naïve (Cont) or 36 hours after receiving an acute dose of CCl<sub>4</sub> (CCl<sub>4</sub>). (Panel A) Hematoxylin/eosin staining of formalin-fixed liver sections (magnification 10x). (Panel B) Circulating levels of alanine aminotransferase (ALT) and aspartate aminotransferase (AST). (Panel C) RT-PCR analysis of hepatic expression of pro-inflammatory cyto/chemokines TNF- $\alpha$ , CCL2, CXCL1, CX<sub>3</sub>CL1. The values are expressed as fold increase over control levels and are means  $\pm$ SD of 6-8 animals in each experimental group. (Panel D) The changes in the liver distribution of CD11c<sup>+</sup>/MHCII<sup>high</sup>/CD11b<sup>+</sup>/CD103<sup>-</sup> HDCs were analysed by flow cytometry in mice either untreated or receiving CCl<sub>4</sub>. (Panel E) The plasma membrane expression of maturation marker CD80 was evaluated in HDCs gated for CD11b. The values are expressed as means  $\pm$ SD of three different cell preparations.

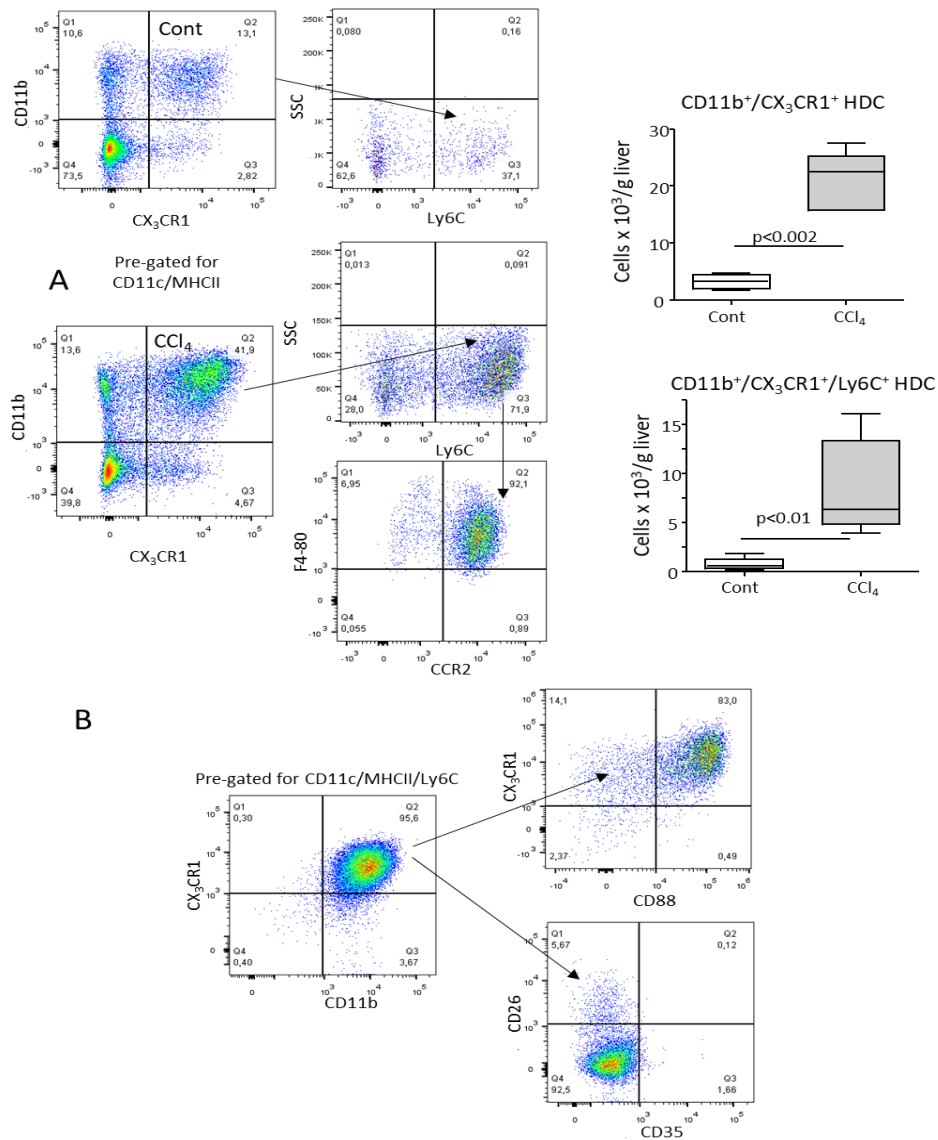


**Figure 16.** Characterization of hepatic dendritic cells (HDCs) expanding in response to acute liver injury.

(Panel A) CD11c<sup>+</sup>/MHCII<sup>high</sup>/CD11b<sup>+</sup> HDCs from either naive (Cont) or CCl<sub>4</sub>-treated mice (CCl<sub>4</sub>) were analyzed by flow cytometry for the expression of CX<sub>3</sub>CR1 and the monocyte markers Ly6C, F4-80 and CCR2. The values are expressed as means ±SD of three different cell preparations. (Panel B) Relative distribution of the dendritic cell and macrophages markers CD26, CD35 and CD88 among CD11c<sup>+</sup>/MHCII<sup>high</sup>/CD11b<sup>+</sup>/Ly6C<sup>+</sup>/CX<sub>3</sub>CR1<sup>+</sup> HDCs.

*The interference with CX<sub>3</sub>CR1 affects monocyte maturation to dendritic cells in injured livers*

To better characterize the possible role of CX<sub>3</sub>CR1-mediated signals in modulating hepatic moDC responses further experiments using CX<sub>3</sub>CR1-deficient homozygous mice having the green fluorescent protein (gfp) inserted in the CX<sub>3</sub>CR1 gene (CX<sub>3</sub>CR1<sup>gfp/gfp</sup>). Using these animals, we observed that the expansion of myeloid dendritic cells associated with CCl<sub>4</sub> poisoning was strongly reduced in CX<sub>3</sub>CR1<sup>gfp/gfp</sup> mice as compared to CX<sub>3</sub>CR1 proficient (CX<sub>3</sub>CR1<sup>+ /gfp</sup>) animals. Such an effect specifically involved the fraction of liver CD11c<sup>+</sup>/MHCII<sup>high</sup>/CX<sub>3</sub>CR1<sup>+</sup>/CD11b<sup>+</sup>/CD88<sup>+</sup> moDCs (Fig. 17A & B). Conversely, no significant differences were appreciable between CCl<sub>4</sub>-treated CX<sub>3</sub>CR1<sup>gfp/gfp</sup> and CX<sub>3</sub>CR1<sup>+ /gfp</sup> mice in the hepatic distribution of CX<sub>3</sub>CR1<sup>+</sup>/F4-80<sup>+</sup>/CD11b<sup>high</sup> monocytes/macrophages (Fig. 17 C). In a similar manner, the lack of CX<sub>3</sub>CR1 did not affect the liver recruitment of Ly6G<sup>-</sup>/CD11b<sup>high</sup>/Ly6C<sup>high</sup> monocytes that were instead more prevalent in CX<sub>3</sub>CR1<sup>gfp/gfp</sup> mice (Fig. 18A). However, we observed that in the absence of CX<sub>3</sub>CR1 the cells that were CD11b<sup>+</sup>/Ly6C<sup>+</sup> and positive for the common dendritic cell marker CD11c<sup>+</sup> failed to fully express MHCII (Fig. 18B), suggesting a possible role of CX<sub>3</sub>CR1 signalling in the differentiation of monocytes to moDCs.

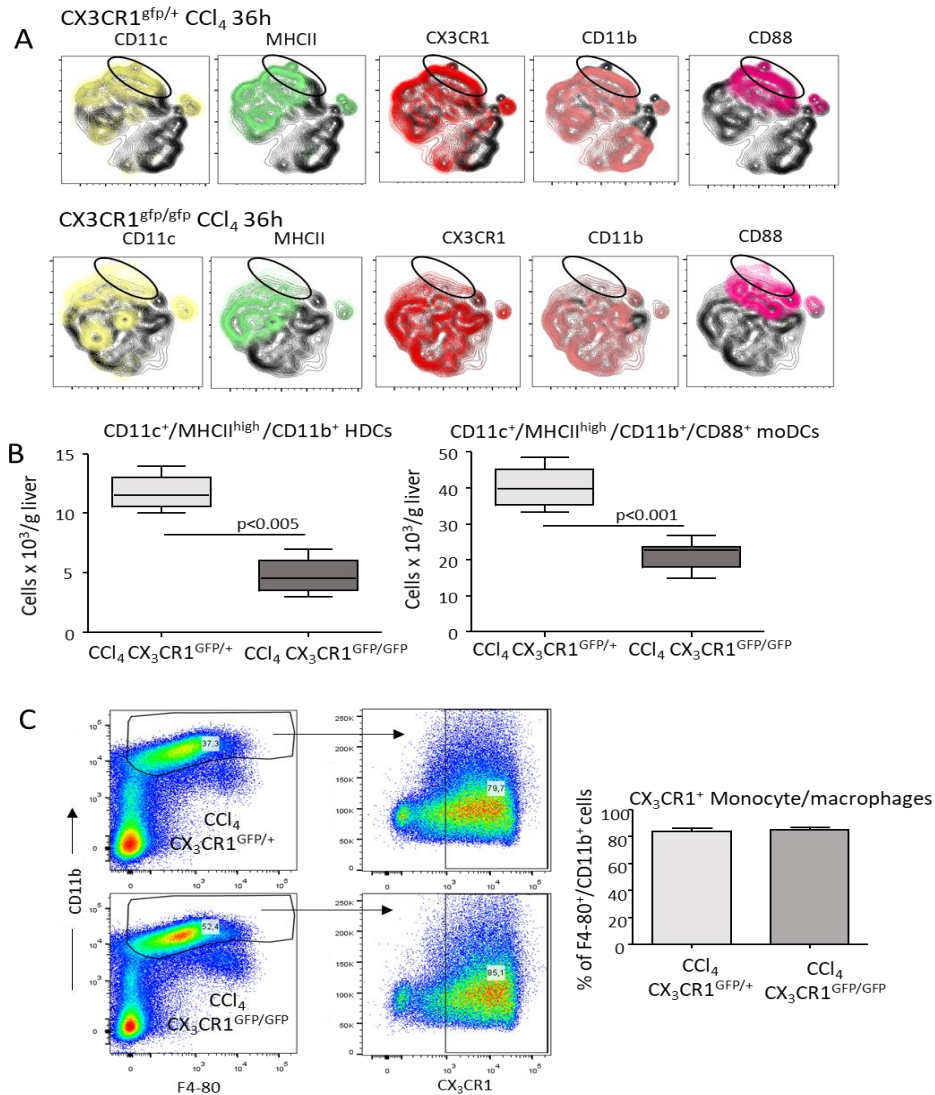


**Figure 17.** The lack of CX<sub>3</sub>CR1 reduced the expansion of monocyte-derived dendritic cells (moDCs) in response to liver inflammation without affecting that of CX<sub>3</sub>CR1<sup>+</sup> monocytes/macrophages.

The liver distribution of CD11b<sup>+</sup> myeloid dendritic cells, moDCs and monocytes were analyzed by flow cytometry in the livers of CX<sub>3</sub>CR1<sup>GFP/+</sup> and CX<sub>3</sub>CR1<sup>GFP/GFP</sup> mice 36 hours after receiving an acute dose of CCl<sub>4</sub>. (Panel A) Flow cytometry plot showing the cluster of moDCs identified as co-expressing CD11c, MHCII, CX<sub>3</sub>CR1, CD11b and CD88 in the livers of CX<sub>3</sub>CR1<sup>GFP/+</sup> and CX<sub>3</sub>CR1<sup>GFP/GFP</sup> mice 36 hours after receiving an acute dose of CCl<sub>4</sub>. (Panel B) Prevalence of CD11c<sup>+</sup>/MHCII<sup>high</sup>/CD11b<sup>+</sup> myeloid dendritic cells and CD11c<sup>+</sup>/MHCII<sup>high</sup>/CD11b<sup>+</sup>/CD88<sup>+</sup> moDCs in CX<sub>3</sub>CR1<sup>GFP/+</sup> and CX<sub>3</sub>CR1<sup>GFP/GFP</sup> mice receiving CCl<sub>4</sub>. (Panel C) Distribution of F4-80<sup>+</sup>/CD11b<sup>high</sup>/CX<sub>3</sub>CR1<sup>+</sup> monocytes/macrophages in the livers of CX<sub>3</sub>CR1<sup>GFP/+</sup> and CX<sub>3</sub>CR1<sup>GFP/GFP</sup> mice 36 hours after receiving an acute dose of CCl<sub>4</sub>. The values are expressed as means ±SD of three different cell preparations or 5-6 animals.

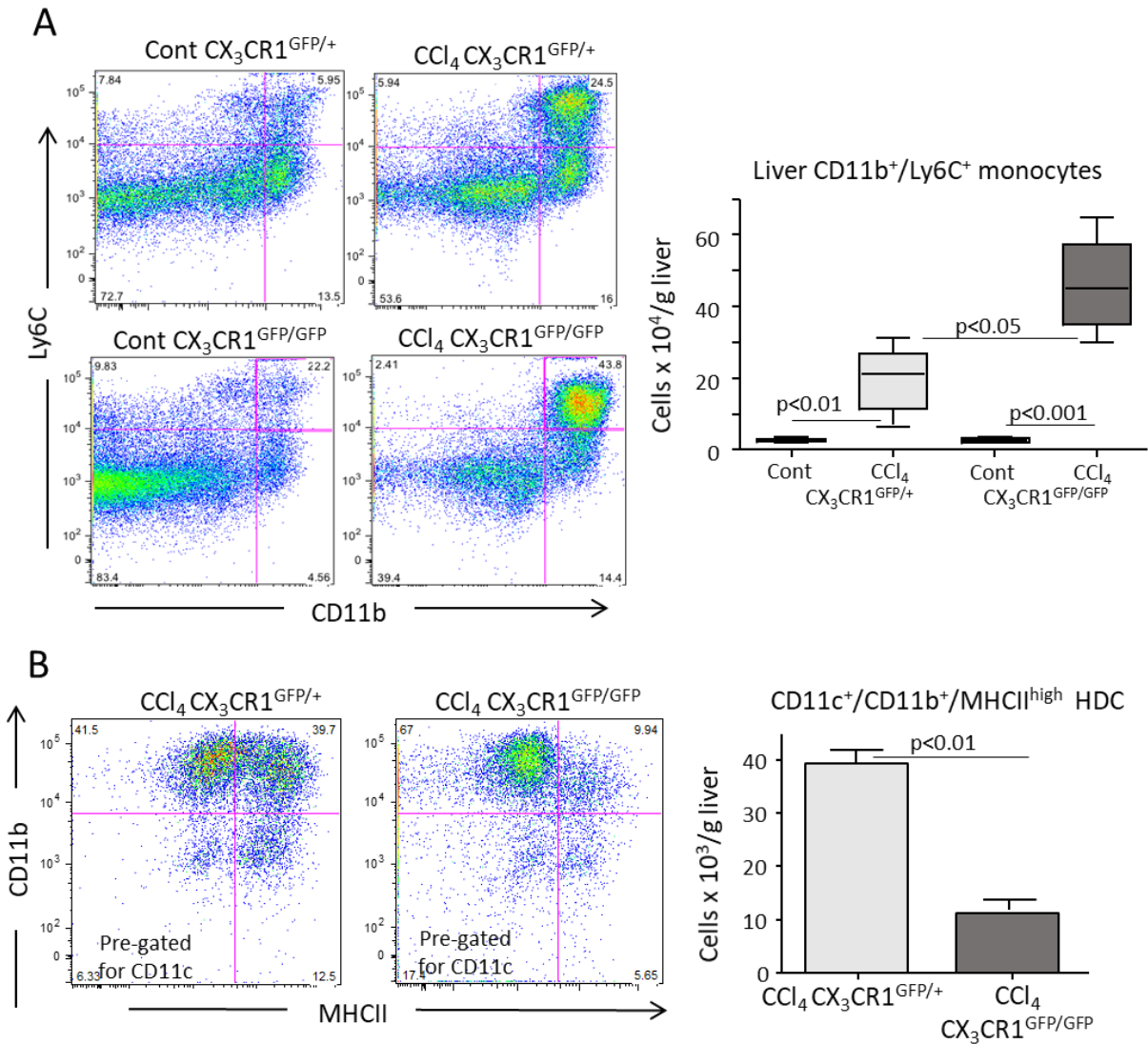


**Figure 18.** The lack of  $CX_3CR1$  reduced the differentiation of monocyte-derived dendritic cells (moDCs) in response to liver inflammation.

The liver distribution of  $CD11b^+$  myeloid dendritic cells, moDCs and monocytes were analyzed by flow cytometry in the livers of  $CX_3CR1^{GFP/+}$  and  $CX_3CR1^{GFP/GFP}$  mice 36 hours after receiving an acute dose of  $CCl_4$ . (Panel A) Hepatic distribution of  $Ly6G^-/CD11b^{high}/Ly6C^{high}$  monocytes in control and  $CCl_4$ -treated  $CX_3CR1^{GFP/+}$  and  $CX_3CR1^{GFP/GFP}$  mice. (Panel B) Impaired expression of MHCII by  $CD11c^+/CD11b^+$  myeloid cells in  $CCl_4$ -treated  $CX_3CR1^{GFP/+}$  and  $CX_3CR1^{GFP/GFP}$  mice. The values are expressed as means  $\pm$ SD of three different cell preparations or 5-6 animals.

### *CX<sub>3</sub>CR1 drives monocyte maturation to dendritic cells in vitro*

To better characterize the role of CX<sub>3</sub>CR1 in directing monocyte differentiation to moDCs in further experiments moDCs were generated in vitro by culturing bone marrow myeloid cells with granulocyte-macrophage colony stimulating factor (GM-CSF) and interleukin-4 (IL-4) (Lutz, et al. 2017). In these experiments we observed that Ly6G<sup>-</sup>/CD11b<sup>+</sup>/CD88<sup>+</sup>/CD11c<sup>+</sup>/MHCII<sup>high</sup> moDC originating from GM-CSF/IL-4-treated bone marrow myeloid cells expressed CX<sub>3</sub>CR1 (Fig. 19A). Thus, we used these cells to further investigate the role of CX<sub>3</sub>CR1 in moDC differentiation. As shown in Figure 19B the fraction of moDCs maturing from the bone marrow of CX<sub>3</sub>CR1<sup>gfp/gfp</sup> mice was 35% lower as compared to that from CX<sub>3</sub>CR1<sup>+gfp</sup> animals. The absence of CX<sub>3</sub>CR1 also influenced the spontaneous differentiation of moDCs when bone marrow myeloid cells were cultured seven days in calf serum-supplemented medium without GM-CSF/IL-4 (24±2.1% vs 13±2.1% p<0.01). In this setting, the lack of CX<sub>3</sub>CR1 specifically hampered MHCII expression by CD11b<sup>+</sup>/CD11c<sup>+</sup> pre-dendritic cells (Fig. 19C). Conversely, the addition of fractalkine (40 ng/mL) to the medium promoted moDC differentiation (28±0.6% vs 32±1.2% p<0.05), indicating a CX<sub>3</sub>CR1 action in the processes leading to full moDC development. To further evaluate such a possibility, we investigated CX<sub>3</sub>CR1 effects on the mRNA levels of the transcription factors Zbtb46, interferon responsive factor-4 (IRF-4) and interferon responsive factor-8 (IRF-8) that have been implicated in moDC maturation induced by GM-CSF/IL-4 (Lutz, et al. 2017; Satpathy, et al. 2019; Tamura, et al. 2005; Bajaaná, et al, 2016). All the three transcription factors were significantly up-regulated in the cells exposed to GM-CSF/IL-4 (Fig. 20). The lack of CX<sub>3</sub>CR1 significantly reduced Zbtb46 and IRF-8 mRNAs, while IRF-4 mRNA was unaffected (Fig. 20), further pointing to a role of CX<sub>3</sub>CR1 in the implicated in the monocyte differentiation to moDCs.

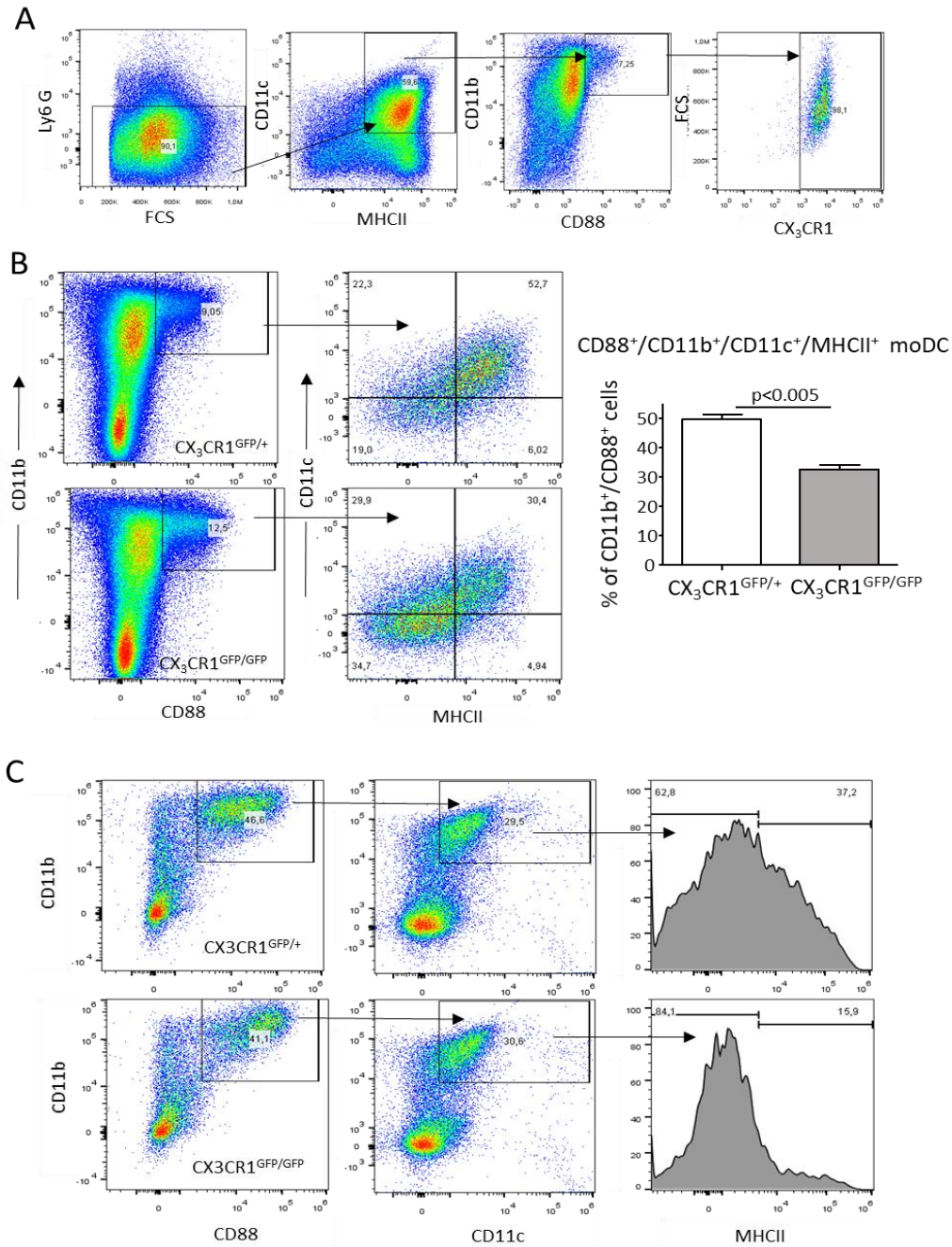


**Figure 19.** The lack of CX<sub>3</sub>CR1 affects the *in vitro* differentiation of monocyte-derived dendritic cells (moDCs).

MoDCs were obtained “*in vitro*” by 7 days culture of bone marrow myeloid cells from either CX<sub>3</sub>CR1<sup>gfp/+</sup> and CX<sub>3</sub>CR1<sup>gfp/gfp</sup> mice with granulocyte-macrophage colony stimulating factor (GM-CSF) and interleukin-4 (IL-4). (Panel A) CX<sub>3</sub>CR1 expression in Ly6G<sup>+</sup>/CD11b<sup>+</sup>/CD88<sup>+</sup>/CD11c<sup>+</sup>/MHCII<sup>high</sup> moDC originating from GM-CSF/IL-4-treated bone marrow myeloid cells. (Panel B) Effect of CX<sub>3</sub>CR1 on the “*in vitro*” differentiation of CD11b<sup>+</sup>/CD88<sup>+</sup>/CD11c<sup>+</sup>/MHCII<sup>high</sup> moDCs. (Panel C) Effect of CX<sub>3</sub>CR1 deficiency on the expression of MHCII by CD11b<sup>+</sup>/CD88<sup>+</sup>/CD11c<sup>+</sup> pre-dendritic cells.



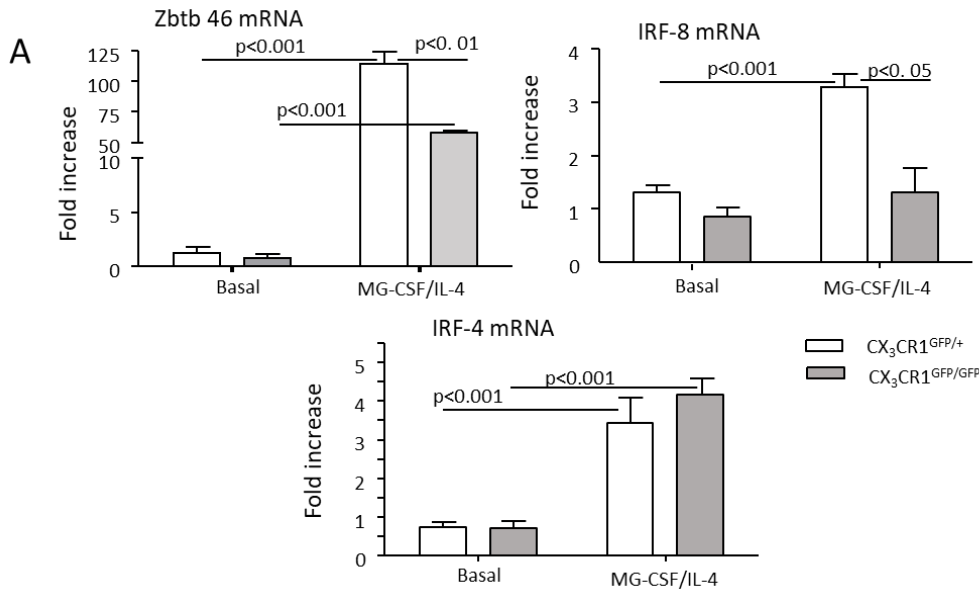


**Figure 20.** The lack of CX<sub>3</sub>CR1 affects the *in vitro* expression of transcription factors involved in the differentiation of monocyte-derived dendritic cells (moDCs).

MoDCs were obtained “*in vitro*” by 7 days culture of bone marrow myeloid cells from either CX<sub>3</sub>CR1<sup>GFP/+</sup> and CX<sub>3</sub>CR1<sup>GFP/GFP</sup> mice with granulocyte-macrophage colony stimulating factor (GM-CSF) and interleukin-4 (IL-4) and the expression of the transcription factors Zbtb46, IRF-4 and IRF-8 implicated in moDC differentiation was evaluated by RT-PCR. The values are expressed as means ±SD of 3-5 different cell preparations.

*Interference with CX<sub>3</sub>CR1-mediated moDCs differentiation ameliorates acute liver injury and inflammation.*

Several studies have implicated moDCs in sustaining tissue injury and inflammation in different tissues (Segura, et al. 2013; Chow, et al. 2017). On this latter respect, we have previously reported that the H<sub>2</sub>S donor NaHS lowers hepatic TNFα levels and ameliorates parenchymal injury in NASH by selectively affecting the development of CX<sub>3</sub>CR1-expressing HDCs (Sutti, et al. 2015). Since NaHS might have also anti-inflammatory actions here we took advantage of a more specific CX<sub>3</sub>CR1 antagonist using CX3-AT, a NH<sub>2</sub>-terminal CX<sub>3</sub>CL1-derived peptide that has been previously reported to block CX<sub>3</sub>CR1 in lymphocytes (Mionnet, et al. 2010; Staumont-Sallé, et al. 2014). For these experiments, mice were treated with a single dose of CX3-AT (150 μg in saline i.p.) 24 hours after the administration of CCl<sub>4</sub> and the effects on hepatic inflammation were

monitored in the following 12 hours. At this dosage CX3-AT was not hepatotoxic and did not affect the liver distribution of monocyte/macrophages and CX<sub>3</sub>CR1<sup>+</sup> type-2 myeloid HDCs (not shown).

In line with the data obtained using CX<sub>3</sub>CR1-deficient mice, CX3-AT treatment affected moDC expansion in response to CCl<sub>4</sub>-induced liver injury (Fig. 22A), specifically reducing the fraction of CX<sub>3</sub>CR1<sup>+</sup> moDCs (Fig. 22B). We also observed that CX3-AT addition lowered moDC expression of the maturation marker CD80 (Fig. 22C) without interfering with the hepatic expression of CX<sub>3</sub>CL1 and CX<sub>3</sub>CR1 (Fig. 22D). Similarly, no appreciable changes were observed in the liver distribution of T-lymphocytes, NK and NKT cells that also rely on CX<sub>3</sub>CR1 signaling (Fig. 23). In the animals receiving CX3-AT liver histology showed a significant reduction of parenchymal necrosis and inflammatory infiltrates (Fig. 24A). Consistently, CX3-AT treatment ameliorated transaminase release (Fig. 24B) and reduced the hepatic expression of the pro-inflammatory cyto/chemokines TNF- $\alpha$ , CCL2 and CXCL1 (Fig. 24C). Altogether, these data indicated that CX<sub>3</sub>CR1-dependent moDCs effectively contributed to hepatic inflammation in response to liver injury.

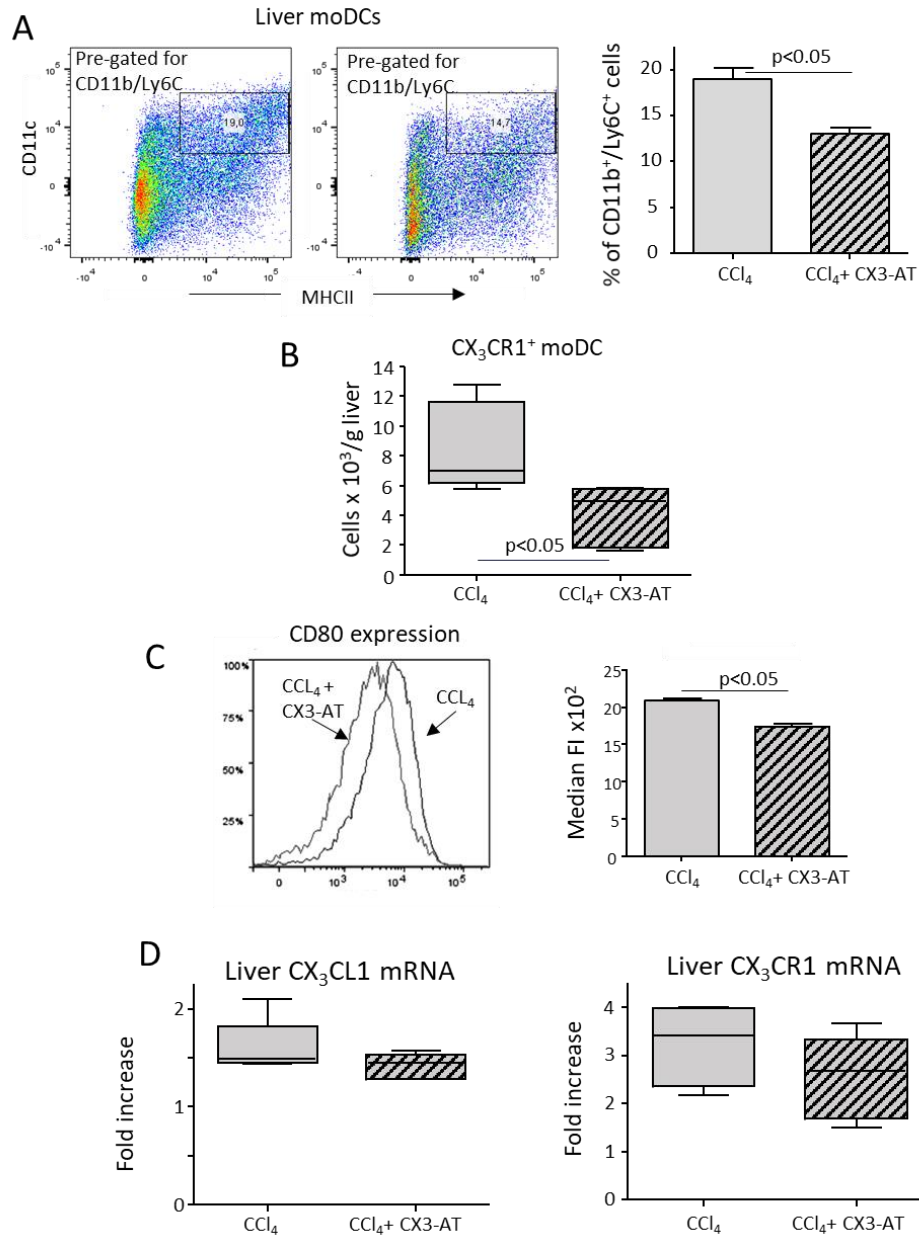


**Figure 22.** The CX<sub>3</sub>CL1 antagonist CX3-AT reduces the expansion of monocyte-derived dendritic cells (moDCs) in response to hepatic injury.

Liver dendritic cells were analyzed by flow cytometry in mice receiving CCl<sub>4</sub> alone or in combination with CX3-AT. (Panels A-B) Liver distribution of CD11b<sup>+</sup>/Ly6C<sup>+</sup> moDCs and CX<sub>3</sub>CR1-expressing moDCs. (Panel C) Plasma membrane expression of the maturation marker CD80 in moDCs for CCl<sub>4</sub>-treated mice receiving or not CX3-AT. The values are expressed as means ±SD of 3 different cell preparations. (Panel D) RT-PCR analysis of the hepatic transcripts for CX<sub>3</sub>CL1 and CX<sub>3</sub>CR1. The values are expressed as fold increase over control levels and are means ±SD of 6-8 animals in each experimental group.

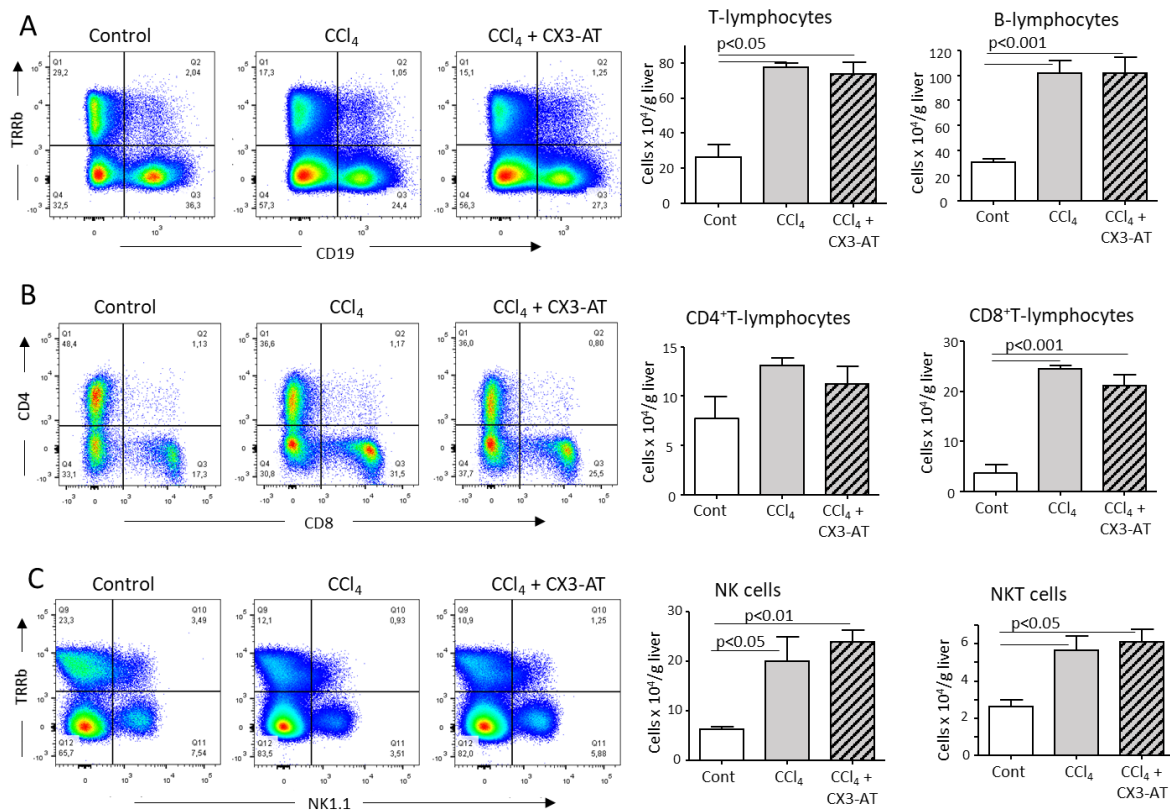


**Figure 23:** CX3-AT does not affect the liver distribution of different lymphocyte sub-sets during hepatic inflammation.

Liver lymphocytes were analyzed by flow cytometry in naïve mice, in animals receiving CCl<sub>4</sub> alone and in combination with CX3-AT. (Panel A) Liver distribution of TCR-β<sup>+</sup>/CD19<sup>-</sup> T- and TCR-β<sup>+</sup>/CD19<sup>+</sup> B-lymphocytes. (Panel B) Liver distribution of CD4<sup>+</sup>/CD8<sup>-</sup> helper and CD4<sup>+</sup>/CD8<sup>+</sup> cytotoxic T-lymphocytes. (Panel C) Liver distribution of TCR-β<sup>-</sup>/NK1.1<sup>+</sup> NK and TCR-β<sup>+</sup>/NK1.1<sup>+</sup> NKT cells. The values are expressed as means ±SD of 5 different cell preparations.

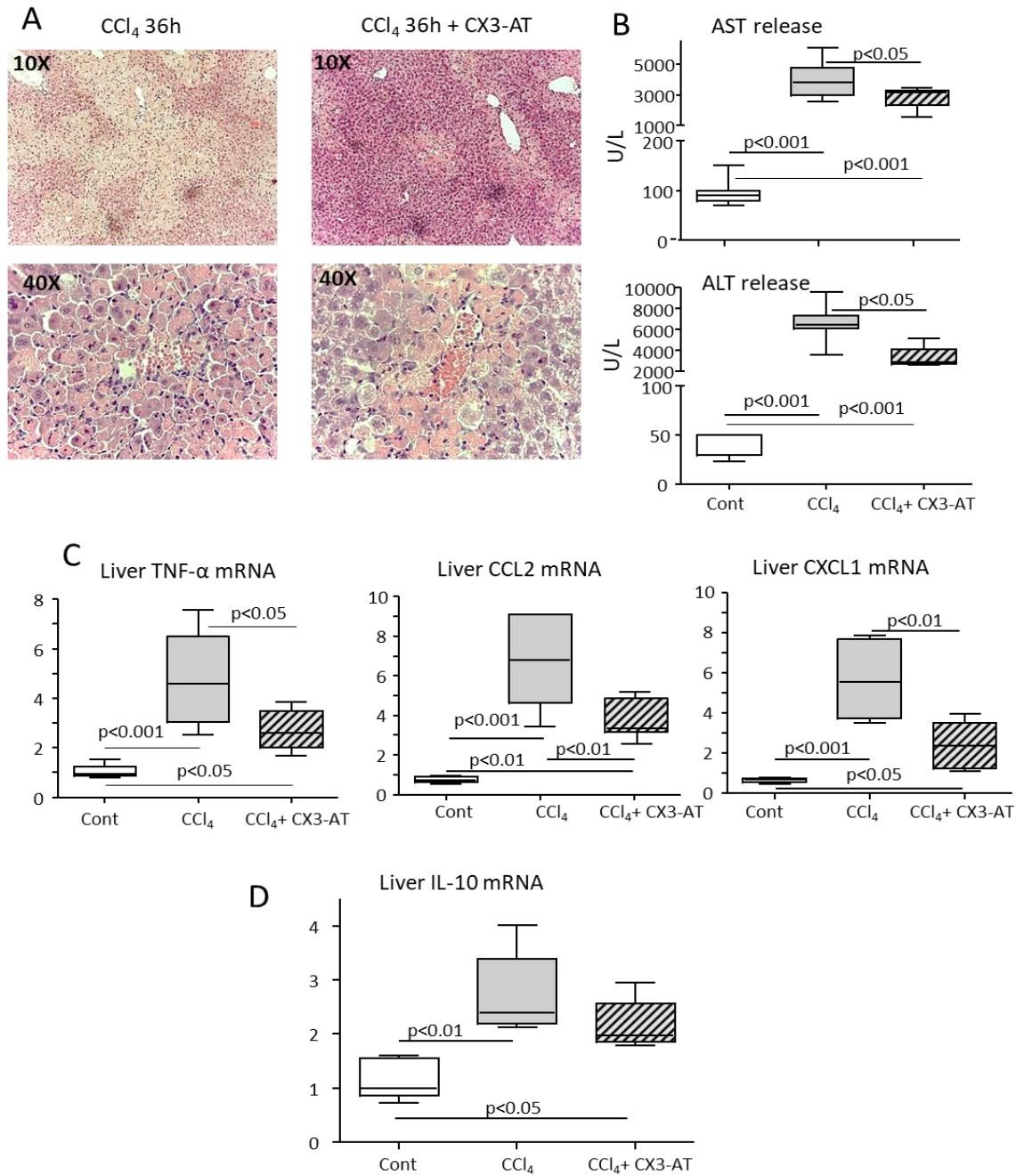


**Figure 24.** The CX<sub>3</sub>CL1 antagonist CX3-AT improves liver injury and inflammation in mice receiving CCl<sub>4</sub>.

Parenchymal damage and lobular inflammation were analyzed in mice receiving CCl<sub>4</sub> alone and in combination with CX3-AT. (Panel A) Hematoxylin/eosin staining of formalin-fixed liver sections (magnification 10x and 40x). (Panel B) Circulating levels of alanine aminotransferase (ALT) aspartate aminotransferase (AST). (Panel C and D) RT-PCR analysis of the hepatic expression of pro-inflammatory cyto/chemokines TNF- $\alpha$ , CCL2, CXCL1 and of IL-10. The values are expressed as fold increase over control levels and are means  $\pm$ SD of 6-8 animals in each experimental group.

## Discussion

Growing evidence indicates that HDCs play an important role in modulating hepatic immune and inflammatory responses both at homeostasis and in liver diseases (Rahman, et al. 2013; Eckert, et al. 2016). Along with that, experiments using different models of acute and chronic liver injury have evidenced that myeloid HDCs expand and mature in response to inflammatory stimuli sustaining the evolution of hepatic damage (Connolly, et al. 2009; Henning, et al. 2013; Connolly, et al. 2011). However, the specific features of these HDCs have not been investigated in detail. Our present data add on the role of HDCs in liver pathology by showing that HDCs expansion in response to inflammatory stimuli involves cells featuring CD11b as type-2 classical HDCs along with the fractalkine receptor CX<sub>3</sub>CR1. The presence of CX<sub>3</sub>CR1 in HDCs has been previously documented in the liver at homeostasis (Rahman, et al. 2013; Sutti, et al. 2017). However, CX<sub>3</sub>CR1<sup>high</sup> HDCs in inflamed livers differ from CX<sub>3</sub>CR1<sup>low</sup> HDCs in naïve mice because they express the monocyte markers F4-80 and CCR2 and are Ly6C<sup>high</sup>. Furthermore, the formers are also characterized by the presence of the complement C5a receptor (C5aR1 or CD88), while are negative for the dipeptidyl peptidase-4 (CD26), two surface markers that, discriminate CD11b<sup>+</sup> monocyte-derived DCs (moDCs) (CD88<sup>+</sup>/CD26<sup>-</sup>) from type-1 and type-2 classical DCs (CD88<sup>-</sup>/CD26<sup>+</sup>) (Nakano, et al. 2015). On these bases, we propose that the differentiation of dendritic cells from liver infiltrating monocytes might represent a mechanism to rapidly expand the pool of HDCs in response to pro-inflammatory stimuli. In line with this, Ly6C<sup>+</sup>/CX<sub>3</sub>CR1<sup>+</sup>/CD88<sup>+</sup> moDCs also account for HDC expansion occurring at the onset of experimental NASH, confirming a previous implication of moDC in sustaining liver injury and inflammation in experimental model of chronic steatohepatitis (Sutti, et al. 2015). Furthermore, Huang and co-workers (Huang, et al. 2013) have reported that CD11b<sup>+</sup> moDCs contribute to the formation of intrahepatic myeloid-cell aggregates for T-cell expansion (iMATEs) responsible for CD8<sup>+</sup> T-lymphocyte stimulation during viral infection. Nonetheless, we are well aware that the above surface markers do not allow a definitive differentiation of moDCs from liver infiltrating inflammatory monocyte-derived macrophages that are also Ly6C<sup>high</sup>/CX<sub>3</sub>CR1<sup>+</sup> and can express to variable extend CD11c, MHCII and CD88 (Krenker, et al. 2017; Weston, et al. 2019).

The experiment using CX<sub>3</sub>CR1-deficient mice have shown that the expansion of moDCs in response to liver injury requires CX<sub>3</sub>CR1. It is noteworthy that in line with a previous report (Karlmark, et al. 2010), the lack of CX<sub>3</sub>CR1 in CCl<sub>4</sub>-treated mice does not affect the pool of liver infiltrating monocyte-derived macrophages, further indicating that CX<sub>3</sub>CR1<sup>+</sup> moDCs might represent a different cell subset. At present, CX<sub>3</sub>CR1 functions in moDCs are still poorly characterized. David and co-workers have shown that CX<sub>3</sub>CR1 contributes to liver dendritic cell replenishment after selective depletion by directing bone marrow-derived precursors (Rahman, et al. 2013). A recent report has also shown that CX<sub>3</sub>CR1/CX<sub>3</sub>CL1 interaction is critical for monocyte adhesion to endothelial cells and their migration into atherosclerotic plaques (Riopel, et al. 2019). However, the effects observed in CX<sub>3</sub>CR1-deficient mice receiving CCl<sub>4</sub> do not involve the hepatic recruitment of monocytes, but rather imply a reduced capacity of dendritic cells precursors to fully express MHCII. Moreover, the lack of CX<sub>3</sub>CR1 reduces in vitro moDC maturation from bone marrow myeloid cells incubated with MG-CSF/IL-4. Altogether these data suggest that CX<sub>3</sub>CR1-mediated signals are required for moDCs differentiation. Supporting this view, we have observed that in MG-CSF/IL-4-treated myeloid cells CX<sub>3</sub>CR1 influences the expression of Zbtb46 and IRF-8, two transcription factors implicated in driving monocyte differentiation to moDC (Satpathy, et al. 2019; Tamura, et al. 2005). However, we can't exclude that CX<sub>3</sub>CR1 might have additional effects on moDCs, as this receptor is required for the survival of liver infiltrating monocyte-derived macrophages (Karlmark, et al. 2010).

It is well established that moDCs not only are effective in antigen presentation to lymphocytes, but also produce pro-inflammatory mediators contributing to sustain inflammatory processes (Segura, et al. 2013; Chow. et al, 2017; Hochheiser, et al. 2015). On this later respect we have observed that interfering with liver CX<sub>3</sub>CR1<sup>+</sup> moDCs differentiation using the CX<sub>3</sub>CR1 blocker CX<sub>3</sub>-AT ameliorates lobular inflammation and parenchymal damage following acute CCl<sub>4</sub> poisoning. These findings are consistent with previous data showing that the H<sub>2</sub>S donor NaHS lowers hepatic TNF $\alpha$  levels and ameliorates parenchymal injury in an experimental model of chronic steatohepatitis by selectively affecting the development of CX<sub>3</sub>CR1-expressing HDCs (Sutti, et al. 2015). Taken together these observations indicate that CX<sub>3</sub>CR1<sup>+</sup> moDCs can contribute to hepatic injury and inflammation through the production of pro-inflammatory mediators. Such an

interpretation is in line with the data of Connolly and co-workers (Connolly, et al. 2009) showing that TNF $\alpha$ -producing HDCs drive hepatic inflammation in mice with thioacetamide-induced fibrosis.

## **Conclusions**

The present results add functional data on the complex role of dendritic cells in the mechanisms of liver injury indicating that the rapid expansion of HDCs in response to hepatic injury involves monocyte differentiation to inflammatory moDCs. Moreover, our data point to the involvement of CX<sub>3</sub>CR1/CX<sub>3</sub>CL1 dyad in modulating moDC differentiation within the liver. These results, along with previous observations by our laboratory on the involvement of CX<sub>3</sub>CR1 expressing moDC in the pathogenesis of NASH, open the possibility of using antagonists of CX<sub>3</sub>CR1 as a therapeutic opinion to prevent the evolution of steatohepatitis.



## Section 3

### **Role of ICOS/ICOSL dyad in the interaction between T-cell and macrophages during NASH evolution.**

#### **Foreword**

A large body of evidence indicates that hepatic macrophages play a key role in directing the evolution of NASH (Tacke, et al. 2017). During chronic liver diseases liver macrophage consist of ontogenically distinct populations that include liver resident Kupffer cells and monocyte-derived macrophages (MoMFs) (Tacke, et al. 2017). These latter are the main responsible for the production of pro-inflammatory mediators responsible for the perpetuation for hepatocyte injury and liver inflammation, but also support the activation of hepatic stellate cells and extracellular matrix deposition during NASH progression to fibrosis and cirrhosis (Tacke, et al. 2017). Consistently, reducing MoMF liver ameliorates experimental NASH and reduces fibrosis evolution in a phase 2 clinical trial (Friedman, et al. 2018). What is less clear is how MoMFs interacts with other inflammatory cells within the liver and particularly with lymphocytes. In this respect several studies have demonstrated that lymphocyte derived cytokines such as IFN- $\gamma$ , IL-17 and LIGHT can stimulate pro-inflammatory responses MoMFs (Tang et al .2011; Luo et al. 2013; Wolf et al. 2014). However, the presence of more specific interactions between liver lymphocytes, particularly T-cells and MoMFs has so far received little attention. Among the signals involved in the interaction of T-cells with other myeloid cells a special role is played by the co-stimulatory molecules Inducible T-cell Co-Stimulator (ICOS; CD278 ) and its ligand ICOSL (CD275, also named B7h, B7-H2, B7RP-1, LICOS) (Wikenheiser and Stumhofer 2016). ICOS belongs to the CD28 family of co-stimulatory molecules and is selectively expressed by activated T cells, while its ligand ICOSL/ICOSL is constitutively present on the surface of a variety of myeloid cells including dendritic cells, macrophages, B-cells, but also on endothelial cells, lung epithelium cells and fibroblasts (Wikenheiser and Stumhofer 2016). The triggering of ICOS on T-cells by

ICOSL/ICOSL has been shown to modulate their cytokine secretion pattern (Wikenheiser and Stumhofer 2016) and favour regulatory T cell (Treg) differentiation (Li and Xiong 2020). In addition, ICOS/ICOSL interaction plays an important role in the development and differentiation of Follicular T-helper cells (Tfh) in the germinal centres of lymphatic nodes (Wikenheiser and Stumhofer 2016). This action is critical in the selection and survival of B cells expressing high-affinity B cell receptors, as well as in facilitating their differentiation into memory B cell and plasma cells (Wikenheiser and Stumhofer 2016). However, recent reports have shown that ICOS/ICOSL interaction can also trigger reverse signals able to modulate the functions of ICOSL-expressing cells. For instance, in dendritic cells ICOSL-mediated signals favor maturation and stimulate cytokine secretion and antigen presentation (Tang et al 2009; Occhipinti et al. 2013), while in monocytes they prevent the differentiation to osteoclast stimulated by RANK ligand (Gigliotti et al.2016). A recent study has also shown that by binding to  $\alpha\text{v}\beta\text{3}$  integrin on podocytes ICOSL ameliorates kidney injury and the development of proteinuria (Koh et al. 2019). From these observations the present study investigated the possible involvement of ICOS/ICOSL dyad in the evolution of liver inflammation and fibrosis in NASH.

## Results

Preliminary analysis of ICOS and ICOSL expression within the livers of mice with NASH induced by feeding the MCD diet for different times showed a decline in the ICOS transcript with the development of steatohepatitis, while ICOSL mRNA showed a progressive increase paralleling the evolution of liver damage (Fig. 25). Further analysis using flow cytometry of liver myeloid cells demonstrated that the fraction of ICOS-positive liver lymphocytes was not significantly modified in mice receiving the MCD diet for 6 weeks (Fig. 26A). Nonetheless, while in control mice most of ICOS-expressing lymphocytes were CD4<sup>+</sup> T cells, we observed that NASH was characterized by a lowering of, respectively 41% and 30% for CD4<sup>+</sup>/ICOS<sup>+</sup> and CD4<sup>-</sup>/CD8<sup>-</sup>/ICOS<sup>+</sup> T cells and by a parallel 4 folds expansion of the pool of ICOS<sup>+</sup>/CD8<sup>+</sup> T-lymphocytes (Fig. 26). These changes only partially reflected the modifications in liver T cell distributions as the fraction of CD4<sup>+</sup> T cells was unchanged (4.1±1.4% vs 4.3±1.9%), whereas CD8<sup>+</sup> T-cell prevalence increased by about 5 folds (1.7±1.2% vs 10.2±2.4%; p<0.03) in mice with NASH. On the other hand, we observed that both the intensity of ICOSL signal and the prevalence of ICOSL-positive leucocytes were increased in mice with NASH (Figure 27A). In both control and NASH mice ICOSL-expressing cells largely segregated with the fraction of CD11b<sup>+</sup>/F4-80<sup>+</sup> monocytes macrophages (MoMFs), while CD11b<sup>-</sup>/F4-80<sup>+</sup> Kupffer cells were largely negative. Furthermore, the increased prevalence of ICOSL-positive cells paralleled with the expansion of MoMF pool that characterizes the evolution of NASH (Fig. 27B). In line with these findings the comparison of mice with NAFLD/NASH induced by the feeding with high fat diet or CDAA diet for 24 weeks we observed a positive correlation between the expression of ICOSL and that of inflammatory markers such as TNF- $\alpha$  (r=0.66, p=0.04) and DC11b (r=0.77, p=0.01). Interestingly, the serum content of the soluble forms of both ICOS and ICOSL were significantly higher in 24 patients with NAFLD/NASH at various stage of the disease evolution than in a group of healthy individuals (Fig. 28), suggesting that an up-regulation of co-stimulatory ICOS /ICOSL system is a feature of NASH and can be related to the disease evolution.

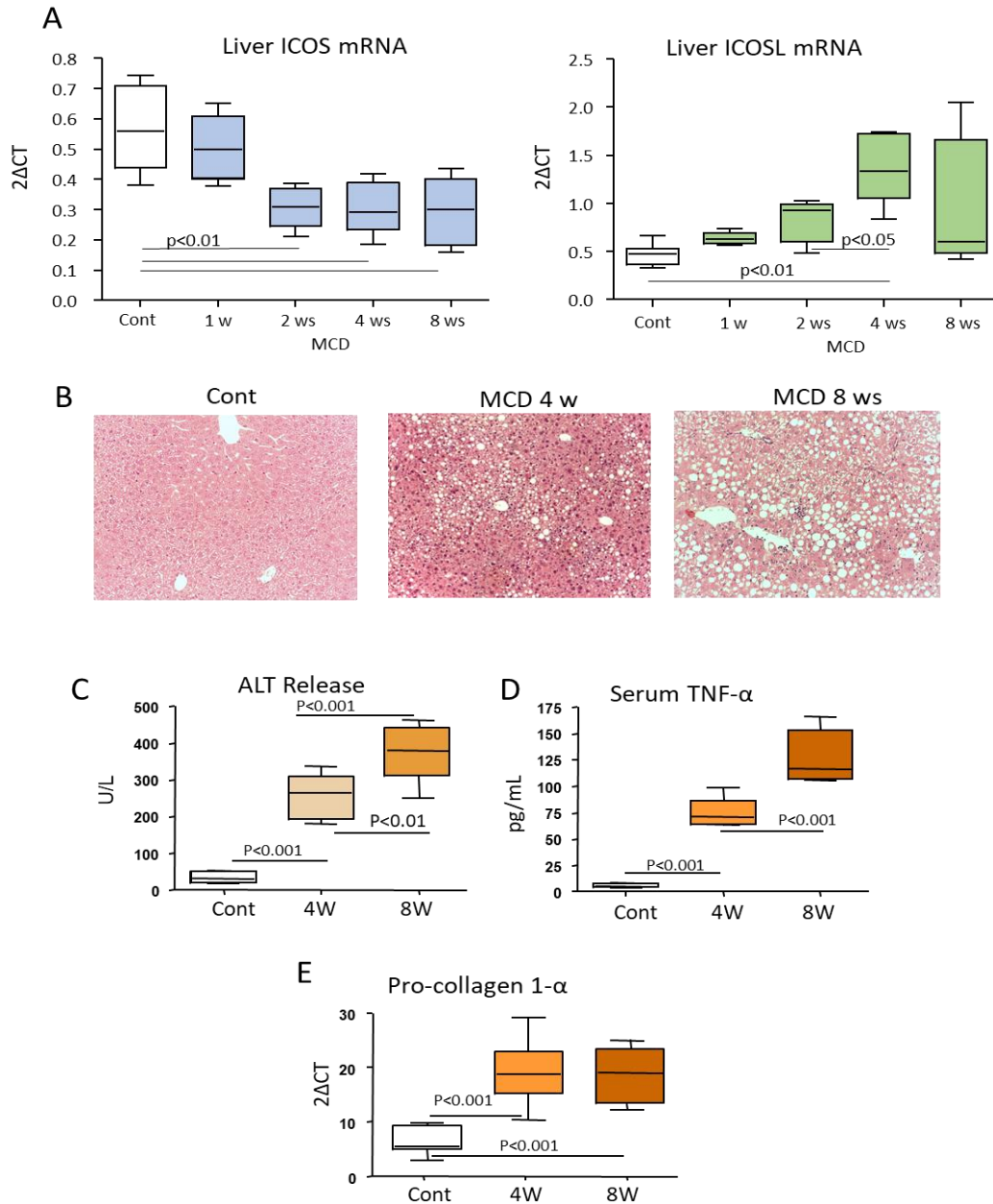


**Figure 25:** Time dependent changes in the transcripts of ICOS and ICOSL during the evolution of NASH induced by mice feeding with a methionine/choline deficient (MCD) diet.

Wild type C57BL/6 mice received MCD or control diets for up to 8 weeks and the animals were investigated for (Panel A) the hepatic mRNA levels of ICOS and ICOSL and the extent of liver injury as monitored by: (Panel B) Hematoxylin/eosin staining of liver sections (magnification 200x); (Panel C) Alanine aminotransferase (ALT) release; (Panel D) Immuno-enzymatic determination of circulating TNF- $\alpha$ . (Panel E) the mRNA expression of pro-collagen-1 $\alpha$ . RT-PCR values are expressed as 2<sup>ΔCT</sup> over the  $\beta$ -actin gene. The values refer to 5-6 animals per group and the boxes include the values within 25<sup>th</sup> and 75<sup>th</sup> percentile, while the horizontal bars represent the medians. The extremities of the vertical bars (10<sup>th</sup>-90<sup>th</sup> percentile) comprise 80% percent of the values.

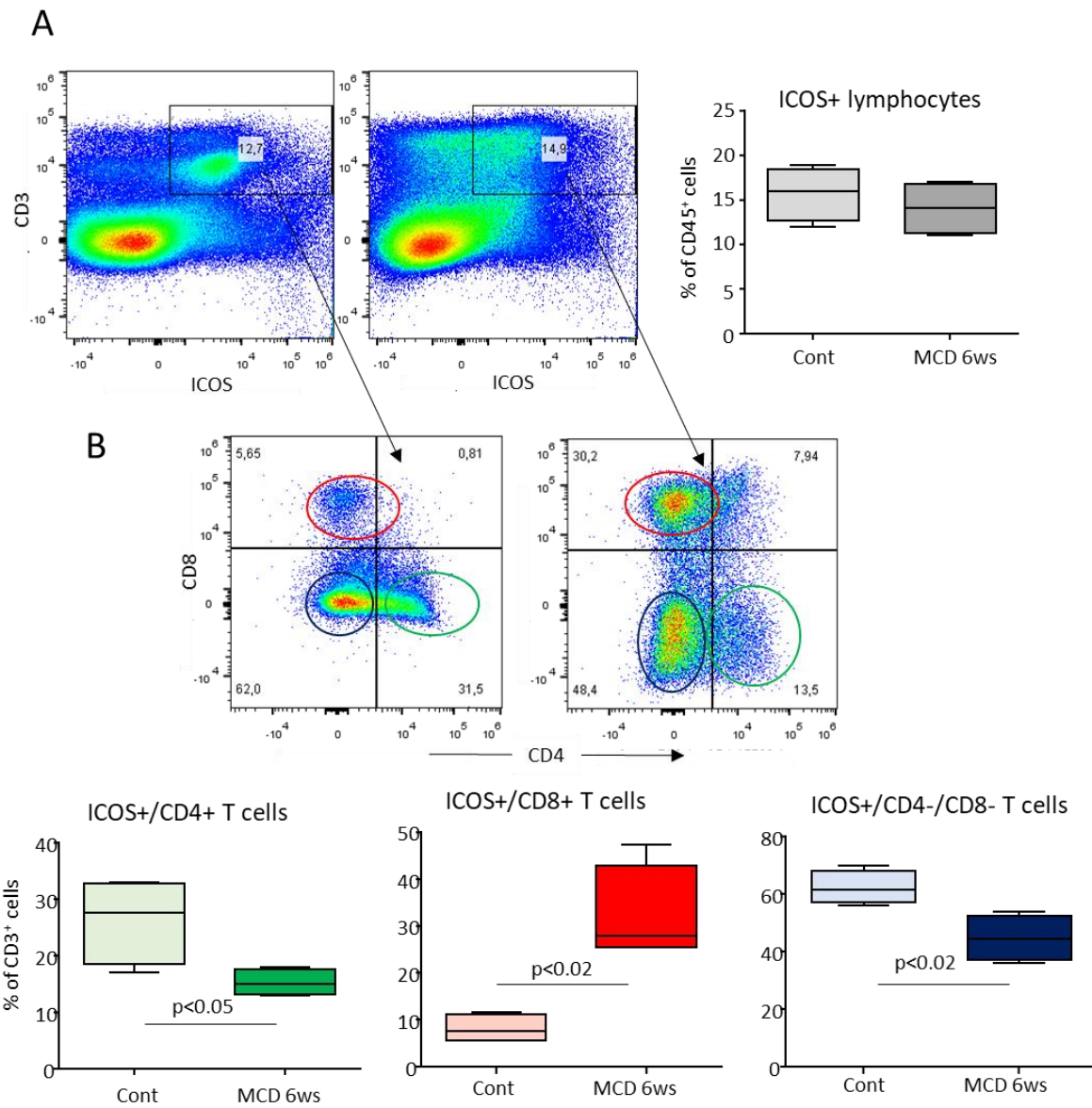


**Figure 26:** Changes in the T lymphocyte expression of ICOS in liver of mice with NASH induced by feeding with a methionine/choline deficient (MCD) diet.

Wild type C57BL/6 mice received MCD or control diets for 6 weeks and hepatic lymphocytes were analyzed by flow cytometry. (Panel A) ICOS expression by the whole pool of CD3<sup>+</sup> T lymphocytes. (Panel B) localization of ICOS-positive T cell in relation to the distribution of CD4<sup>+</sup> helper and CD8<sup>+</sup> cytotoxic and double negative T cells. The values refer to 3-4 animals per group and the boxes include the values within 25<sup>th</sup> and 75<sup>th</sup> percentile, while the horizontal bars represent the medians. The extremities of the vertical bars (10<sup>th</sup>-90<sup>th</sup> percentile) comprise 80% percent of the values.

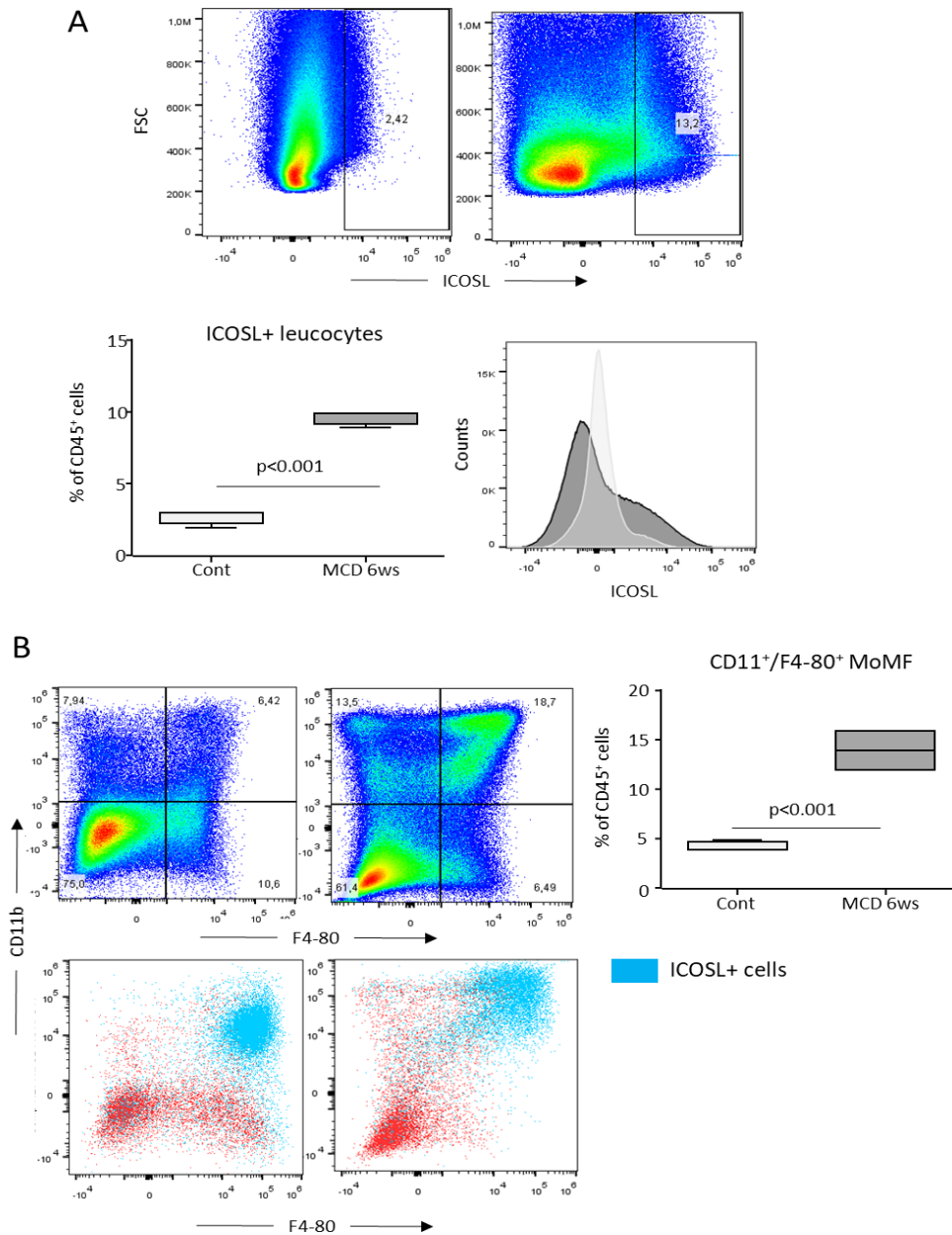


**Figure 27:** Changes in expression of ICOSL among myeloid cells in liver of mice with NASH induced by feeding with a methionine/choline deficient (MCD) diet.

Wild type C57BL/6 mice received MCD or control diets for 6 weeks and hepatic myeloid cells were analyzed by flow cytometry. (Panel A) ICOS expression by the whole pool of liver myeloid cells. (Panel B) localization of ICOSL-positive cell in relation to the distribution of CD11<sup>+</sup>/F4-80 hepatic monocyte/macrophages. The values refer to 3-4 animals per group and the boxes include the values within 25<sup>th</sup> and 75<sup>th</sup> percentile, while the horizontal bars represent the medians. The extremities of the vertical bars (10<sup>th</sup>-90<sup>th</sup> percentile) comprise 80% percent of the values.

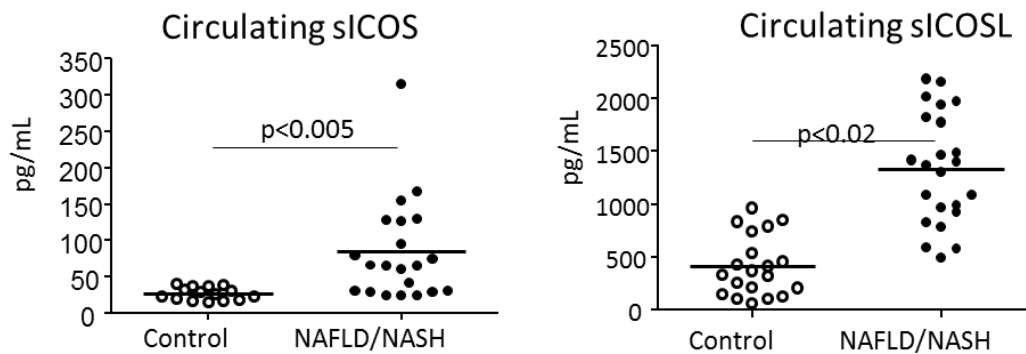


**Figure 28:** Changes in the circulating levels of soluble ICOS and ICOSL in patients with NAFLD/NASH.

The levels of the soluble forms of ICOS (sICOS) and ICOSL (sICOSL) were measured by ELISA assay in the sera of 20 healthy controls and 22 patients with NAFLD/NASH. The bars represent the median values.

In subsequent experiments we investigated whether the lack of ICOSL might influence inflammatory and immune responses involved in NASH evolution. For these experiments we took advantage of ICOSL deficient mice (ICOSL<sup>-/-</sup>) that received the MCD diet for 6 weeks. Figure 29 show that liver histology of MCD-fed ICOSL<sup>-/-</sup> mice did not revealed appreciable differences in the extension of steatosis as compared to wild-type animals. Conversely, transaminase release as well as the transcripts for inflammatory markers such as CD11b, TNF- $\alpha$ , CXCL10 were significantly lower in ICOSL<sup>-/-</sup> than wild type mice (Fig. 29). On the same vein, we observed that Sirius Red staining for collagen as well as the levels mRNAs for fibrosis markers such as pro-collagen-1 $\alpha$  and smooth muscle  $\alpha$ -actin ( $\alpha$ -SMA) were lowered in the absence of ICOSL (Fig. 30).

Previous studies have shown that ICOSL<sup>-/-</sup> mice are characterized by a reduction in the number and size of the lymphatic germinal centres in the spleen and reduced production of IgG1 (Wikenheiser and Stumhofer 2016). Furthermore, Watanabe and co-workers (Watanabe et al. 2010) have observed that defects in ICOS-mediated co-stimulation results in a defect in the development of NKT cells in the thymus that reflects on a reduction in liver and spleen NKT cells in ICOS<sup>-/-</sup> mice. However, in our hand liver CD3<sup>+</sup>/CD4<sup>+</sup>, CD3<sup>+</sup>/CD8<sup>+</sup> T-lymphocytes and CD3<sup>+</sup>/NK1.1<sup>+</sup> NKT cells were not significantly different between MCD-fed ICOSL<sup>-/-</sup> and wild type mice (not shown). As expected, the lack of ICOS-mediated signals affected IgG production and

NASH associated titers of IgG against oxidative stress derived epitopes (anti-OSE IgG) were appreciably lower in ICOS<sup>-/-</sup> mice (0.30±0.17 optical units in wild type vs 0.05±0.03 in ICOSL<sup>-/-</sup> mice; p<0.02). Such an impairment of B-cell maturation did not influence the distribution of liver B220<sup>+</sup>/IgM<sup>+</sup> B lymphocytes that were similar in the two strains (not shown). Although ICOS/ICOSL dyad has been shown to contribute in regulating Th-1 responses in different experimental settings, the liver transcripts for lymphocyte Th-1 transcription factor T-bet and for interferon- $\gamma$  (INF- $\gamma$ ) were significantly higher in ICOSL<sup>-/-</sup> mice with NASH than in wild type littermates (T-bet = 0.10±0.03<sup>-2</sup> $\Delta$ CT vs 15.5±0.50<sup>-2</sup> $\Delta$ CT; p<0.05; INF- $\gamma$  = 0.16±0.04<sup>-2</sup> $\Delta$ CT vs 0.23±0.04<sup>-2</sup> $\Delta$ CT; p<0.02). This indicated that the costimulatory functions of ICOS/ICOSL dyad in T-cells were not responsible for the improvement of liver damage and inflammation observed in ICOSL<sup>-/-</sup> mice.

From these data we went on to investigate whether reverse signals mediated by ICOSL in MoMFs might influence their functions during the progression of NASH. Flow cytometry analysis of liver CD11b<sup>+</sup>/F4-80<sup>+</sup> MoMFs revealed that the lack of ICOSL did not affected the prevalence of CD11b<sup>high</sup>/F4-80<sup>+</sup> MoMFs (Fig. 31). The fraction of CD11b<sup>high</sup>/F4-80<sup>+</sup> MoMFs includes inflammatory M1 macrophages that express high level of the lymphocyte antigen 6 (Ly6C) also known as tissue plasminogen activator receptor (When et al 2020). The analysis of the fraction of CD11b<sup>high</sup>/Ly6C<sup>high</sup> MoMFs in the livers of wild type and ICOSL<sup>-/-</sup> mice receiving the MCD diet demonstrated an appreciable a reduction of these cells in ICOSL<sup>-/-</sup> mice (Fig. 31A). We previously shown that the Ly6C expression characterizes monocyte derived dendritic cells (moDCs) that are expanded in the liver of mice with NASH and support inflammation (Sutti et al. 2015; Sutti et al. 2019). Since ICOS/ICOSL action can contribute to moDC maturation (Tang et al 2009; Occhipinti et al. 2013), we also explored whether defect of ICOSL might affect liver MoDC pool in NASH. However, as shown in Figure 31B no significant changes were observed between wild type and ICOSL<sup>-/-</sup> mice neither in the fraction of whole liver CD11c<sup>+</sup>/MHCII<sup>+</sup> dendritic cells not in the subset of CD11c<sup>+</sup>/MHCII<sup>+</sup>/CD11b<sup>+</sup>/Ly6C<sup>+</sup> MoDC. Altogether these data suggested that the improvement of steatohepatitis in these animals might be related to an effect of ICOSL-mediated reverse signals on the activity of pro-inflammatory M1 macrophages.



Recent reports have shown that pro-inflammatory activation of liver MoMFs involves the expression of the Triggering Receptor Expressed on Myeloid cells 1 (TREM-1) (Arts et al. 2013; Nguyen-Lefebvre et al. 2018). TREM-1 is a cell-surface-activating receptor belonging to Ig superfamily that is involved in amplifying inflammatory responses in granulocytes and macrophages (Arts et al. 2013). TREM-1 transduce its signals by associating with the adaptor molecule DAP12 which recruits the protein kinase SYK to activate downstream signals involving phosphoinositide-3 kinase (PI3K), phospholipase C extracellular regulated kinase (ERK) (Arts et al. 2013). TREM-1 ligands involve DAMPs such as HMGB1 and HSP70, but also bacterial products and TREM-1-mediated stimulation greatly increases cell production of pro-inflammatory mediators including cytokines and chemokines (Arts et al. 2013). Within the liver TREM-1 is almost exclusively expressed by MoMFs and its activity promotes hepatic inflammation and the progression of chronic damage to fibrosis (Nguyen-Lefebvre et al. 2018). Furthermore, a recent study has also shown that TREM-1 was overexpressed in the liver of mice with experimental NASH and blocking TREM-1 attenuates liver injury and inflammation in these animals (Rao et al. 2019). By evaluating the TREM-1 transcripts in mice receiving the MCD diet we confirmed that NASH was associated to a 12 folds up-regulation of TREM-1 (Fig. 29). Moreover, in the absence of ICOSL TREM-1 expression was lowered by about 25% (Fig. 29). Interestingly, TREM-1 expression was also down regulated by about 30% also in ICOS-deficient mice (ICOS<sup>-/-</sup>) receiving the MCD diet for 6 weeks ( $0.31 \pm 0.12^{-2}\Delta\text{CT}$  in ICOS<sup>-/-</sup> vs  $0.49 \pm 0.15^{-2}\Delta\text{CT}$  in wild type mice;  $p < 0.05$ ) in parallel with the lowering with inflammatory markers (TNF- $\alpha$  =  $0.85 \pm 0.28^{-2}\Delta\text{CT}$  vs  $1.77 \pm 0.30^{-2}\Delta\text{CT}$ ;  $p < 0.001$ ; CXCL10 =  $8.02 \pm 3.02^{-2}\Delta\text{CT}$  vs  $16.3 \pm 4.50^{-2}\Delta\text{CT}$ ;  $p < 0.01$ ; CD11b =  $3.14 \pm 0.63^{-2}\Delta\text{CT}$  vs  $6.14 \pm 1.94^{-2}\Delta\text{CT}$ ;  $p < 0.02$ ), suggesting that the signals involving ICOS/ICOSL dyad were responsible for sustaining TREM-1 mediated macrophage M1 responses. Supporting such an interpretation we observed that TREM-1 transcripts were significantly lower ( $3.2 \pm 0.8^{-2}\Delta\text{CT}$  vs  $0.8 \pm 0.3^{-2}\Delta\text{CT}$ ;  $p < 0.02$ ) in peritoneal macrophages obtained from ICOSL<sup>-/-</sup> mice receiving intraperitoneal injection of thioglycolate as compared to macrophages from wild type animals.

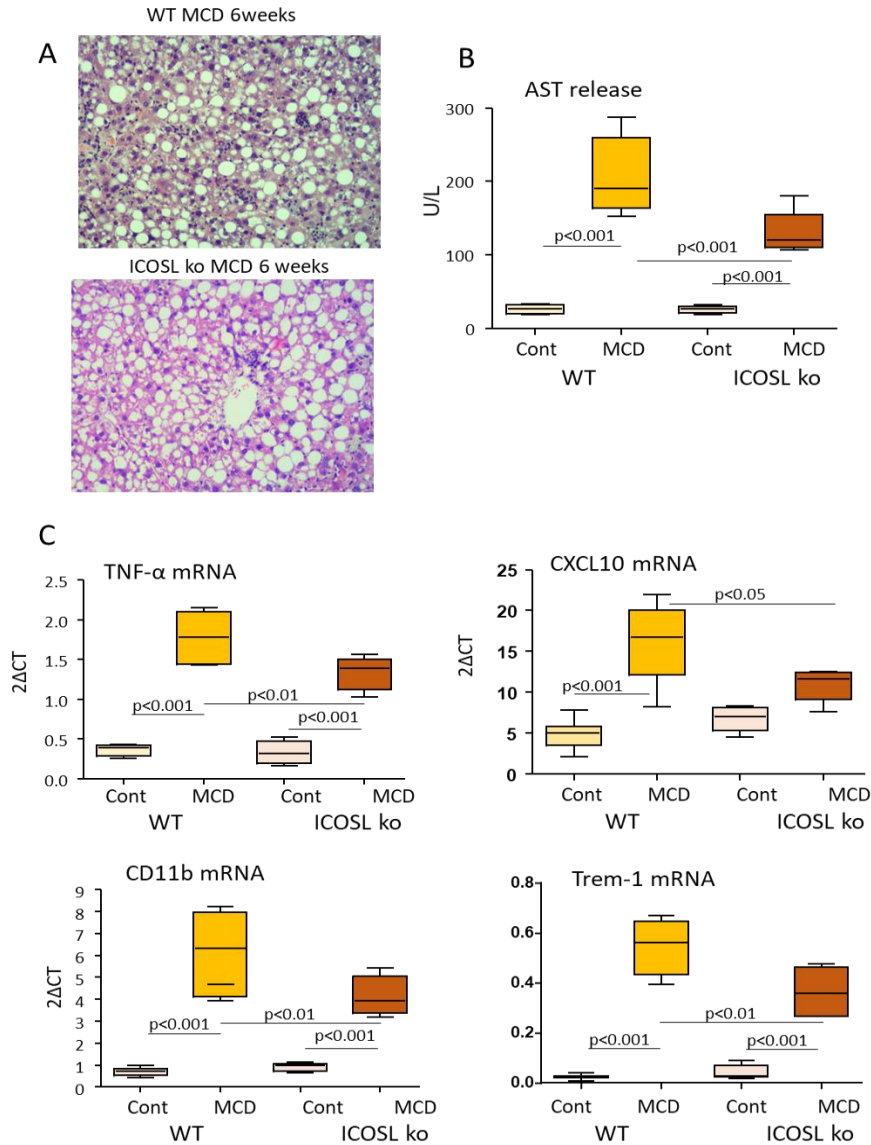


**Figure 29:** ICOSL deficiency reduces the severity of liver injury and inflammation in mice with NASH.

ICOSL deficient (ICOS ko) and wild type (WT) mice were fed with either control or MCD diets for 6 weeks and the animals were investigated for the severity of steatohepatitis. (Panel A) Haematoxylin/eosin staining of liver sections (Magnification 200x); (Panel B) Alanine aminotransferase (ALT) release; (Panel C) The hepatic mRNA levels of pro-inflammatory markers TNF- $\alpha$ , CXCL10, CD11b and TREM-1. RT-PCR values are expressed as fold increase over control values after normalization to the  $\beta$ -actin gene. The values in the panels B, C and E refer to 5-7 animals per group and the boxes include the values within 25<sup>th</sup> and 75<sup>th</sup> percentile, while the horizontal bars represent the median. The extremities of the vertical bars (10<sup>th</sup>-90<sup>th</sup> percentile) include 80% of the values.

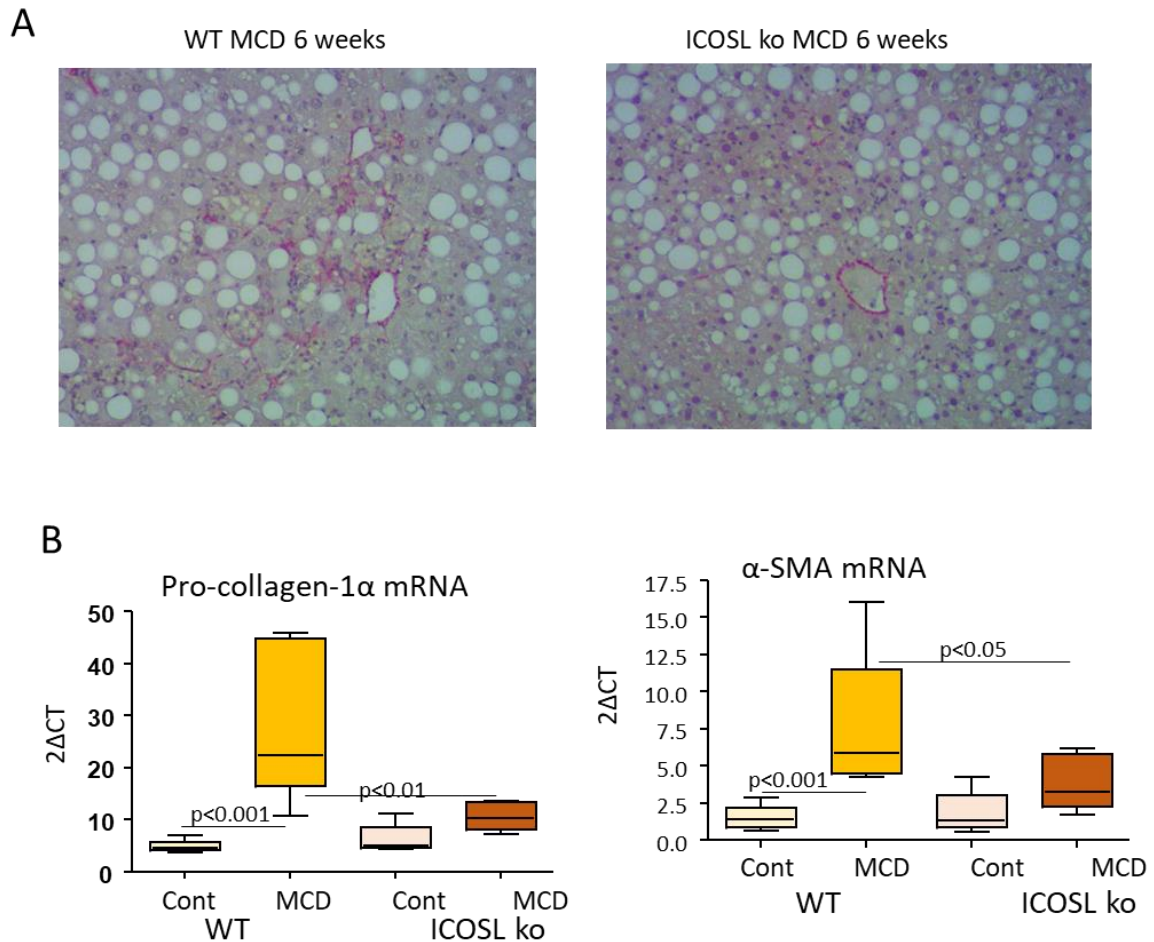


**Figure 30:** ICOSL deficiency improves NASH evolution to fibrosis.

ICOSL deficient (ICOS ko) and wild type (WT) mice were fed with either control or MCD diets for 6 weeks and the animals were investigated for the extension of liver fibrosis. (Panel A) Collagen deposition as detected by Sirius Red staining in representative liver sections from wild type (WT) and ICOSL deficient (ICOS ko) mice receiving the MCD diet for 6-weeks (Magnification 200x). (Panel B) Hepatic expression of fibrogenesis markers  $\alpha$ 1-procollagen,  $\alpha$ -smooth muscle actin ( $\alpha$ -SMA) and Transforming Growth Factor- $\beta$ 1 (TGF- $\beta$ 1). RT-PCR values are expressed as fold increase over control values after normalization to the  $\beta$ -actin gene. (B) The values refer to 5-7 animals per group and the boxes include the values within 25<sup>th</sup> and 75<sup>th</sup> percentile, while the horizontal bars represent the median. The extremities of the vertical bars (10<sup>th</sup>-90<sup>th</sup> percentile) include 80% of the values.

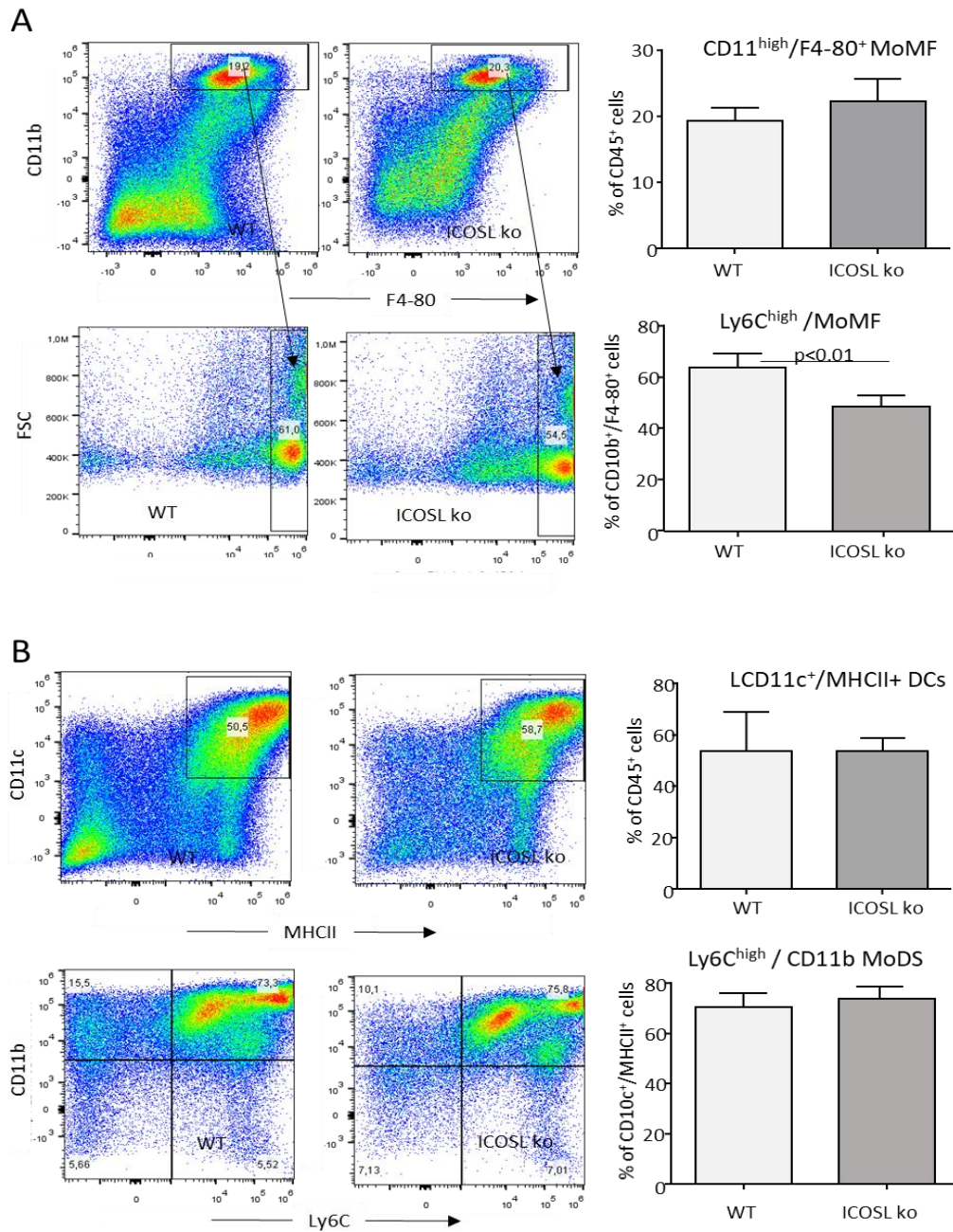


**Figure 31:** ICOSL deficiency reduces the liver infiltration of pro-inflammatory monocyte/macrophages.

ICOSL deficient (ICOS ko) and wild type (WT) mice were fed with either control or MCD diets for 6 weeks and the animals were investigated by flow cytometry for the prevalence of pro-inflammatory monocyte/macrophages (MoMFs) and monocyte-derived dendritic cells (MoDCs). (Panel A) Prevalence of liver CD11b<sup>high</sup>/F4-80<sup>+</sup> MoMF and Ly6C<sup>high</sup> MoMFs. (Panel B) Prevalence of liver CD11c<sup>+</sup>/MHCII<sup>+</sup> dendritic cells (DCs) and of CD11c<sup>+</sup>/MHCII<sup>+</sup>/CD1b<sup>+</sup>/Ly6C<sup>+</sup> monocyte-derived DCs (moDCs). The values refer to 3-4 animals per group  $\pm$  SD.

## Discussion

So far, the mechanisms by which adaptive immunity can support hepatic inflammation in NASH have not been investigated in detail. In principle, the network of cytokines generated by Th-1, Th-17 and CD8<sup>+</sup> lymphocytes is capable to provide a potent stimulus for the M1 activation of hepatic macrophage, which, in turn, supports lymphocyte functions through the release of a variety of mediators including interleukin-12, (IL-12), interleukin-23 (IL-23) and the lymphocyte chemokines CXCL9-10-11 (Tacke 2017). In line with this view mice deficient for the lymphocyte cytokine LIGHT (Lymphotoxin-like Inducible protein that competes with Glycoprotein D for Herpesvirus entry on T cells; TNFSF14) are protected against steatohepatitis when receiving a high fat choline-deficient diet (Wolf et al. 2014) and IFN- $\gamma$  deficient mice develop less steatohepatitis and fibrosis than wild-type littermates when fed with a methionine/choline deficient (MCD) diet (Luo et al. 2013). However, it is well possible that the network of signals involved in supporting chronic inflammation might be far more complex.

Here we show that direct interaction between macrophages and lymphocyte through the interaction with the co-stimulatory molecules ICOS and ICOSL could provide additional stimuli for sustaining pro-inflammatory responses during the progression of NASH. So far most of the studies regarding ICOS/ICOSL functions have been focalized on the effects on T-cells, where ICOS is up-regulated upon activation (Wikenheiser and Stumhofer 2016). The triggering by ICOSL of ICOS on CD4<sup>+</sup> T-cell has been shown to modulate their Th-1 or Th2 functions depending on the environment stimulation (Wikenheiser and Stumhofer 2016). In addition, ICOS/ICOSL interaction plays an important role in the development and differentiation of Follicular T-helper cells (Tfh) in the germinal centres of lymphatic nodules (Wikenheiser and Stumhofer 2016). However, recent reports have shown that ICOS/ICOSL interaction can also trigger reverse signals able to modulate the functions of ICOSL-expressing cells. For instance, in monocyte-derived dendritic cells ICOSL-mediated signals favor maturation stimulating cytokine secretion and antigen presentation (Tang et al 2009; Occhipinti et al. 2013), while they prevent monocytes differentiation to osteoclasts stimulated by RANK ligand (Gigliotti et al. 2016). These observations suggest the possibility that

ICOS expressing T-cells might modulate the function of monocytes/macrophages through the interaction with ICOSL. On this respect we have observed that, while overall liver expression of ICOS does not change in NASH, the progression of steatohepatitis is characterized by a dept change in the distribution of ICOS among T cells with a reduction of CD4<sup>+</sup>/ICOS<sup>+</sup> and CD4<sup>-</sup>/CD8<sup>-</sup>/ICOS<sup>+</sup> T cells and a parallel expansion of the CD8<sup>+</sup>/ICOS<sup>+</sup> pool. The expansion of activated cytotoxic T-cells is a feature of NASH in either rodents and humans (Sutti, et al.2014; Wolf, et al. 2014; Grohmann, et al. 2018; Ghazarian, et al.2017; Breuer et al. 2020) and their ablation is effective in ameliorating steatohepatitis in wild-type mice receiving a high fat/high carbohydrate diet (Bhattacharjee, et al. 2017; Breuer et al. 2020). Nonetheless, the mechanisms implicating CD8<sup>+</sup> T cells in the pathogenesis of NASH are not well characterized. Wolf and coworkers have shown that  $\beta 2m^{-/-}$  mice lacking CD8<sup>+</sup> T- and NKT cells are protected from steatohepatitis in relation to the capacity of CD8<sup>+</sup> T- and NKT cells to produce LIGHT (Wolf, et al.2014). More recently Breuer et al. (2020) have reported that IL-10-expressing CD8<sup>+</sup> T cells isolated from the liver of mice with obesity-associated NASH have the capability to stimulate macrophage and hepatic stellate cell (HSC) activation. However they did not investigate the mechanisms involved. Here we propose the possibility that ICOS expressing CD8<sup>+</sup> T cell might promote macrophage activation through reverse signaling involving ICOSL. Such a hypothesis is based on the observation that the pool of ICOS<sup>+</sup>/CD8<sup>+</sup> T cells expand in NASH livers and that the lack of both ICOS and ICOSL reduces NASH associated inflammation and fibrosis. In particular, we have observed that the absence of ICOSL reduces the fraction of Ly6C pro-inflammatory macrophages and that this associated with the lowering in the expression of TREM-1, a membrane receptor implicated in maintaining M1 activation of liver macrophages (Arts et al. 2013). The implication of ICOSL ligand in sustaining pro-inflammatory MoMFs along with the selective upregulation of ICOS in CD8<sup>+</sup> T lymphocytes might also explain how the expansion of these cells can support the evolution of steatohepatitis. In a recent report Torres-Hernandez and co-workers (2019) have demonstrated that during the evolution of NASH ICOS is required for the differentiation of a specific subset of  $\gamma\delta$ T cells producing IL-17A which are involved in modulating hepatic inflammation in NASH.  $\gamma\delta$ T cells are a distinct subset of CD3<sup>+</sup> T cells defined by expressing  $\gamma\delta$ T cell receptor (TCR) instead of the conventional  $\alpha\beta$ TCR and constitute about 15%~25% of all liver

T cells. Through  $\gamma\delta$ TCR,  $\gamma\delta$ T cells can rapidly respond to a variety of protein and non-protein antigens promoting inflammatory responses (Hammerich and Tacke 2014). Although we cannot exclude that the absence of ICOSL might influence the differentiation of liver  $\gamma\delta$ T cells in mice fed with the MCD-diet this possibility appears unlikely to explain the improvement of steatohepatitis in these animals since we have observed that ICOS-expressing  $CD4^+/CD8^-$  T cells which include  $\gamma\delta$ T cells are lowered in the liver of NASH mice without further changes in ICOSL<sup>-/-</sup> animals. Nonetheless further analysis are required to better define whether modulation of  $\gamma\delta$ T cells can contribute to improving NASH in ICOSL-deficient mice also considering that the mechanisms proposed by Torres-Hernandez and co-workers for explaining the amelioration of steatohepatitis in mice lacking  $\gamma\delta$ T cells implicate a suppression of INF- $\gamma$  production by  $CD4^+$  T cells that has not been verified in our experimental setting where INF- $\gamma$  expression was instead increased in the liver of MCD-fed ICOSL<sup>-/-</sup> mice as compared to wild type littermates. To our knowledge the only study that has so far addressed the role of ICOS and ICOSL in tissue healing responses is a work by Tanaka and coworkers who have reported that that ICOS deficiency prevents lung fibrosis induced in mice by bleomycin administration whereas ICOSL deficiency aggravates it (Tanaka et al 2010). Such a divergent behaviours associate with opposite effects on lung inflammatory cell recruitment and in the production of inflammatory cytokines (Tanaka et al 2010). The partial inconsistency of these results with our data in the liver the difference in the experimental systems as well as by the fact in the lung the severity of fibrosis inversely correlates with ICOSL expression (Tanaka et al 2010) whereas the reverse occurs in the liver.

In conclusion these results demonstrate the implication of ICOS/ICOSL dyad in modulating liver inflammatory reactions during the evolution of NASH and propose the contribution of reverse ICOSL signalling in the interaction between  $CD8^+$  T lymphocytes and macrophages. The results might have possible implications in developing new approaches for the treatment of NASH since monoclonal antibodies targeting ICOS and ICOSL are already under trial for immune-modulatory therapies in cancer.

## General Discussion

In the recent years, the contribution of adaptive immunity to the pathogenesis of NASH has received increasing interest. On this respect, several studies have given clear evidence that the expansion and activation of CD4<sup>+</sup> and CD8<sup>+</sup> T lymphocytes are implicated in supporting hepatic inflammation during the evolution of NAFLD/NASH (Sutti, et al.2014; Wolf, et al. 2014; Grohmann, et al. 2018; Ghazarian, et al.2017; Breuer et al. 2020). Recent data have also given some insight in how lymphocytes can interact with innate immunity cells favouring their pro-inflammatory and pro-fibrogenic actions. Nonetheless, many aspects concerning the implication of immune mechanisms in NASH remain elusive. The work performed during my doctoral training tackle some of these aspects investigating the role of B and CD8<sup>+</sup> T lymphocytes in the mechanisms of NASH associated hepatic inflammation.

From the observation that circulating IgG targeting oxidative stress derived epitopes characterize either experimental and human NASH and are an independent predictor of the disease evolution to fibrosis it has been possible to demonstrate that B cell activation is an early event in the onset of NASH preceding T-cell responses. On the same vein, interfering with B-cells maturation reduces Th-1 activation of liver CD4<sup>+</sup> T-lymphocytes and ameliorates liver injury and the development of fibrosis. The contribution of B cells to the evolution to fibrosis of chronic liver disease has been recently confirmed by a study performed in a model of cholestatic liver diseases using mice with deficiency of biliary transport proteins Mdr2 in which B cells depletion by anti-CD20 mAb improves both hepatic inflammation and fibrosis (Thapa et al. 2020). So far, the clinical relevance of the above findings has not been investigated in detail. We have shown that in about 60% of NAFLD/NASH patients B- and T-lymphocytes form focal aggregates, resembling ectopic lymphoid structures and that the size and the prevalence of these aggregates positively correlate with the scores of lobular inflammation and fibrosis. Furthermore, McPherson and co-workers have observed that serum IgA are more frequently elevated among patients with NASH than in subjects with simple steatosis and are as well an independent predictor of advanced liver fibrosis (McPherson et al.2014). This latter observation is relevant also for a better



understanding of the mechanisms implicated in the evolution of NASH to hepatocellular carcinoma. In fact, Shalapour and co-workers (Shalapour et al. 2017) have observed that both in humans and in mice advanced NASH is characterized by the accumulation of IgA-producing plasma cells that suppress anti-tumor cytotoxic CD8<sup>+</sup> T-cells through the expression of PD-L1 and IL-10, thus favoring HCC emergence. In these conditions, genetic or pharmacological interference with IgA-producing plasma cells restore the cytotoxic activity of CD8<sup>+</sup> T-cells and attenuate hepatic carcinogenesis (Shalapour et al. 2017). If further confirmed by human studies, the data concerning direct involvement of B cells in the mechanisms supporting chronic liver injury and might open the way for new therapeutic approaches to NASH by using already available treatments that interfere with B-cell functions.

A key problem in understanding how immune mechanisms promote the evolution of NASH concern the interplay among the different lymphocyte subsets and between adaptive and innate immune cells. The data so far available indicate the ablation of B-lymphocytes, CD8<sup>+</sup> T and NKT cells reduces MoMF activation and ameliorates liver injury, lobular inflammation and fibrosis in different mice model of NASH (Wolf et al. 2014; Breuer et al. 2020). This suggests the possibility that these cells might interact with MoMFs by a variety of mechanisms. The experiments performed using ICOSL-deficient animals open a new approach in investigating the problem by showing that, beside cytokine and chemokine production, CD8<sup>+</sup> T lymphocytes, can dialogue with MoMFs through membrane signals involving the co-stimulatory molecules ICOS and ICOSL. The main function ICOSL is the triggering of ICOS on activated T cells that leads to functional modulation (Wikenheiser and Stumhofer 2016; Li and Xiong 2020). However, recent reports have shown that the ICOS/ICOSL interaction can trigger bidirectional signals able to influence the response of ICOSL-expressing cells such as dendritic cells and osteoclasts (Occhipinti et. al 2013; Gigliotti et al 2016). As MoMFs, dendritic cells and osteoclasts are derived from monocytes and express ICOSL upon differentiation, suggesting that ICOSL signalling might be critical for the functions of monocyte-derived cells. Our results in NASH suggest a novel role of ICOSL in the interaction between CD8<sup>+</sup> lymphocytes and MoMFs that appear critical to support the combined pro-inflammatory capability and pro-fibrogenetic activities of Ly6C<sup>high</sup> MoMF without affecting the Ly6C<sup>low</sup> population that has anti-fibrotic activity (Wen et al. 2020). Interestingly a recent

report by Sun and co-workers has also implicated the co-stimulatory signals in the pathogenesis of NASH. The authors reported in fact that the co-stimulatory molecule OX40 (CD134) and its ligand OX40L (CD252) are upregulated in the liver of mice with steatohepatitis. Interestingly, soluble OX40 is also elevated in the plasma of NASH patients positively correlating with the severity of steatohepatitis (Sun et al. 2018). OX40 is largely expressed on activated T-cells in both mice and humans (Bashiardes, et al. 2016). Upon ligation by OX40L, present on APCs, activated T-cells, endothelial cells and mast cells OX40 promotes T-cell survival, differentiation and activation (Bashiardes, et al. 2016). Along this, OX40 deficiency in mice with experimental NASH selectively lowers Th-1 and Th-17 differentiation of hepatic CD4<sup>+</sup> T-cells ameliorating steatosis, transaminase release and the prevalence of M1 macrophages (Sun et al. 2018). Altogether these observations suggest the possibility that the involvement of adaptive immunity in the progression of NASH might implicate a complex network of signals involving co-stimulatory molecules and possible co-inhibitory molecules expressed by a variety of myeloid cells.

Previous studies have demonstrated that reversed ICOSL signalling induces partial maturation of mouse dendritic cells (Tang et al 2009), while enhance cytokine secretion and the capacity to cross-present endocytosed antigens in human dendritic cells (Occhipinti et al 2013). Our data show that hepatic dendritic cell expansion that characterize the onset of NASH involves CD11b<sup>high</sup>/Ly6C<sup>high</sup> monocyte-derived myeloid dendritic cells (MoDCs). Preliminary data in ICOSL-deficient mice with NASH do not evidence appreciable changes in these cells as compared to wild type animals, indicating that ICOSL is dispensable for MoDC maturation in inflamed liver. On this later respect, we have observed that the presence of the fractalkine receptor CX<sub>3</sub>CR1 is important for MoDC expansion and maturation. Furthermore, interference with CX<sub>3</sub>CR1 acute liver damage supporting previous data (Sutti et al 2015) that implicate MoDCs in supporting lobular inflammation in NASH. Nonetheless, due to the difficulty to specifically distinguish between MoMFs and MoDCs using surface markers and flow cytometry further studies are required to better characterize the involvement of MoDCs in stimulating the activation of adaptive immunity as well as in defining their contribution to inflammatory response.

In conclusion the data obtained during my doctoral training have given further evidence of the complexity of the mechanisms involved in the progression of NASH pointing to the importance

of specific interactions between adaptive and innate immunity cells in supporting the disease evolution. Targeting these interactions might offer the possibility for developing novel therapeutic approaches to NASH.

## References

- Ahmed M. Non-alcoholic fatty liver disease in 2015. *World J Hepatol.* 2015;7(11):1450-1459. doi:10.4254/wjh.v7.i11.1450.
- Akazawa Y, Guicciardi ME, Cazanave SC, et al. Degradation of cIAPs contributes to hepatocyte lipoapoptosis. *Am J Physiol Gastrointest Liver Physiol.* 2013;305(9):G611-G619. doi:10.1152/ajpgi.00111.2013
- Albano E, Mottaran E, Vidali M, et al. Immune response towards lipid peroxidation products as a predictor of progression of non-alcoholic fatty liver disease to advanced fibrosis. *Gut.* 2005;54(7):987-993. doi:10.1136/gut.2004.057968
- Angulo P, Keach JC, Batts KP, Lindor KD. Independent predictors of liver fibrosis in patients with nonalcoholic steatohepatitis. *Hepatology.* 1999 Dec;30(6):1356-62. doi: 10.1002/hep.510300604.
- Arts RJ, Joosten LA, van der Meer JW, Netea MG. TREM-1: intracellular signaling pathways and interaction with pattern recognition receptors. *J Leukoc Biol.* 2013;93(2):209-215. doi:10.1189/jlb.0312145
- Baek C, Wehr A, Karlmark KR, et al. Pharmacological inhibition of the chemokine CCL2 (MCP-1) diminishes liver macrophage infiltration and steatohepatitis in chronic hepatic injury. *Gut.* 2012;61(3):416-426. doi:10.1136/gutjnl-2011-300304
- Baffy G, Brunt EM, Caldwell SH. Hepatocellular carcinoma in non-alcoholic fatty liver disease: an emerging menace. *J Hepatol.* 2012;56(6):1384-1391. doi:10.1016/j.jhep.2011.10.027.
- Bajaña S, Turner S, Paul J, Ainsua-Enrich E, Kovats S. IRF4 and IRF8 Act in CD11c+ Cells To Regulate Terminal Differentiation of Lung Tissue Dendritic Cells. *J Immunol.* 2016;196(4):1666-1677. doi:10.4049/jimmunol.1501870
- Bamboatz M, Ocuin LM, Balachandran VP, Obaid H, Plitas G, DeMatteo RP. Conventional DCs reduce liver ischemia/reperfusion injury in mice via IL-10 secretion. *J Clin Invest.* 2010;120(2):559-569. doi:10.1172/JCI40008
- Bashiardes S, Shapiro H, Rozin S, Shibolet O, Elinav E. Non-alcoholic fatty liver and the gut microbiota. *Mol Metab.* 2016;5(9):782-794. Published 2016 Jun 14. doi:10.1016/j.molmet.2016.06.003
- Baumgardner JN, Shankar K, Hennings L, Albano E, Badger TM, Ronis MJ. N-acetylcysteine attenuates progression of liver pathology in a rat model of nonalcoholic steatohepatitis. *J Nutr.* 2008;138(10):1872-1879. doi:10.1093/jn/138.10.1872
- Béland K, Marceau G, Labardy A, Bourbonnais S, Alvarez F. Depletion of B cells induces remission of autoimmune hepatitis in mice through reduced antigen presentation and help to T cells. *Hepatology.* 2015;62(5):1511-1523. doi:10.1002/hep.27991
- Bhattacharjee J, Kirby M, Softic S, et al. Hepatic Natural Killer T-cell and CD8+ T-cell Signatures in Mice with Nonalcoholic Steatohepatitis. *Hepatol Commun.* 2017;1(4):299-310. doi:10.1002/hep4.1041

Biegls V, Trautwein C. Innate immune signaling and gut-liver interactions in non-alcoholic fatty liver disease. *Hepatobiliary Surg Nutr.* 2014;3(6):377-385. doi:10.3978/j.issn.2304-3881.2014.12.04

Biegls V, van Gorp PJ, Walenbergh SM, et al. Specific immunization strategies against oxidized low-density lipoprotein: a novel way to reduce nonalcoholic steatohepatitis in mice. *Hepatology.* 2012;56(3):894-903. doi:10.1002/hep.25660

Brandl K, Schnabl B. Intestinal microbiota and nonalcoholic steatohepatitis. *Curr Opin Gastroenterol.* 2017;33(3):128-133. doi:10.1097/MOG.0000000000000349

Breuer DA, Pacheco MC, Washington MK, Montgomery SA, Hasty AH, Kennedy AJ. CD8<sup>+</sup> T cells regulate liver injury in obesity-related nonalcoholic fatty liver disease. *Am J Physiol Gastrointest Liver Physiol.* 2020;318(2):G211-G224. doi:10.1152/ajpgi.00040.2019

Brunt EM, Kleiner DE, Wilson LA, Belt P, Neuschwander-Tetri BA; NASH Clinical Research Network (CRN). Nonalcoholic fatty liver disease (NAFLD) activity score and the histopathologic diagnosis in NAFLD: distinct clinicopathologic meanings. *Hepatology.* 2011;53(3):810-820. doi:10.1002/hep.24127

Bruzzì S, Sutti S, Giudici G, et al. B2-Lymphocyte responses to oxidative stress-derived antigens contribute to the evolution of nonalcoholic fatty liver disease (NAFLD). *Free Radic Biol Med.* 2018;124:249-259. doi:10.1016/j.freeradbiomed.2018.06.015

Cai J, Zhang XJ, Li H. The Role of Innate Immune Cells in Nonalcoholic Steatohepatitis. *Hepatology.* 2019;70(3):1026-1037. doi:10.1002/hep.30506

Cai Y, Li H, Liu M, et al. Disruption of adenosine 2A receptor exacerbates NAFLD through increasing inflammatory responses and SREBP1c activity. *Hepatology.* 2018;68(1):48-61. doi:10.1002/hep.29777

Caligiuri A, Gentilini A, Marra F. Molecular Pathogenesis of NASH. *Int J Mol Sci.* 2016;17(9):1575. doi:10.3390/ijms17091575.

Cazanave SC, Gores GJ. Mechanisms and clinical implications of hepatocyte lipoapoptosis. *Clin Lipidol.* 2010;5(1):71-85. doi:10.2217/clp.09.85

Cazanave SC, Mott JL, Elmi NA, et al. JNK1-dependent PUMA expression contributes to hepatocyte lipoapoptosis. *J Biol Chem.* 2009;284(39):26591-26602. doi:10.1074/jbc.M109.0224917.

Chalasani N, Deeg MA, Crabb DW. Systemic levels of lipid peroxidation and its metabolic and dietary correlates in patients with nonalcoholic steatohepatitis. *Am J Gastroenterol.* 2004;99(8):1497-1502. doi:10.1111/j.1572-0241.2004.30159

Chalasani N, Vuppalanchi R, Navarro V, et al. Acute liver injury due to flavocoxid (Limbrel), a medical food for osteoarthritis: a case series. *Ann Intern Med.* 2012;156(12):857-W300. doi:10.7326/0003-4819-156-12-201206190-00006

Chaney A. Treating the patient with nonalcoholic fatty liver disease. *Nurse Pract.* 2015;40(11):36-43. doi:10.1097/01.NPR.0000472248.28703.18

Chatzigeorgiou A, Chung KJ, Garcia-Martin R, et al. Dual role of B7 costimulation in obesity-related nonalcoholic steatohepatitis and metabolic dysregulation. *Hepatology.* 2014;60(4):1196-1210. doi:10.1002/hep.27233

Chow KV, Sutherland RM, Zhan Y, Lew AM. Heterogeneity, functional specialization and differentiation of monocyte-derived dendritic cells. *Immunol Cell Biol.* 2017;95(3):244-251. doi:10.1038/icb.2016.104

Connolly MK, Ayo D, Malhotra A, et al. Dendritic cell depletion exacerbates acetaminophen hepatotoxicity. *Hepatology.* 2011;54(3):959-968. doi:10.1002/hep.24429

Connolly MK, Bedrosian AS, Mallen-St Clair J, et al. In liver fibrosis, dendritic cells govern hepatic inflammation in mice via TNF-alpha. *J Clin Invest.* 2009;119(11):3213-3225. doi:10.1172/JCI37581

Cyster JG. Lymphoid organ development and cell migration. *Immunol Rev.* 2003; 195:5-14. doi:10.1034/j.1600-065x.2003.00075

Czaja MJ. JNK regulation of hepatic manifestations of the metabolic syndrome. *Trends Endocrinol Metab.* 2010;21(12):707-713. doi:10.1016/j.tem.2010.08.010

DeFuria J, Belkina AC, Jagannathan-Bogdan M, et al. B cells promote inflammation in obesity and type 2 diabetes through regulation of T-cell function and an inflammatory cytokine profile. *Proc Natl Acad Sci U S A.* 2013;110(13):5133-5138. doi:10.1073/pnas.1215840110

Dhirapong A, Lleo A, Yang GX, et al. B cell depletion therapy exacerbates murine primary biliary cirrhosis. *Hepatology.* 2011;53(2):527-535. doi:10.1002/hep.24044

DiLillo DJ, Horikawa M, Tedder TF. B-lymphocyte effector functions in health and disease. *Immunol Res.* 2011;49(1-3):281-292. doi:10.1007/s12026-010-8189-3

Dixon LJ, Flask CA, Papouchado BG, Feldstein AE, Nagy LE. Caspase-1 as a central regulator of high fat diet-induced non-alcoholic steatohepatitis. *PLoS One.* 2013;8(2):e56100. doi:10.1371/journal.pone.0056100

Doherty DG. Immunity, tolerance and autoimmunity in the liver: A comprehensive review. *J Autoimmun.* 2016;66:60-75. doi:10.1016/j.jaut.2015.08.020

Duarte S, Baber J, Fujii T, Coito AJ. Matrix metalloproteinases in liver injury, repair and fibrosis. *Matrix Biol.* 2015;44-46:147-156. doi:10.1016/j.matbio.2015.01.004

Duwaerts CC, Maher JJ. Mechanisms of Liver Injury in Non-Alcoholic Steatohepatitis. *Curr Hepatol Rep.* 2014;13(2):119-129. doi:10.1007/s11901-014-0224-8

Echeverri Tirado LC, Yassin LM. B cells interactions in lipid immune responses: implications in atherosclerotic disease. *Lipids Health Dis.* 2017;16(1):30. Published 2017 Feb 6. doi:10.1186/s12944-016-0390-5

Eckert C, Klein N, Kornek M, Lukacs-Kornek V. The complex myeloid network of the liver with diverse functional capacity at steady state and in inflammation. *Front Immunol.* 2015;6:179. Published 2015 Apr 20. doi:10.3389/fimmu.2015.00179

Eguchi A, Feldstein AE. Adipocyte cell death, fatty liver disease and associated metabolic disorders. *Dig Dis.* 2014;32(5):579-585. doi:10.1159/000360509

Estes C, Anstee QM, Arias-Loste MT, et al. Modeling NAFLD disease burden in China, France, Germany, Italy, Japan, Spain, United Kingdom, and United States for the period 2016-2030. *J Hepatol.* 2018;69(4):896-904. doi:10.1016/j.jhep.2018.05.036

Estes C, Razavi H, Loomba R, Younossi Z, Sanyal AJ. Modeling the epidemic of nonalcoholic fatty liver disease demonstrates an exponential increase in burden of disease. *Hepatology*. 2018;67(1):123-133. doi:10.1002/hep.29466

Feldstein AE, Canbay A, Angulo P, et al. Hepatocyte apoptosis and fas expression are prominent features of human nonalcoholic steatohepatitis. *Gastroenterology*. 2003;125(2):437-443. doi:10.1016/s0016-5085(03)00907-7

Feldstein AE. Novel insights into the pathophysiology of nonalcoholic fatty liver disease. *Semin Liver Dis*. 2010;30(4):391-401. doi:10.1055/s-0030-1267539

Ferreira Solari NE, Inzaugarat ME, Baz P, et al. The role of innate cells is coupled to a Th1-polarized immune response in pediatric nonalcoholic steatohepatitis. *J Clin Immunol*. 2012;32(3):611-621. doi:10.1007/s10875-011-9635-2

Figueira FR, Umpierre D, Casali KR, et al. Aerobic and combined exercise sessions reduce glucose variability in type 2 diabetes: crossover randomized trial. *PLoS One*. 2013;8(3):e57733. doi:10.1371/journal.pone.0057733

Francisco V, Pino J, Campos-Cabaleiro V, et al. Obesity, Fat Mass and Immune System: Role for Leptin. *Front Physiol*. 2018;9:640. doi:10.3389/fphys.2018.00640

Friedman SL, Neuschwander-Tetri BA, Rinella M, Sanyal AJ. Mechanisms of NAFLD development and therapeutic strategies. *Nat Med*. 2018;24(7):908-922. doi:10.1038/s41591-018-0104-9

Friedman SL, Ratziu V, Harrison SA, et al. A randomized, placebo-controlled trial of cenicriviroc for treatment of nonalcoholic steatohepatitis with fibrosis. *Hepatology*. 2018;67(5):1754-1767. doi:10.1002/hep.29477

Friedman SL. Mechanisms of hepatic fibrogenesis. *Gastroenterology*. 2008;134(6):1655-1669. doi:10.1053/j.gastro.2008.03.003

Gadd VL, Skoien R, Powell EE, et al. The portal inflammatory infiltrate and ductular reaction in human nonalcoholic fatty liver disease. *Hepatology*. 2014;59(4):1393-1405. doi:10.1002/hep.26937

Gambino R, Musso G, Cassader M. Redox balance in the pathogenesis of nonalcoholic fatty liver disease: mechanisms and therapeutic opportunities. *Antioxid Redox Signal*. 2011;15(5):1325-1365. doi:10.1089/ars.2009.3058

Ganz M, Szabo G. Immune and inflammatory pathways in NASH. *Hepatology Int*. 2013;7:771-781. doi:10.1007/s12072-013-9468-6

Garcia-Martinez I, Santoro N, Chen Y, et al. Hepatocyte mitochondrial DNA drives nonalcoholic steatohepatitis by activation of TLR9. *J Clin Invest*. 2016;126(3):859-864. doi:10.1172/JCI83885

Ghazarian M, Revelo XS, Nøhr MK, et al. Type I Interferon Responses Drive Intrahepatic T cells to Promote Metabolic Syndrome. *Sci Immunol*. 2017;2(10):eaai7616. doi:10.1126/sciimmunol.aai7616

Gigliotti CL, Boggio E, Clemente N, et al. ICOS-Ligand Triggering Impairs Osteoclast Differentiation and Function In Vitro and In Vivo. *J Immunol*. 2016;197(10):3905-3916. doi:10.4049/jimmunol.1600424

Giles DA, Moreno-Fernandez ME, Stankiewicz TE, et al. Regulation of Inflammation by IL-17A and IL-17F Modulates Non-Alcoholic Fatty Liver Disease Pathogenesis. *PLoS One*. 2016;11(2): e0149783. doi:10.1371/journal.pone.0149783

Gomes AL, Teijeiro A, Burén S, et al. Metabolic Inflammation-Associated IL-17A Causes Non-alcoholic Steatohepatitis and Hepatocellular Carcinoma. *Cancer Cell*. 2016;30(1):161-175. doi:10.1016/j.ccell.2016.05.020

Gramlich T, Kleiner DE, McCullough AJ, Matteoni CA, Boparai N, Younossi ZM. Pathologic features associated with fibrosis in nonalcoholic fatty liver disease. *Hum Pathol*. 2004;35(2):196-199. doi:10.1016/j.humpath.2003.09.018

Grohmann M, Wiede F, Dodd GT, et al. Obesity Drives STAT-1-Dependent NASH and STAT-3-Dependent HCC. *Cell*. 2018;175(5):1289-1306. doi:10.1016/j.cell.2018.09.053

Gruber S, Hendriks T, Tsiantoulas D, et al. Sialic Acid-Binding Immunoglobulin-like Lectin G Promotes Atherosclerosis and Liver Inflammation by Suppressing the Protective Functions of B-1 Cells. *Cell Rep*. 2016;14(10):2348-2361. doi:10.1016/j.celrep.2016.02.027

Guo B, Li Z. Endoplasmic reticulum stress in hepatic steatosis and inflammatory bowel diseases. *Front Genet*. 2014;5:242. doi:10.3389/fgene.2014.00242

Hammerich L, Tacke F. Role of gamma-delta T cells in liver inflammation and fibrosis. *World J Gastrointest Pathophysiol*. 2014;5(2):107-113. doi:10.4291/wjgp.v5.i2.107

Harbrecht BG, Nweze I, Smith JW, Zhang B. Insulin inhibits hepatocyte iNOS expression induced by cytokines by an Akt-dependent mechanism. *Am J Physiol Gastrointest Liver Physiol*. 2012;302(1):G116-G122. doi:10.1152/ajpgi.00114.2011

Harley IT, Stankiewicz TE, Giles DA, et al. IL-17 signaling accelerates the progression of nonalcoholic fatty liver disease in mice. *Hepatology*. 2014;59(5):1830-1839. doi:10.1002/hep.26746

Harmon DB, Srikakulapu P, Kaplan JL, et al. Protective Role for B-1b B Cells and IgM in Obesity-Associated Inflammation, Glucose Intolerance, and Insulin Resistance. *Arterioscler Thromb Vasc Biol*. 2016;36(4):682-691. doi:10.1161/ATVBAHA.116.307166

Heier EC, Meier A, Julich-Haertel H, et al. Murine CD103<sup>+</sup> dendritic cells protect against steatosis progression towards steatohepatitis. *J Hepatol*. 2017;66(6):1241-1250. doi:10.1016/j.jhep.2017.01.008

Henao-Mejia J, Elinav E, Jin C, et al. Inflammasome-mediated dysbiosis regulates progression of NAFLD and obesity. *Nature*. 2012;482(7384):179-185. doi:10.1038/nature10809

Hendriks T, Watzenböck ML, Walenbergh SM, et al. Low levels of IgM antibodies recognizing oxidation-specific epitopes are associated with human non-alcoholic fatty liver disease. *BMC Med*. 2016;14(1):107. doi:10.1186/s12916-016-0652-0

Henning JR, Graffeo CS, Rehman A, et al. Dendritic cells limit fibroinflammatory injury in nonalcoholic steatohepatitis in mice. *Hepatology*. 2013;58(2):589-602. doi:10.1002/hep.26267

Heymann F, Peusquens J, Ludwig-Portugall I, et al. Liver inflammation abrogates immunological tolerance induced by Kupffer cells. *Hepatology*. 2015;62(1):279-291. doi:10.1002/hep.27793



Heymann F, Tacke F. Immunology in the liver--from homeostasis to disease. *Nat Rev Gastroenterol Hepatol*. 2016;13(2):88-110. doi:10.1038/nrgastro.2015.200

Hochheiser K, Kurts C. Selective Dependence of Kidney Dendritic Cells on CX3CR1--Implications for Glomerulonephritis Therapy. *Adv Exp Med Biol*. 2015;850:55-71. doi:10.1007/978-3-319-15774-0\_5

Hooper AJ, Adams LA, Burnett JR. Genetic determinants of hepatic steatosis in man. *J Lipid Res*. 2011;52(4):593-617. doi:10.1194/jlr.R008896.

Huang LR, Wohlleber D, Reisinger F, et al. Intrahepatic myeloid-cell aggregates enable local proliferation of CD8(+) T cells and successful immunotherapy against chronic viral liver infection. *Nat Immunol*. 2013;14(6):574-583. doi:10.1038/ni.2573

Huebener P, Pradere JP, Hernandez C, et al. The HMGB1/RAGE axis triggers neutrophil-mediated injury amplification following necrosis [published correction appears in *J Clin Invest*. 2019 Mar 4;130:1802]. *J Clin Invest*. 2015;125(2):539-550. doi:10.1172/JCI76887

Ibrahim J, Nguyen AH, Rehman A, et al. Dendritic cell populations with different concentrations of lipid regulate tolerance and immunity in mouse and human liver. *Gastroenterology*. 2012;143(4):1061-1072. doi:10.1053/j.gastro.2012.06.003

Ikura Y, Ohsawa M, Suekane T, et al. Localization of oxidized phosphatidylcholine in nonalcoholic fatty liver disease: impact on disease progression. *Hepatology*. 2006;43(3):506-514. doi:10.1002/hep.21070

Inzaugarat ME, Ferreyra Solari NE, Billordo LA, Abecasis R, Gadano AC, Cherñavsky AC. Altered phenotype and functionality of circulating immune cells characterize adult patients with nonalcoholic steatohepatitis. *J Clin Immunol*. 2011;31(6):1120-1130. doi:10.1007/s10875-011-9571-1

James OF, Day CP. Non-alcoholic steatohepatitis (NASH): a disease of emerging identity and importance. *J Hepatol*. 1998;29(3):495-501. doi:10.1016/s0168-8278(98)80073-1.

Karlmark KR, Zimmermann HW, Roderburg C, et al. The fractalkine receptor CX<sub>3</sub>CR1 protects against liver fibrosis by controlling differentiation and survival of infiltrating hepatic monocytes. *Hepatology*. 2010;52(5):1769-1782. doi:10.1002/hep.23894

Kelly A, Fahey R, Fletcher JM, et al. CD141<sup>+</sup> myeloid dendritic cells are enriched in healthy human liver. *J Hepatol*. 2014;60(1):135-142. doi:10.1016/j.jhep.2013.08.007

Kesar V, Odin JA. Toll-like receptors and liver disease. *Liver Int*. 2014;34(2):184-196. doi:10.1111/liv.12315

Ketelhuth DF, Hansson GK. Adaptive Response of T and B Cells in Atherosclerosis. *Circ Res*. 2016;118(4):668-678. doi:10.1161/CIRCRESAHA.115.306427

Koh KH, Cao Y, Mangos S, et al. Nonimmune cell-derived ICOS ligand functions as a renoprotective  $\alpha\beta 3$  integrin-selective antagonist. *J Clin Invest*. 2019;129(4):1713-1726. doi:10.1172/JCI123386

Kowalczyk-Quintas C, Schuepbach-Mallepell S, Vigolo M, et al. Antibodies That Block or Activate Mouse B Cell Activating Factor of the Tumor Necrosis Factor (TNF) Family (BAFF), Respectively, Induce B Cell Depletion or B Cell Hyperplasia. *J Biol Chem*. 2016;291(38):19826-19834. doi:10.1074/jbc.M116.725929

Kremer M, Thomas E, Milton RJ, et al. Kupffer cell and interleukin-12-dependent loss of natural killer T cells in hepatosteatosis. *Hepatology*. 2010;51(1):130-141. doi:10.1002/hep.23292

Krenkel O, Tacke F. Liver macrophages in tissue homeostasis and disease. *Nat Rev Immunol*. 2017;17(5):306-321. doi:10.1038/nri.2017.11

Krueger PD, Kim TS, Sung SS, Braciale TJ, Hahn YS. Liver-resident CD103+ dendritic cells prime antiviral CD8+ T cells in situ. *J Immunol*. 2015;194(7):3213-3222. doi:10.4049/jimmunol.1402622

Lanthier N. Targeting Kupffer cells in non-alcoholic fatty liver disease/non-alcoholic steatohepatitis: Why and how?. *World J Hepatol*. 2015;7(19):2184-2188. doi:10.4254/wjh.v7.i19.2184

Laurent A, Nicco C, Tran Van Nhieu J, et al. Pivotal role of superoxide anion and beneficial effect of antioxidant molecules in murine steatohepatitis. *Hepatology*. 2004;39(5):1277-1285. doi:10.1002/hep.20177

Lefebvre E, Moyle G, Reshef R, et al. Antifibrotic Effects of the Dual CCR2/CCR5 Antagonist Cenicriviroc in Animal Models of Liver and Kidney Fibrosis. *PLoS One*. 2016;11(6):e0158156. doi:10.1371/journal.pone.0158156

Ley K, Gerdes N, Winkels H. ATVB Distinguished Scientist Award: How Costimulatory and Coinhibitory Pathways Shape Atherosclerosis. *Arterioscler Thromb Vasc Biol*. 2017;37(5):764-777. doi:10.1161/ATVBAHA.117.308611

Li B, Selmi C, Tang R, Gershwin ME, Ma X. The microbiome and autoimmunity: a paradigm from the gut-liver axis. *Cell Mol Immunol*. 2018;15(6):595-609. doi:10.1038/cmi.2018.7

Li DY, Xiong XZ. ICOS<sup>+</sup> Tregs: A Functional Subset of Tregs in Immune Diseases. *Front Immunol*. 2020;11:2104. doi:10.3389/fimmu.2020.02104

Li F, Hao X, Chen Y, et al. The microbiota maintain homeostasis of liver-resident  $\gamma\delta$ T-17 cells in a lipid antigen/CD1d-dependent manner. *Nat Commun*. 2017;7:13839. doi:10.1038/ncomms13839

Li Z, Soloski MJ, Diehl AM. Dietary factors alter hepatic innate immune system in mice with nonalcoholic fatty liver disease. *Hepatology*. 2005;42(4):880-885. doi:10.1002/hep.20826

Lindenmeyer CC, McCullough AJ. The Natural History of Nonalcoholic Fatty Liver Disease-An Evolving View. *Clin Liver Dis*. 2018;22(1):11-21. doi:10.1016/j.cld.2017.08.003.

Liu B, Yu H, Sun G, et al. OX40 promotes obesity-induced adipose inflammation and insulin resistance. *Cell Mol Life Sci*. 2017;74(20):3827-3840. doi:10.1007/s00018-017-2552-7

Locatelli I, Sutti S, Jindal A, et al. Endogenous annexin A1 is a novel protective determinant in nonalcoholic steatohepatitis in mice. *Hepatology*. 2014;60(2):531-544. doi:10.1002/hep.27141

Locatelli I, Sutti S, Vacchiano M, Bozzola C, Albano E. NF- $\kappa$ B1 deficiency stimulates the progression of non-alcoholic steatohepatitis (NASH) in mice by promoting NKT-cell-mediated responses. *Clin Sci (Lond)*. 2013;124(4):279-287. doi:10.1042/CS20120289

Lonardo A, Loria P. Apolipoprotein synthesis in nonalcoholic steatohepatitis. *Hepatology*. 2002;36(2):514-515. doi:10.1053/jhep.2002.34443

Lund FE. Cytokine-producing B lymphocytes-key regulators of immunity. *Curr Opin Immunol*. 2008;20(3):332-338. doi:10.1016/j.coi.2008.03.003

Luo XY, Takahara T, Kawai K, et al. IFN- $\gamma$  deficiency attenuates hepatic inflammation and fibrosis in a steatohepatitis model induced by a methionine- and choline-deficient high-fat diet. *Am J Physiol Gastrointest Liver Physiol*. 2013;305(12):G891-G899. doi:10.1152/ajpgi.00193.2013

Lutz MB, Strobl H, Schuler G, Romani N. GM-CSF Monocyte-Derived Cells and Langerhans Cells As Part of the Dendritic Cell Family. *Front Immunol*. 2017;8:1388. doi:10.3389/fimmu.2017.01388

Ma X, Hua J, Mohamood AR, Hamad AR, Ravi R, Li Z. A high-fat diet and regulatory T cells influence susceptibility to endotoxin-induced liver injury. *Hepatology*. 2007;46(5):1519-1529. doi:10.1002/hep.21823

Mackay F, Schneider P. Cracking the BAFF code. *Nat Rev Immunol*. 2009;9(7):491-502. doi:10.1038/nri2572

Malhi H, Gores GJ. Molecular mechanisms of lipotoxicity in nonalcoholic fatty liver disease. *Semin Liver Dis*. 2008;28(4):360-369. doi:10.1055/s-0028-1091980

Mansouri A, Gattolliat CH, Asselah T. Mitochondrial Dysfunction and Signaling in Chronic Liver Diseases. *Gastroenterology*. 2018;155(3):629-647. doi:10.1053/j.gastro.2018.06.083

Maricic I, Marrero I, Eguchi A, et al. Differential Activation of Hepatic Invariant NKT Cell Subsets Plays a Key Role in Progression of Nonalcoholic Steatohepatitis. *J Immunol*. 2018;201(10):3017-3035. doi:10.4049/jimmunol.1800614

Marra F, DeFranco R, Robino G, et al. Thiazolidinedione treatment inhibits bile duct proliferation and fibrosis in a rat model of chronic cholestasis. *World J Gastroenterol*. 2005;11(32):4931-4938. doi:10.3748/wjg.v11.i32.4931

Marra F, Gastaldelli A, Svegliati Baroni G, Tell G, Tiribelli C. Molecular basis and mechanisms of progression of non-alcoholic steatohepatitis. *Trends Mol Med*. 2008;14(2):72-81. doi:10.1016/j.molmed.2007.12.003

Marrero I, Maricic I, Feldstein AE, et al. Complex Network of NKT Cell Subsets Controls Immune Homeostasis in Liver and Gut. *Front Immunol*. 2018;9:2082. Published 2018 Sep 11. doi:10.3389/fimmu.2018.02082

Martinon F, Burns K, Tschopp J. The inflammasome: a molecular platform triggering activation of inflammatory caspases and processing of proIL-beta. *Mol Cell*. 2002;10(2):417-426. doi:10.1016/s1097-2765(02)00599-3

Masarone M, Rosato V, Dallio M, et al. Role of Oxidative Stress in Pathophysiology of Nonalcoholic Fatty Liver Disease. *Oxid Med Cell Longev*. 2018;2018:9547613. doi:10.1155/2018/9547613

Mastrodonato M, Calamita G, Rossi R, et al. Altered distribution of caveolin-1 in early liver steatosis. *Eur J Clin Invest*. 2011;41(6):642-651. doi:10.1111/j.1365-2362.2010.02459

McLaughlin T, Ackerman SE, Shen L, Engleman E. Role of innate and adaptive immunity in obesity-associated metabolic disease. *J Clin Invest*. 2017;127(1):5-13. doi:10.1172/JCI88876

McPherson S, Henderson E, Burt AD, Day CP, Anstee QM. Serum immunoglobulin levels predict fibrosis in patients with non-alcoholic fatty liver disease. *J Hepatol.* 2014;60(5):1055-1062. doi:10.1016/j.jhep.2014.01.010

Mionnet C, Buatois V, Kanda A, et al. CX3CR1 is required for airway inflammation by promoting T helper cell survival and maintenance in inflamed lung. *Nat Med.* 2010;16(11):1305-1312. doi:10.1038/nm.2253

Miyake T, Abe M, Tokumoto Y, et al. B cell-activating factor is associated with the histological severity of nonalcoholic fatty liver disease. *Hepatol Int.* 2013;7(2):539-547. doi:10.1007/s12072-012-9345-8

Mofrad P, Contos MJ, Haque M, et al. Clinical and histologic spectrum of nonalcoholic fatty liver disease associated with normal ALT values. *Hepatology.* 2003;37(6):1286-1292. doi:10.1053/jhep.2003.50229.

Molina MF, Abdelnabi MN, Fabre T, Shoukry NH. Type 3 cytokines in liver fibrosis and liver cancer. *Cytokine.* 2019;124:154497. doi:10.1016/j.cyto.2018.07.028

Mridha AR, Wree A, Robertson AAB, et al. NLRP3 inflammasome blockade reduces liver inflammation and fibrosis in experimental NASH in mice. *J Hepatol.* 2017;66(5):1037-1046. doi:10.1016/j.jhep.2017.01.022

Musso G, Gambino R, Biroli G, et al. Hypoadiponectinemia predicts the severity of hepatic fibrosis and pancreatic Beta-cell dysfunction in nondiabetic nonobese patients with nonalcoholic steatohepatitis. *Am J Gastroenterol.* 2005;100(11):2438-2446. doi:10.1111/j.1572-0241.2005.00297

Musso G, Gambino R, Cassader M. Recent insights into hepatic lipid metabolism in non-alcoholic fatty liver disease (NAFLD). *Prog Lipid Res.* 2009;48(1):1-26. doi:10.1016/j.plipres.2008.08.001

Nakano H, Moran TP, Nakano K, Gerrish KE, Bortner CD, Cook DN. Complement receptor C5aR1/CD88 and dipeptidyl peptidase-4/CD26 define distinct hematopoietic lineages of dendritic cells. *J Immunol.* 2015;194(8):3808-3819. doi:10.4049/jimmunol.1402195

Nguyen-Lefebvre AT, Ajith A, Portik-Dobos V, et al. The innate immune receptor TREM-1 promotes liver injury and fibrosis. *J Clin Invest.* 2018;128(11):4870-4883. doi:10.1172/JCI98156

Nobili V, Parola M, Alisi A, et al. Oxidative stress parameters in paediatric non-alcoholic fatty liver disease. *Int J Mol Med.* 2010;26(4):471-476. doi:10.3892/ijmm\_00000487

Novo E, Parola M. Redox mechanisms in hepatic chronic wound healing and fibrogenesis. *Fibrogenesis Tissue Repair.* 2008;1(1):5. Published 2008 Oct 13. doi:10.1186/1755-1536-1-5

Novobrantseva TI, Majeau GR, Amatucci A, et al. Attenuated liver fibrosis in the absence of B cells. *J Clin Invest.* 2005;115(11):3072-3082. doi:10.1172/JCI24798

Occhipinti S, Dianzani C, Chiocchetti A, et al. Triggering of B7h by the ICOS modulates maturation and migration of monocyte-derived dendritic cells. *J Immunol.* 2013;190(3):1125-1134. doi:10.4049/jimmunol.1201816

Oh Y, Park O, Swierczewska M, et al. Systemic PEGylated TRAIL treatment ameliorates liver cirrhosis in rats by eliminating activated hepatic stellate cells. *Hepatology.* 2016;64(1):209-223. doi:10.1002/hep.28432

Papac-Milicevic N, Busch CJ, Binder CJ. Malondialdehyde Epitopes as Targets of Immunity and the Implications for Atherosclerosis. *Adv Immunol.* 2016;131:1-59. doi:10.1016/bs.ai.2016.02.001

Petrasek J, Csak T, Szabo G. Toll-like receptors in liver disease. *Adv Clin Chem.* 2013;59:155-201. doi:10.1016/b978-0-12-405211-6.00006-1

Postic C, Girard J. Contribution of de novo fatty acid synthesis to hepatic steatosis and insulin resistance: lessons from genetically engineered mice. *J Clin Invest.* 2008;118(3):829-838. doi:10.1172/JCI34275

Pratt DS, Kaplan MM. Evaluation of abnormal liver-enzyme results in asymptomatic patients. *N Engl J Med.* 2000;342(17):1266-1271. doi:10.1056/NEJM200004273421707.

Radaeva S, Sun R, Jaruga B, Nguyen VT, Tian Z, Gao B. Natural killer cells ameliorate liver fibrosis by killing activated stellate cells in NKG2D-dependent and tumor necrosis factor-related apoptosis-inducing ligand-dependent manners. *Gastroenterology.* 2006;130(2):435-452. doi:10.1053/j.gastro.2005.10.055

Rahman AH, Aloman C. Dendritic cells and liver fibrosis. *Biochim Biophys Acta.* 2013;1832(7):998-1004. doi:10.1016/j.bbadis.2013.01.005

Rao S, Huang J, Shen Z, Xiang C, Zhang M, Lu X. Inhibition of TREM-1 attenuates inflammation and lipid accumulation in diet-induced nonalcoholic fatty liver disease [published online ahead of print, 2019 Feb 25]. *J Cell Biochem.* 2019;120(7):11867-11877. doi:10.1002/jcb.28468

Rau M, Rehman A, Dittrich M, et al. Fecal SCFAs and SCFA-producing bacteria in gut microbiome of human NAFLD as a putative link to systemic T-cell activation and advanced disease. *United European Gastroenterol J.* 2018;6(10):1496-1507. doi:10.1177/2050640618804444

Rau M, Schilling AK, Meertens J, et al. Progression from Nonalcoholic Fatty Liver to Nonalcoholic Steatohepatitis Is Marked by a Higher Frequency of Th17 Cells in the Liver and an Increased Th17/Resting Regulatory T Cell Ratio in Peripheral Blood and in the Liver. *J Immunol.* 2016;196(1):97-105. doi:10.4049/jimmunol.1501175

Ray PD, Huang BW, Tsuji Y. Reactive oxygen species (ROS) homeostasis and redox regulation in cellular signaling. *Cell Signal.* 2012;24(5):981-990. doi:10.1016/j.cellsig.2012.01.008

Rinella ME. Nonalcoholic fatty liver disease: a systematic review [published correction appears in *JAMA.* 2015 Oct 13;314(14):1521]. *JAMA.* 2015;313(22):2263-2273. doi:10.1001/jama.2015.5370.

Ringelhan M, Pfister D, O'Connor T, Pikarsky E, Heikenwalder M. The immunology of hepatocellular carcinoma. *Nat Immunol.* 2018;19(3):222-232. doi:10.1038/s41590-018-0044-z

Riopel M, Vassallo M, Ehinger E, et al. CX3CL1-Fc treatment prevents atherosclerosis in Ldlr KO mice. *Mol Metab.* 2019;20:89-101. doi:10.1016/j.molmet.2018.11.011

Rolla R, Vay D, Mottaran E, et al. Detection of circulating antibodies against malondialdehyde-acetaldehyde adducts in patients with alcohol-induced liver disease. *Hepatology.* 2000;31(4):878-884. doi:10.1053/he.2000.5373

Rolla S, Alchera E, Imarisio C, et al. The balance between IL-17 and IL-22 produced by liver-infiltrating T-helper cells critically controls NASH development in mice. *Clin Sci (Lond).* 2016;130(3):193-203. doi:10.1042/CS20150405

Rosser EC, Mauri C. Regulatory B cells: origin, phenotype, and function. *Immunity*. 2015;42(4):607-612. doi:10.1016/j.immuni.2015.04.005

Satpathy AT, KC W, Albring JC, et al. Zbtb46 expression distinguishes classical dendritic cells and their committed progenitors from other immune lineages. *J Exp Med*. 2012;209(6):1135-1152. doi:10.1084/jem.20120030

Schneider KM, Bieghs V, Heymann F, et al. CX3CR1 is a gatekeeper for intestinal barrier integrity in mice: Limiting steatohepatitis by maintaining intestinal homeostasis. *Hepatology*. 2015;62(5):1405-1416. doi:10.1002/hep.27982

Schneider P, Takatsuka H, Wilson A, et al. Maturation of marginal zone and follicular B cells requires B cell activating factor of the tumor necrosis factor family and is independent of B cell maturation antigen. *J Exp Med*. 2001;194(11):1691-1697. doi:10.1084/jem.194.11.1691

Segura E, Amigorena S. Inflammatory dendritic cells in mice and humans. *Trends Immunol*. 2013;34(9):440-445. doi:10.1016/j.it.2013.06.001

Seijkens T, Kusters P, Chatzigeorgiou A, Chavakis T, Lutgens E. Immune cell crosstalk in obesity: a key role for costimulation?. *Diabetes*. 2014;63(12):3982-3991. doi:10.2337/db14-0272

Seki E, Brenner DA. Toll-like receptors and adaptor molecules in liver disease: update. *Hepatology*. 2008;48(1):322-335. doi:10.1002/hep.22306

Seki S, Kitada T, Yamada T, Sakaguchi H, Nakatani K, Wakasa K. In situ detection of lipid peroxidation and oxidative DNA damage in non-alcoholic fatty liver diseases. *J Hepatol*. 2002;37(1):56-62. doi:10.1016/s0168-8278(02)00073-9

Sell H, Habich C, Eckel J. Adaptive immunity in obesity and insulin resistance. *Nat Rev Endocrinol*. 2012;8(12):709-716. doi:10.1038/nrendo.2012.114

Shalapour S, Lin XJ, Bastian IN, et al. Inflammation-induced IgA+ cells dismantle anti-liver cancer immunity [published correction appears in *Nature*. 2017 Nov 22;:] [published correction appears in *Nature*. 2018 Sep;561(7721):E1]. *Nature*. 2017;551(7680):340-345. doi:10.1038/nature24302

Sheth SG, Gordon FD, Chopra S. Nonalcoholic steatohepatitis [published correction appears in *Ann Intern Med* 1997 Oct 15;127(8 Pt 1):658]. *Ann Intern Med*. 1997;126(2):137-145. doi:10.7326/0003-4819-126-2-199701150-00008

Sivitz WI, Yorek MA. Mitochondrial dysfunction in diabetes: from molecular mechanisms to functional significance and therapeutic opportunities. *Antioxid Redox Signal*. 2010;12(4):537-577. doi:10.1089/ars.2009.2531

Smallwood MJ, Nissim A, Knight AR, Whiteman M, Haigh R, Winyard PG. Oxidative stress in autoimmune rheumatic diseases. *Free Radic Biol Med*. 2018;125:3-14. doi:10.1016/j.freeradbiomed.2018.05.086

Smith BW, Adams LA. Non-alcoholic fatty liver disease. *Crit Rev Clin Lab Sci*. 2011;48(3):97-113. doi:10.3109/10408363.2011.596521

Staumont-Sallé D, Fleury S, Lazzari A, et al. CX<sub>3</sub>CL1 (fractalkine) and its receptor CX<sub>3</sub>CR1 regulate atopic dermatitis by controlling effector T cell retention in inflamed skin. *J Exp Med*. 2014;211(6):1185-1196. doi:10.1084/jem.20121350

Strowig T, Henao-Mejia J, Elinav E, Flavell R. Inflammasomes in health and disease. *Nature*. 2012;481(7381):278-286. Published 2012 Jan 18. doi:10.1038/nature10759

Sumida Y, Eguchi Y, Ono M. Current status and agenda in the diagnosis of nonalcoholic steatohepatitis in Japan. *World J Hepatol*. 2010;2(10):374-383. doi:10.4254/wjh.v2.i10.374

Sumpter TL, Dangi A, Matta BM, et al. Hepatic stellate cells undermine the allostimulatory function of liver myeloid dendritic cells via STAT3-dependent induction of IDO. *J Immunol*. 2012;189(8):3848-3858. doi:10.4049/jimmunol.1200819

Sun G, Jin H, Zhang C, et al. OX40 Regulates Both Innate and Adaptive Immunity and Promotes Nonalcoholic Steatohepatitis. *Cell Rep*. 2018;25(13):3786-3799.e4. doi:10.1016/j.celrep.2018.12.006

Sutti S, Heymann F, Bruzzi S, et al. CX<sub>3</sub>CR1 modulates the anti-inflammatory activity of hepatic dendritic cells in response to acute liver injury. *Clin Sci (Lond)*. 2017;131(17):2289-2301. doi:10.1042/CS20171025

Sutti S, Bruzzi S, Heymann F, et al. CX<sub>3</sub>CR1 Mediates the Development of Monocyte-Derived Dendritic Cells during Hepatic Inflammation. *Cells*. 2019;8(9):1099. doi:10.3390/cells8091099

Sutti S, Jindal A, Bruzzi S, Locatelli I, Bozzola C, Albano E. Is there a role for adaptive immunity in nonalcoholic steatohepatitis?. *World J Hepatol*. 2015;7(13):1725-1729. doi:10.4254/wjh.v7.i13.1725

Sutti S, Jindal A, Locatelli I, et al. Adaptive immune responses triggered by oxidative stress contribute to hepatic inflammation in NASH. *Hepatology*. 2014;59(3):886-897. doi:10.1002/hep.26749

Sutti S, Locatelli I, Bruzzi S, et al. CX<sub>3</sub>CR1-expressing inflammatory dendritic cells contribute to the progression of steatohepatitis. *Clin Sci (Lond)*. 2015;129(9):797-808. doi:10.1042/CS20150053

Svegliati-Baroni G, Faraci G, Fabris L, et al. Insulin resistance and necroinflammation drives ductular reaction and epithelial-mesenchymal transition in chronic hepatitis C. *Gut*. 2011;60(1):108-115. doi:10.1136/gut.2010.219741

Syn WK, Agboola KM, Swiderska M, et al. NKT-associated hedgehog and osteopontin drive fibrogenesis in non-alcoholic fatty liver disease. *Gut*. 2012;61(9):1323-1329. doi:10.1136/gutjnl-2011-301857

Szabo G, Csak T. Inflammasomes in liver diseases. *J Hepatol*. 2012;57(3):642-654. doi:10.1016/j.jhep.2012.03.035

Tacke F, Zimmermann HW. Macrophage heterogeneity in liver injury and fibrosis. *J Hepatol*. 2014;60(5):1090-1096. doi:10.1016/j.jhep.2013.12.025

Tacke F. Targeting hepatic macrophages to treat liver diseases. *J Hepatol*. 2017;66(6):1300-1312. doi:10.1016/j.jhep.2017.02.026

Tahan V, Canbakan B, Balci H, et al. Serum gamma-glutamyltranspeptidase distinguishes non-alcoholic fatty liver disease at high risk. *Hepatogastroenterology*. 2008;55(85):1433-1438. 8795706.

- Tajiri K, Shimizu Y, Tsuneyama K, Sugiyama T. Role of liver-infiltrating CD3+CD56+ natural killer T cells in the pathogenesis of nonalcoholic fatty liver disease. *Eur J Gastroenterol Hepatol.* 2009;21(6):673-680. doi:10.1097/MEG.0b013e32831bc3d6
- Takaki A, Kawai D, Yamamoto K. Multiple hits, including oxidative stress, as pathogenesis and treatment target in non-alcoholic steatohepatitis (NASH). *Int J Mol Sci.* 2013;14(10):20704-20728. doi:10.3390/ijms141020704
- Tamura T, Tailor P, Yamaoka K, et al. IFN regulatory factor-4 and -8 govern dendritic cell subset development and their functional diversity. *J Immunol.* 2005;174(5):2573-2581. doi:10.4049/jimmunol.174.5.2573
- Tanaka C, Fujimoto M, Hamaguchi Y, Sato S, Takehara K, Hasegawa M. Inducible costimulator ligand regulates bleomycin-induced lung and skin fibrosis in a mouse model independently of the inducible costimulator/inducible costimulator ligand pathway. *Arthritis Rheum.* 2010;62(6):1723-1732. doi:10.1002/art.27428
- Tang G, Qin Q, Zhang P, et al. Reverse signaling using an inducible costimulator to enhance immunogenic function of dendritic cells. *Cell Mol Life Sci.* 2009;66(18):3067-3080. doi:10.1007/s00018-009-0090-7
- Tang Y, Bian Z, Zhao L, et al. Interleukin-17 exacerbates hepatic steatosis and inflammation in non-alcoholic fatty liver disease. *Clin Exp Immunol.* 2011;166(2):281-290. doi:10.1111/j.1365-2249.2011.04471
- Tang ZH, Liang S, Potter J, Jiang X, Mao HQ, Li Z. Tim-3/galectin-9 regulate the homeostasis of hepatic NKT cells in a murine model of nonalcoholic fatty liver disease. *J Immunol.* 2013;190(4):1788-1796. doi:10.4049/jimmunol.1202814
- Thapa M, Chinnadurai R, Velazquez VM, et al. Liver fibrosis occurs through dysregulation of MyD88-dependent innate B-cell activity. *Hepatology.* 2015;61(6):2067-2079. doi:10.1002/hep.27761
- Thapa M, Tedesco D, Gumber S, et al. Blockade of BAFF Reshapes the Hepatic B Cell Receptor Repertoire and Attenuates Autoantibody Production in Cholestatic Liver Disease. *J Immunol.* 2020;204(12):3117-3128. doi:10.4049/jimmunol.1900391
- Torres DM, Harrison SA. Diagnosis and therapy of nonalcoholic steatohepatitis. *Gastroenterology.* 2008;134(6):1682-1698. doi:10.1053/j.gastro.2008.02.077.
- Tosello-Tramont AC, Krueger P, Narayanan S, Landes SG, Leitinger N, Hahn YS. NKp46(+) natural killer cells attenuate metabolism-induced hepatic fibrosis by regulating macrophage activation in mice. *Hepatology.* 2016;63(3):799-812. doi:10.1002/hep.28389
- Torres-Hernandez A, Wang W, Nikiforov Y, Tejada K, Torres L, Kalabin A, Adam S, Wu J, Lu L, Chen R, Lemmer A, Camargo J, Hundeyin M, Diskin B, Aykut B, Kurz E, Kochen Rossi JA, Khan M, Liria M, Sanchez G, Wu N, Su W, Adams S, Haq MIU, Farooq MS, Vasudevaraja V, Leinwand J, Miller G.  $\gamma\delta$  T Cells Promote Steatohepatitis by Orchestrating Innate and Adaptive Immune Programming. *Hepatology.* 2020;71:477-494. doi: 10.1002/hep.30952.



Tsiantoulas D, Sage AP, Mallat Z, Binder CJ. Targeting B cells in atherosclerosis: closing the gap from bench to bedside. *Arterioscler Thromb Vasc Biol.* 2015;35(2):296-302. doi:10.1161/ATVBAHA.114.303569

Tsung A, Zheng N, Jeyabalan G, et al. Increasing numbers of hepatic dendritic cells promote HMGB1-mediated ischemia-reperfusion injury. *J Leukoc Biol.* 2007;81(1):119-128. doi:10.1189/jlb.0706468

Urtasun R, Lopategi A, George J, et al. Osteopontin, an oxidant stress sensitive cytokine, up-regulates collagen-I via integrin  $\alpha(V)\beta(3)$  engagement and PI3K/pAkt/NF $\kappa$ B signaling. *Hepatology.* 2012;55(2):594-608. doi:10.1002/hep.24701

Ushio-Fukai M. Compartmentalization of redox signaling through NADPH oxidase-derived ROS. *Antioxid Redox Signal.* 2009;11(6):1289-1299. doi:10.1089/ars.2008.2333

Vernon G, Baranova A, Younossi ZM. Systematic review: the epidemiology and natural history of non-alcoholic fatty liver disease and non-alcoholic steatohepatitis in adults. *Aliment Pharmacol Ther.* 2011;34(3):274-285. doi:10.1111/j.1365-2036.2011.04724

Wang J, Brymora J, George J. Roles of adipokines in liver injury and fibrosis. *Expert Rev Gastroenterol Hepatol.* 2008;2(1):47-57. doi:10.1586/17474124.2.1.47

Watanabe S, Ohnuki K, Hara Y, Ishida Y, Ikarashi Y, Ogawa S, Kishimoto H, Tanabe K, Abe R. Suppression of Con A-induced hepatitis induction in ICOS-deficient mice *Immunol Lett* 2010;128:51–58

Wehr A, Baeck C, Heymann F, et al. Chemokine receptor CXCR6-dependent hepatic NK T Cell accumulation promotes inflammation and liver fibrosis. *J Immunol.* 2013;190(10):5226-5236. doi:10.4049/jimmunol.1202909

Weiß J, Rau M, Geier A. Non-alcoholic fatty liver disease: epidemiology, clinical course, investigation, and treatment. *Dtsch Arztebl Int.* 2014;111(26):447-452. doi:10.3238/arztebl.2014.0447.

Wen Y, Lambrecht J, Ju C, Tacke F. Hepatic macrophages in liver homeostasis and diseases-diversity, plasticity and therapeutic opportunities [published online ahead of print, 2020 Oct 12]. *Cell Mol Immunol.* 2020;10.1038/s41423-020-00558-8. doi:10.1038/s41423-020-00558-8

Weston CJ, Shepherd EL, Claridge LC, et al. Vascular adhesion protein-1 promotes liver inflammation and drives hepatic fibrosis. *J Clin Invest.* 2015;125(2):501-520. doi:10.1172/JCI73722

Weston CJ, Zimmermann HW, Adams DH. The Role of Myeloid-Derived Cells in the Progression of Liver Disease. *Front Immunol.* 2019;10:893. Published 2019 Apr 24. doi:10.3389/fimmu.2019.00893

Wikenheiser DJ, Stumhofer JS. ICOS Co-Stimulation: Friend or Foe?. *Front Immunol.* 2016;7:304. Published 2016 Aug 10. doi:10.3389/fimmu.2016.00304

Winer DA, Winer S, Shen L, et al. B cells promote insulin resistance through modulation of T cells and production of pathogenic IgG antibodies. *Nat Med.* 2011;17(5):610-617. doi:10.1038/nm.2353

Wolf MJ, Adili A, Piotrowitz K, et al. Metabolic activation of intrahepatic CD8+ T cells and NKT cells causes nonalcoholic steatohepatitis and liver cancer via cross-talk with hepatocytes. *Cancer Cell.* 2014;26(4):549-564. doi:10.1016/j.ccell.2014.09.003

Wree A, Eguchi A, McGeough MD, et al. NLRP3 inflammasome activation results in hepatocyte pyroptosis, liver inflammation, and fibrosis in mice. *Hepatology*. 2014;59(3):898-910. doi:10.1002/hep.26592

Xu R, Zhang Z, Wang FS. Liver fibrosis: mechanisms of immune-mediated liver injury. *Cell Mol Immunol*. 2012;9(4):296-301. doi:10.1038/cmi.2011.53

Ye D, Yang K, Zang S, et al. Lipocalin-2 mediates non-alcoholic steatohepatitis by promoting neutrophil-macrophage crosstalk via the induction of CXCR2 [published correction appears in *J Hepatol*. 2017 Mar;66(3):669]. *J Hepatol*. 2016;65(5):988-997. doi:10.1016/j.jhep.2016.05.041

Yeh MM, Brunt EM. Pathological features of fatty liver disease. *Gastroenterology*. 2014;147(4):754-764. doi:10.1053/j.gastro.2014.07.056

Ying W, Wollam J, Ofrecio JM, et al. Adipose tissue B2 cells promote insulin resistance through leukotriene LTB4/LTB4R1 signaling. *J Clin Invest*. 2017;127(3):1019-1030. doi:10.1172/JCI90350

Yki-Järvinen H. Non-alcoholic fatty liver disease as a cause and a consequence of metabolic syndrome. *Lancet Diabetes Endocrinol*. 2014;2(11):901-910. doi:10.1016/S2213-8587(14)70032-4

Yoon JC, Lim JB, Park JH, Lee JM. Cell-to-cell contact with hepatitis C virus-infected cells reduces functional capacity of natural killer cells. *J Virol*. 2011;85(23):12557-12569. doi:10.1128/JVI.00838-11

Younes R, Bugianesi E. Should we undertake surveillance for HCC in patients with NAFLD?. *J Hepatol*. 2018;68(2):326-334. doi:10.1016/j.jhep.2017.10.006

Younossi Z, Anstee QM, Marietti M, et al. Global burden of NAFLD and NASH: trends, predictions, risk factors and prevention. *Nat Rev Gastroenterol Hepatol*. 2018;15(1):11-20. doi:10.1038/nrgastro.2017.109

Younossi ZM, Koenig AB, Abdelatif D, Fazel Y, Henry L, Wymer M. Global epidemiology of nonalcoholic fatty liver disease-Meta-analytic assessment of prevalence, incidence, and outcomes. *Hepatology*. 2016;64(1):73-84. doi:10.1002/hep.28431

Younossi ZM, Mishra A,. Epidemiology and Natural History of Non-alcoholic Fatty Liver Disease. *J Clin Exp Hepatol*. 2012;2(2):135-144. doi:10.1016/S0973-6883(12)60102-9

Zhang F, Jiang WW, Li X, et al. Role of intrahepatic B cells in non-alcoholic fatty liver disease by secreting pro-inflammatory cytokines and regulating intrahepatic T cells. *J Dig Dis*. 2016;17(7):464-474. doi:10.1111/1751-2980.12362

Zhang M, Ueki S, Kimura S, et al. Roles of dendritic cells in murine hepatic warm and liver transplantation-induced cold ischemia/reperfusion injury. *Hepatology*. 2013;57(4):1585-1596. doi:10.1002/hep.26129

Zhang X, Han J, Man K, et al. CXC chemokine receptor 3 promotes steatohepatitis in mice through mediating inflammatory cytokines, macrophages and autophagy. *J Hepatol*. 2016;64(1):160-170. doi:10.1016/j.jhep.2015.09.005

## Acknowledgement

Firstly, I would like to express my sincere gratitude to my advisor *Prof. Emanuele Albano* for his immense knowledge and plentiful experience have encouraged me in all the time of my academic research and daily life. I could not have imagined having a better advisor and mentor for my Ph.D study.

I would also like to thank *Asst. Prof. Salvatore Sutti* who made me more passionate towards scientific research. I would like to thank *Associazione Italiana per lo Studio del Fegato (A.I.S.F)* for supporting me with a Research Grant.

I would like to thank lab mates, colleagues and research team – *Laila Lavanya, Alessia Provera, Suguna Reddy, Simone* for a cherished time spent together in the lab.

Finally, I must express my very profound gratitude to my parents, my brothers [Ramesh Rathod, Nagesh] and to my friends [*Christudas Marcilian, Ranadhir Reddy, Feba Mariam, Lavanya Gadipudi, Deepika Pantham*] for providing me with wonderful support and continuous encouragement to reach my dreams.